AV-R-87/714
AV Project No.: 91118

# DIFFUSION AND TRANSPORT MODEL ENHANCEMENT

for

Ronald E. Meyers
Principal Investigator
Physical Processes in
Transport and Diffusion

U.S. Army ASL
(SLCAS-AR-M)
White Sands Missile Range, NM 88002-5501

28 December 1987

**AeroVironment Inc.**
825 Myrtle Avenue • Monrovia, California 91016-3424 • USA
Telephone 818/357-9983

AV-R-87/714
AV Project No.: 91118

# DIFFUSION AND TRANSPORT MODEL ENHANCEMENT

by

Paolo Zannetti
AeroVironment Inc.
825 Myrtle Avenue
Monrovia, CA 91016

for

Ronald E. Meyers
Principal Investigator
Physical Processes in
Transport and Diffusion

U.S. Army ASL
(SLCAS-AR-M)
White Sands Missile Range, NM 88002-5501

28 December 1987

Contract No. DAAL03-86-D-0001
Delivery Order 0621
Scientific Service Program

UNCLASSIFIED

SECURITY CLASSIFICATION OF THIS PAGE

# REPORT DOCUMENTATION PAGE

Form Approved
OMB No 0704-0188
Exp Date Jun 30 1986

| | |
|---|---|
| 1a REPORT SECURITY CLASSIFICATION<br>UNCLASSIFIED | 1b. RESTRICTIVE MARKINGS |
| 2a. SECURITY CLASSIFICATION AUTHORITY | 3. DISTRIBUTION / AVAILABILITY OF REPORT<br>May not be released by other than sponsoring organization without approval of US Army Research Office. |
| 2b DECLASSIFICATION / DOWNGRADING SCHEDULE | |
| 4 PERFORMING ORGANIZATION REPORT NUMBER(S)<br>Delivery Order 0621 | 5. MONITORING ORGANIZATION REPORT NUMBER(S)<br>TCN 87-551 |
| 6a. NAME OF PERFORMING ORGANIZATION<br>Dr. Paolo Zannetti<br>6b. OFFICE SYMBOL (If applicable) | 7a. NAME OF MONITORING ORGANIZATION<br>U.S. Army Research Office |
| 6c. ADDRESS (City, State, and ZIP Code)<br>c/o AeroVironment, Inc.<br>825 Myrtle Avenue<br>Monrovia, CA 91016 | 7b. ADDRESS (City, State, and ZIP Code)<br>P.O. Box 12211<br>Research Triangle Park, NC 27709-2211 |
| 8a. NAME OF FUNDING / SPONSORING ORGANIZATION<br>U. S. Army ASL<br>8b. OFFICE SYMBOL (If applicable)<br>SLCAS-AR-M | 9. PROCUREMENT INSTRUMENT IDENTIFICATION NUMBER |
| 8c. ADDRESS (City, State, and ZIP Code)<br>Mr. Ronald E. Meyers<br>White Sands Missile Range, NM 88002-5501 | 10. SOURCE OF FUNDING NUMBERS<br>PROGRAM ELEMENT NO. / PROJECT NO. / TASK NO. / WORK UNIT ACCESSION NO |

11. TITLE (Include Security Classification)

Diffusion and Transport Model Enhancement (Unclassified)

12. PERSONAL AUTHOR(S)
Paolo Zannetti

| 13a. TYPE OF REPORT | 13b. TIME COVERED | 14. DATE OF REPORT (Year, Month, Day) | 15. PAGE COUNT |
|---|---|---|---|
| FINAL REPORT | FROM 17 Aug '87 TO 31 Dec '87 | 1987 December 30 | 109 |

16. SUPPLEMENTARY NOTATION Task was performed under a Scientific Services Agreement issued by Battelle, Research Triangle Park Office, 200 Park Drive, P.O. Box 12297, Research Triangle Park, NC 27709

| 17. COSATI CODES | | | 18. SUBJECT TERMS (Continue on reverse if necessary and identify by block number) |
|---|---|---|---|
| FIELD | GROUP | SUB-GROUP | |
| | | | |
| | | | |

19. ABSTRACT (Continue on reverse if necessary and identify by block number)

This report discusses the problem of battlefield assessment of atmospheric transport and diffusion problems, especially for real-time applications. The study is divided into three tasks. Task 1 describes an alternative diffusion algorithm, the Gaussian segment-puff approach, which represents a very cost-effective algorithm for dispersion calculations. Task 2 discusses the use of Kalman filtering techniques for improving the forecasting ability of prognostic meteorological models, using incoming on-line measurements. Task 3 describes the strategies for the software implementation of the filtering techniques. Finally, possible continuation and development of this study are discussed, and, in particular, the use of particle methods and the problem of linking Lagrangian particle models with prognostic Eulerian meteorological models.

| 20. DISTRIBUTION / AVAILABILITY OF ABSTRACT | 21 ABSTRACT SECURITY CLASSIFICATION |
|---|---|
| ☐ UNCLASSIFIED/UNLIMITED ☐ SAME AS RPT. ☐ DTIC USERS | |
| 22a. NAME OF RESPONSIBLE INDIVIDUAL<br>Paolo Zannetti | 22b. TELEPHONE (Include Area Code)<br>(818) 357-9983<br>22c. OFFICE SYMBOL |

DD FORM 1473, 84 MAR 83 APR edition may be used until exhausted. All other editions are obsolete.

SECURITY CLASSIFICATION OF THIS PAGE
UNCLASSIFIED

## TABLE OF CONTENTS

# 1. INTRODUCTION AND OVERVIEW

In several battlefield scenarios, the military is strategically interested (U.S. ARO, 1983; 1985) in the depiction and prediction of the space-time relationships between ambient meteorological conditions, typical battlefield surface and terrain conditions, and natural and battle-induced gaseous and particulate matter. Specific areas of interest include:

- The effects of battlefield surface cover and terrain on meteorological conditions in the surface layer (SL) and in the planetary boundary layer (PBL).

- The effects of the horizontal, slant and vertical variability of natural and battle-induced gaseous and particulate matter on electro-optical (EO) system performance, acoustic wave propagation, and visual range.

- The improvement of methods for characterizing the aerosol environment over a battlefield.

- The advancement of knowledge concerning the formation, growth and ultimate fate of natural aerosols (water fogs and clouds) and manmade aerosols (dusts, smokes, and chemical and biological agents) in battlefield environments -- environments that include complex terrain under adverse weather conditions.

- Aerosol dispersion in the surface layer (Bach, 1984).

A major problem in this area is battlefield obscuration (Ohmstede and Stenmark, 1980), since modern warfare is characterized by immense fire power, which is restricted, however, by limitations on target acquisition. In fact, to operate a weapon system, its target needs to be seen at the wavelength used by that weapon system. Natural or battle-induced pollutants may strongly affect the atmospheric transmissivity of those wavelengths, thus limiting the effective use of the weapon system.

Battlefield scenarios require not only reliable simulations of atmospheric dispersion phenomena, but also real-time simulation capabilities, in order to provide a quick-response, continuous forecasting of atmospheric dynamic behavior to allow decision-makers to plan or modify combat strategies.

This report presents the results of a preliminary study aimed at two of the goals described above:

1. The improvement of the numerical simulation of atmospheric diffusion using a mixed segment-puff method.

2. The development of real-time forecasting techniques, based on the information provided by real-time incoming meteorological measurements.

Section 2 of this report presents an alternative atmospheric diffusion algorithm based on the AVACTA II methodology recently developed by Zannetti (1986) and modified to incorporate the treatment of instantaneous and semi-continuous emission releases. Section 3 discusses the Kalman filter algorithm and presents a cost-effective technique for improving the forecasting ability of prognostic meteorological models, based on the information provided by real-time meteorological measurements. Strategies for software development of the Kalman filter algorithm are presented in Section 4, while Section 5 summarizes the main results of this project and proposes research activities for its continuation and further development.

Additional complementary information is provided in the appendices.

## 2. TASK 1 -- AN ALTERNATIVE DIFFUSION ALGORITHM

### 2.1 The Gaussian Approach

The Gaussian plume model is the most common air pollution model. It is based on a simple formula that describes the three-dimensional concentration field c generated by a point source under stationary meteorological and emission conditions as

$$c = \frac{Q}{2\pi\,\sigma_h\,\sigma_z\,|\bar{\mathbf{u}}|}\ \exp\left[-\frac{1}{2}\left(\frac{\Delta_{cw}}{\sigma_h}\right)^2\right]\ \exp\left[-\frac{1}{2}\left(\frac{z_s + \Delta h - z_r}{\sigma_z}\right)^2\right] \qquad (2\text{-}1)$$

where $c(\mathbf{s}, \mathbf{r})$ is the concentration at the receptor $\mathbf{r} = (x_r, y_r, z_r)$ due to the emissions at the source $\mathbf{s} = (x_s, y_s, z_s)$; Q is the pollutant mass emission rate; $\sigma_h(j_h, d)$ and $\sigma_z(j_z, d)$ are the standard deviations (horizontal and vertical) of the plume concentration spatial distribution (often $\sigma_h$ is referred to as $\sigma_y$); $j_h$ and $j_z$ are the horizontal and vertical turbulence states (often classified by "stability" classes); d is the downwind distance of the receptor from the source

$$d = \left[(\mathbf{r} - \mathbf{s}) \cdot \bar{\mathbf{u}}\right] / |\bar{\mathbf{u}}| \qquad (2\text{-}2)$$

$\bar{\mathbf{u}}$ is the average wind velocity vector $(\bar{u}_x, \bar{u}_y, \bar{u}_z)$ at the emission height; $\Delta_{cw}$ is the crosswind distance between the receptor and source (i.e., between the receptor and the plume centerline)

$$\Delta_{cw} = \left(|\mathbf{r} - \mathbf{s}|^2 - d^2\right)^{1/2} \qquad (2\text{-}3)$$

and $\Delta h(d)$ is the emission plume rise. Eq. 2-1 is applied for $d > 0$; if $d \leq 0$, then $c = 0$.

Eq. 2-1 refers to a stationary state (c is not a function of time), uses meteorological conditions (wind and turbulence states) that must be considered

homogeneous and stationary in the modeled area (i.e., between **s** and **r**), and cannot work in calm conditions where $|\bar{u}| \cong 0$. However, the simplicity of the Gaussian approach, its relative ease of use with clearly measurable meteorological parameters and, especially, the elevation of this methodology to the quantitative decision-controlling level (U.S. EPA, 1978) have stimulated research aimed at removing some of its limitations in treating the complex situations of the real world.

Equation 2-1 is generally written in the form

$$c = \frac{Q}{2\pi\sigma_h\sigma_z\bar{u}} \exp\left[-\frac{1}{2}\left(\frac{y_r}{\sigma_y}\right)^2\right] \exp\left[-\frac{1}{2}\left(\frac{h_e - z_r}{\sigma_z}\right)^2\right] \qquad (2\text{-}4)$$

in which $\bar{u}$ is the average wind speed, $h_e$ is the effective emission height ($h_e = z_s + \Delta h$, where $\Delta h$ is the emission plume rise), and $\sigma_y$ replaces $\sigma_h$. Here a wind-oriented coordinate system is also used in which the wind is blowing toward the x-axis. Eq. 2-4 can be derived in several ways from different assumptions and can be justified by semi-empirical considerations. Even though instantaneous plume concentrations are quite irregular, a sufficiently long averaging time (e.g., one hour) generates, in many cases, bell-shaped concentration distributions that can be well approximated by the Gaussian distribution in both the horizontal and (to a lesser degree) the vertical.

## 2.2 Dynamic Applications of the Gaussian Formula

### 2.2.1 The Segmented Plume Model

The Gaussian steady-state formula described in Eq. 2-1 or 2-4 is valid only during fairly stationary and homogeneous transport conditions (e.g., $\bar{u} \geq 1$ m/s). In order to treat time-varying transport conditions and, especially, changes in wind direction, several authors have developed and used a segmented Gaussian plume (e.g., Hales et al., 1977; Benkley and Bass, 1979; Chan et al., 1979). In the segmented plume approach, the plume is broken up into independent elements (plume segments or sections) whose initial features and time dynamics are a

function of time-varying emission conditions and the local time-varying meteorological conditions encountered by the segments along their motion.

The segmented plume features are illustrated in Figure 2-1, which shows a top view (solid lines) of a segmented plume encountering a progressive change of wind direction along its trajectory. Segments are sections of a Gaussian plume. Each segment, however, generates a concentration field that is still computed by Eq. 2-1 and that represents the contribution of the entire virtual plume passing through that segment, as illustrated by the dotted lines in Figure 2-1. Therefore, only one segment (the closest) affects the concentration computation at each receptor, although the occurrence of a $180^{\circ}$ wind direction change can create a condition where the contribution of two segments (that is, two virtual plumes) should be superimposed at some receptors.

### 2.2.2 Puff Models

Like segmented models, puff models (e.g., Lamb, 1969; Roberts et al., 1970) have been developed to treat nonstationary nonhomogeneous emission and dispersion conditions. Puff methods, however, have the additional advantage of being able, at least theoretically, to simulate calm or low wind conditions.

The Gaussian puff model assumes that each pollutant emission during the time interval $\Delta t$ injects into the atmosphere a "puff" having a mass $\Delta M = Q\,\Delta t$, where Q is the time-varying emission rate. The center of each puff is advected according to the local time-varying wind vector. If, at time t, the center of a puff is located at $\mathbf{p}(t) = (x_p, y_p, z_p)$, then the concentration $\Delta c$ due to that puff at the receptor $\mathbf{r} = (x_r, y_r, z_r)$ can be computed using the basic Gaussian puff formula

$$\Delta c = \frac{\Delta M}{(2\pi)^{3/2}\,\sigma_h^2\,\sigma_z} \exp\left[-\frac{1}{2}\left(\frac{x_p - x_r}{\sigma_h}\right)^2\right] \cdot$$

$$\exp\left[-\frac{1}{2}\left(\frac{y_p - y_r}{\sigma_h}\right)^2\right] \exp\left[-\frac{1}{2}\left(\frac{z_p - z_r}{\sigma_z}\right)^2\right] \qquad (2\text{-}5)$$

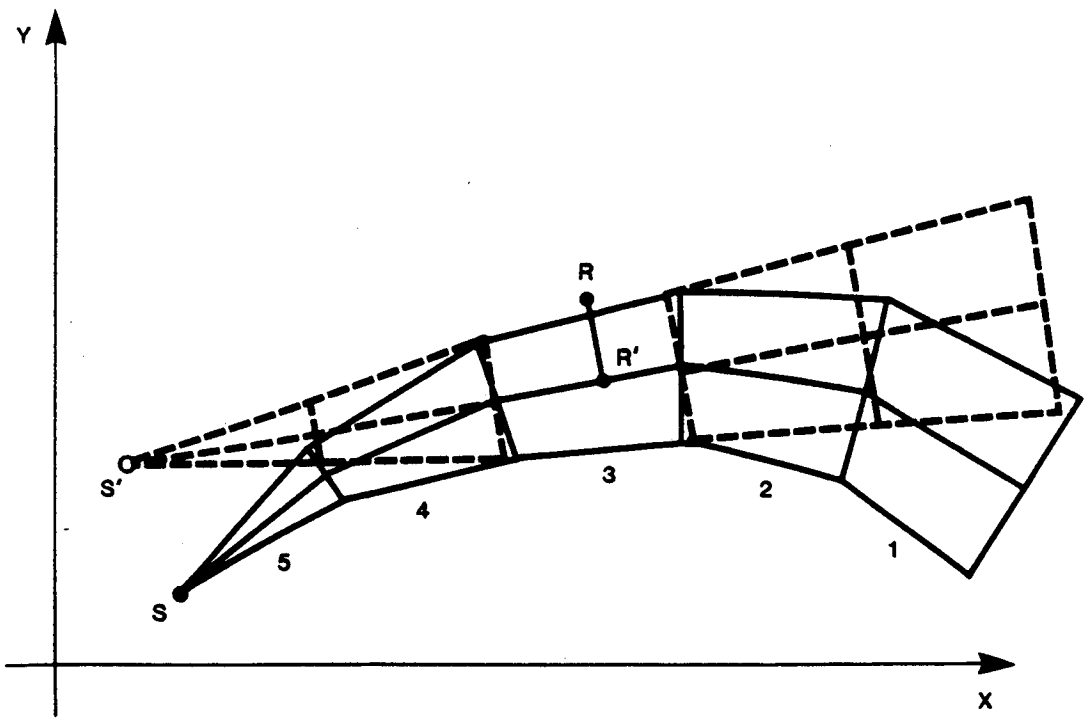


Figure 2-1. Computation of the concentration at the receptor R generated by the segmented plume (solid lines). The comutation os performed by evaluating the contribution of the virtual plume (dotted lines) from the virtual source S' passing through the closest segment (number 3) to the receptor R.

which is often expanded to incorporate reflection and deposition/decay terms. The analytical integration of Eq. 2-5 in stationary, homogeneous transport conditions, gives the Gaussian plume formula of Eq. 2-4.

Eq. 2-5 requires the evaluation of the horizontal ($\sigma_h$) and vertical ($\sigma_z$) dynamics of each puff's growth. The total concentration in a receptor at time t is computed by adding the contribution $\Delta c$ from all existing puffs generated by all sources. Note that Eq. 2-5 differs from Eq. 2-4 mainly because an extra horizontal diffusion term has been substituted for the transport term with the consequent disappearance of the wind speed $\bar{u}$. In a puff model, the wind speed directly affects the concentration computation only by controlling the density of puffs in the region (that is, the lower the wind speed, the closer a puff is to the next one generated by the same source). Therefore, at least in theory, a puff model can handle calm or low-wind conditions, and this approach represents the most advanced and powerful application of the Gaussian formula.

Several studies have discussed the puff modeling approach in detail, improving its application features. Algorithms have been proposed and evaluated for incorporating wind shear effects (Sheih, 1978). Virtual distance (Ludwig et al., 1977) and virtual age (Zannetti, 1981) computations have been defined for evaluating the $\sigma_h$ and $\sigma_z$ dynamics of the puff. Puff merging (Ludwig et al., 1977) or splitting (Zannetti, 1981) has been incorporated for performing cost-effective simulations with relatively large $\Delta t$ (for example, 5 to 10 minutes). An empirical method has been derived (Zannetti, 1981) for evaluating the puff's $\sigma_h$ and $\sigma_z$ growth during calm or low-wind conditions as a function of currently available $\sigma$ functions during transport conditions.

### 2.2.3 Mixed Segment-Puff Methodology

A new mixed methodology has recently been proposed by Zannetti (1986). It combines the advantages of both the segment and puff approaches for realistic and cost-effective simulation of short-term plume dispersion phenomena using the Gaussian formula.

## 2.3 The Selected Algorithm

The mixed segment-puff methodology introduced in Section 2.2.3 above was selected as the basic algorithm for the alternative diffusion approach to be used in this study. This technique is fully described by Zannetti (1986; paper enclosed as Appendix A). This algorithm has been fully implemented into a computer code, AVACTA II, Release 3.1 (Zannetti et al., 1986), which currently provides the most advanced, dynamic use of the Gaussian formula. Among the unique characteristics of this code are:

- the cost-effective description of a plume by a sequence of plume elements, segments or puffs, depending upon their size
- the "split-sigma" approach, in which horizontal diffusion is a function of a "horizontal" stability, while vertical diffusion is a function of a "vertical" one
- the capability of treating calm or low-wind conditions
- the capability of computing the dynamics of the plume elements by directly using the three-dimensional output (wind and stability) of a meteorological model
- the possibility of selecting different computational options, such as different plume rise formulas, sigma functions, reflection assumptions, etc.

Since AVACTA II was originally developed to treat continuous plumes, this methodology was improved during this project in order to comply with the special needs of this study, which requires the capability of treating instantaneous, semi-continuous and continuous emission releases. This improvement is presented below.

## 2.4 Improvement of the Algorithm for the Simulation of Instantaneous or Semi-Continuous Releases

There are two types of application of puff modeling. The first one uses puffs to simulate, as in the original version of AVACTA II, the average (e.g., one-hour average) characteristics of a continuously emitted plume. In this case, it is correct to calculate the puff dynamics using "plume" sigmas, i.e., sigma functions originally proposed for the calculation of plume dynamics. But puff (or better, relative diffusion) simulations apply also to the instantaneous or semi-instantaneous sources, defined as those sources where the release time is short compared with the travel time.

Unfortunately, very little information is available for the description of the diffusion of a single puff, i.e., for the evaluation of the relative diffusion sigmas, even though it is quite clear that the "plume" sigma equations cannot be applied (even though they often are) to relative diffusion calculations.

For relative diffusion, Hanna et al. (1982) recommend the Batchelor's formula

$$\sigma_h^2 = \varepsilon t^3 \tag{2-6}$$

for puff travel times that are less than $10^4$s, where $\varepsilon$ is the eddy dissipation rate. They also recommend calculating $\varepsilon$ locally at first (i.e., when the vertical size of the puff is small), and then at a height $z = z_i/2$ as $\sigma_z$ approaches $0.3\, z_i$, where $z_i$ is the PBL height. The eddy dissipation rate $\varepsilon$ is given by

$$\varepsilon = \frac{u_*^3}{k\, z} \left(\phi_m - \frac{z}{L}\right) \tag{2-7}$$

within the surface layer and

$$\varepsilon = 0.5\, H' \tag{2-8}$$

at heights above the surface layer, where $u_*$ is the friction velocity, k is the von Karman constant, $\phi_m$ is the nondimensional wind shear, z is the altitude of the puff, L is the Monin-Obukov length, and H' is the surface buoyancy flux

$$H' = \frac{g}{\bar{T}} \overline{w'T'} = \frac{H g}{c_p \rho \bar{T}} \quad (2\text{-}9)$$

where H is the surface heat flux defined by

$$H = c_p \rho \overline{w'T'} \quad (2\text{-}10)$$

In neutral conditions, however, $H' = 0$ and $\varepsilon = 0$. In this case, a better fit of the available data gives, above the surface layer

$$\varepsilon = 2 u_*^3 / z \quad (2\text{-}11)$$

For travel times greater than $10^4$s, Hanna et al. (1982) suggest

$$\sigma_h = \text{const } t \quad (2\text{-}12)$$

where const can be determined by forcing Eq. (2-12) to satisfy Eq. (2-6) for $t = 10^4$s, thus giving

$$\text{const} = 100\sqrt{\varepsilon} \quad (2\text{-}13)$$

A similar procedure is proposed for $\sigma_z$, except that $\sigma_z$ remains equal to $0.3\ z_i$ for all times after it first reaches this value.

## 2.5 Implementation of the Improved Algorithm into AVACTA II

The methodology described in Section 2.4 for simulating instantaneous or semi-continuous releases has been added to the AVACTA II computer package. This new version of the code (Release 4.0) and its user's manual are being provided separately to Mr. Ronald E. Meyers of the U.S. Army. This code is written in FORTRAN 77 and can provide a fast and accurate alternative algorithm for the MACH1 computer code. The model can run on virtually any mainframe computer and, with minor modifications, on most microcomputers.

# 3. TASK 2 -- THE KALMAN FILTER ALGORITHM

## 3.1 Introduction to Kalman Filters

The principle of least squares estimation originated at the beginning of the 19th century, but only a century and a half later, starting with the pioneering work of Wiener (1949), the method received a substantial innovation that allowed its "recursive" application, as explained below.

Let us consider, following the discussion by Young (1974), the linear regression problem

$$y = \mathbf{x}^T \mathbf{a} \tag{3-1}$$

in which a variable y is related to n other linearly independent variables $\mathbf{x} = [x_1, x_2, ..., x_n]^T$, through the unknown coefficients $\mathbf{a} = [a_1, a_2, ..., a_n]^T$. Then, if we have k observations of y and **x**, we can obtain an estimate $\mathbf{a}'_k$ of **a** by using the least squares method, as follows

$$\mathbf{a}'_k = \left[ \sum_{i=1}^{k} \mathbf{x}_i \mathbf{x}_i^T \right]^{-1} \sum_{i=1}^{k} \mathbf{x}_i y_i \quad . \tag{3-2}$$

But if the number k is increasing, i.e., if new observations of y and **x** are progressively gathered, the updating of the estimate $\mathbf{a}'_k$ requires a repeated application of Eq. 3-2, which contains a computationally expensive matrix inversion. To avoid this expensive calculation, Plackett (1950) rewrote Eq. 3-2 in a "recursive" form in which $\mathbf{a}'_k$ is a linear sum of the estimate obtained after k-1 observations (i.e., $\mathbf{a}'_{k-1}$), plus a correction term based on the newly-received information $y_k$ and $\mathbf{x}_k$. This recursive form does not require direct matrix inversion, but, nevertheless, provides results mathematically identical to Eq. (3-2).

The next step was provided by Kalman (1960), who expanded the work of Wiener (1949) and solved the general problem of estimating a set of parameters $\mathbf{a}_k$ in which:

- $\mathbf{a}_k$ represents, in a more general form, the "state" of a dynamic system

- parametric invariance (i.e., $\mathbf{a}_k = \mathbf{a}_{k-1}$, for all k) is not assumed any more

- the parameters $\mathbf{a}_k$ vary according to the general stochastic evolution scheme ("state equation" or "message model")

$$\mathbf{a}_k = \mathbf{F}(k, k-1)\,\mathbf{a}_{k-1} + \mathbf{G}(k, k-1)\,\mathbf{w}_k \tag{3-3}$$

where $\mathbf{F}(k, k-1)$ is a n x n transition matrix, $\mathbf{G}(k, k-1)$ is a n x m input matrix, and $\mathbf{w}_k$ is a m x 1 vector of independent random variables with zero mean and covariance matrix $\mathbf{Q}$.

- "noisy" measurements $\mathbf{y}_k = [y_1, y_2, \ldots, y_p]^T_k$ are available that are linearly related to $\mathbf{a}_k$ by the "observation equation" or "observation model"

$$\mathbf{y}_k = \mathbf{H}_k\,\mathbf{a}_k + \mathbf{v}_k \tag{3-4}$$

where $\mathbf{H}_k$ is a p x n coefficient matrix and $\mathbf{v}_k$ is the measurement error assumed to be a vector of independent random variables with zero mean and covariance matrix $\mathbf{R}$.

Then, the equations of the Kalman filtering method allow a recursive computation of

- the estimates $\mathbf{a}'_{k+j}$ (j = 1, 2, ...) of $\mathbf{a}_{k+j}$ by considering only the effect of the most recent observation $\mathbf{y}_k$, instead of resolving at each time the entire problem by the classical least squares regression technique

- the estimate of the covariance matrix of the forecasting error $\mathbf{a}_{k+j} - \mathbf{a}'_{k+j}$, and, therefore, an important indication of the accuracy of the estimates $\mathbf{a}'_{k+j}$ and information on their convergence

In the Kalman filter outlined above, the state vector $\mathbf{a}_k$ can be any numerical description of the state of a dynamic system, e.g., the location of a space ship, concentrations of pollutants in the atmosphere, or a velocity field representing groundwater dynamics. Then, the transition matrix **F** contains our (imperfect) deterministic representation of the phenomenon (e.g., a set of physical equations reduced into a linear matrix form*), and $\mathbf{y}_k$ are the limited measurements available. Then the Kalman filter provides a method for forecasting the evolution of $\mathbf{a}_k$, which takes into account both the "deterministic" component **F** (predictor) and the continuous, on-line information (corrector) provided by the measurements $\mathbf{y}_k$.

### 3.2 Previous Applications to Air Quality Problems

Kalman filters have been used in air pollution problems to obtain more accurate predicted values in episode forecasting and control. This can be done by considering $\mathbf{x}(t) = \mathbf{a}_k$ as the vector of concentrations of a pollutant at the grid points of a grid dispersion model (Bankoff and Hanzevack, 1975; Melli et al., 1981) or at the pollutant monitoring points (Sawaragi et al., 1976) of the study area. The state vector **x**(t) might also be extended to include some additional adaptive parameters (Bankoff and Hanzevack, 1975), but we will not discuss this extension here. Then the transition matrix **F** becomes either the matrix of the spatial discretization (K-model) of the transport and diffusion equation (Bankoff and Hanzevack, 1975; Melli et al., 1981) (including time-dependent emission and meteorological inputs), or a multiple regression matrix (Sawaragi et al., 1976). Model inaccuracies and emissions and meteorology input errors are included in the system noise process **w**(t).

*Non-linear Kalman filters are also available, but will not be discussed here.

A hybrid* air quality application of the Kalman filter was developed by Zannetti and Switzer (1979; paper enclosed as Appendix C), who limited the dimension of the state vector **x** to the number of air quality monitoring stations, but incorporated the contribution of the meteorology by having the transition matrix **F** depend upon the time-varying meteorological conditions. They evaluated the coefficients of **F** in an "adaptive" manner, i.e., using a first-order Markov chain on a learning time period of given fixed length close to the forecasting time.

An important problem arises in the application of the Kalman filter to air pollution problems. In fact, it is necessary to avoid the high dimensionality of the resulting Kalman filter equations. For example, when **F** is the time-evolution transition matrix of the K-model, a simple spatial grid of 20 x 20 x 10 points produces Kalman filter matrices of dimension 4000 x 4000. Methods have been developed to simplify this problem. In particular, either the Green function can be used to reduce the equation of the K-model to a difference equation of relatively small dimension (Hino, 1974), or a discrete form of Chandrasekar-type equations** can be applied for the same goal (Desalu et al., 1974). Alternatively, the region can be partitioned into subregions (Bankoff and Hanzevack, 1975; Melli et al., 1981) and, if the subvectors of the subregions are not coupled (or are weakly coupled), the filter algorithm can be applied separately to each of the subvectors, thus reducing the size of the matrices that must be manipulated. Finally, a multiple linear regression model can be used (Savaragi et al., 1976) for **F**, thus reducing the dimension of the filter to the number of monitoring stations in the area. However, this loses the "physical" information of the diffusion phenomenon.

*This approach is a hybrid one since the matrix **F** is not computed using a set of deterministic equations, but is calculated using statistical methods, in which a different matrix **F** is estimated for each meteorological class (see Appendix C for a complete discussion on this methodology).

**This alternative method completely bypasses direct calculation of the covariance matrices, while still retaining the properties of the Kalman filter.

# 4. TASK 3 — STRATEGIES FOR THE SOFTWARE DEVELOPMENT OF THE KALMAN FILTER ALGORITHM

## 4.1 Real-Time Prediction Using Meteorological Models

Two basic types of meteorological models are used to provide meteorological input to air pollution dispersion models:

1. diagnostic models, which are based on objective analysis of meteorological measurements and provide a mass-consistent evaluation of the three-dimensional wind field

2. prognostic models, which forecast the time evolution of the atmospheric system through the space-time integration of the equations of mass, heat, motion and water

Diagnostic models, such as NEWEST (Tran and Sklarew, 1979) and NOABL (Phillips and Traci, 1978), are just a reasonable interpolation/extrapolation of available data. They make full and good use of all the available measurements, but do not possess forecasting ability. Prognostic models, such as the SIGMET family of mesoscale models developed by Science Applications Inc., the vorticity-mode model developed by Bornstein et al. (1985) and the primitive equations-mode model developed by Pielke et al. (1983), need limited measurements, i.e., only the initial and boundary conditions for the meteorological parameters, and can make virtually no use of incoming meteorological information. Since a good meteorological forecast is an important prerequisite to any real-time air quality forecasting, it is important to incorporate filtering techniques into prognostic meteorological models. This filtering, however, raises the problem of the representativeness of point measurements of meteorological variables, which is discussed in the next section.

## 4.2 The Problem of Spatial and Temporal Representativeness of Field Measurements

As discussed in the previous sections, filtering techniques allow a real-time use of incoming measurements, with a consequent improvement of the forecasting ability. In the case of meteorological forecasting by a mesoscale numerical model, filtering is extremely important, since the information content of incoming measurements is very high and, therefore, its incorporation into the numerical forecasting scheme is essential to achieve reasonably good forecasting capabilities.

The problem, however, is the following. How good are the meteorological measurements? And what is their "representativeness" in space and time? In other words, how large are the errors $\mathbf{v}_k$ in Eq. 3-4? And, still in Eq. 3-4, how many elements of the state vector $\mathbf{a}_k$ (of length n) are described by the observation vector $\mathbf{y}_k$ (of length p)? If, for example, the wind speed is the parameter of concern, what is the relationship between point measurements of wind speed at meteorological stations 10 m above the ground and grid-average wind speed value in cells of, say, 1000 m x 1000 m x 50 m? The answers to the above questions are essential to the correct definition of the p x n coefficient matrix $\mathbf{H}_k$ and the covariance matrix $\mathbf{R}$ of the errors $\mathbf{v}_k$ in Eq. 3-4.

The problem of assessing the "representativeness," in space and time, of meteorological measurements, is, today, a very important one, which is receiving much attention, especially in order to fully understand if, and how, grid-averaged values can be compared with point measurements. The study of this subject is in its infancy, but preliminary definitions and general methodological approaches have been given by Nappo et al. (1982) and Nappo (1983), who defined four types of representativeness:

1. measurement representativeness
2. point-to-point representativeness
3. point-to-volume representativeness
4. temporal representativeness

and three types of semi-quantative measures of representativeness based on:

1. residuals (or deviations)
2. autocorrelation and structure functions
3. frequency distributions (e.g., useful in wind energy studies)

Zannetti (1986; paper provided as Appendix B) analyzed the problems related to the evaluation and validation of air quality models using field measurements. His discussion, which deals with a pollutant concentration field c but can be extended to virtually any meteorological parameter, such as wind, temperature, etc., provides a preliminary method to assess the horizontal extent of the "representativeness volume" of ground-level atmospheric point measurements. Then, depending upon the relative size of this volume compared with the size of the grid cells, several implications for measurement representativeness can be derived.

It is clear that, without a reasonable evaluation of point measurement representativeness, no filtering algorithm can be defined.

### 4.3 A Methodological Approach

For the particular problem of mesoscale meteorological parameters, we propose the following approach

1. use of a diagnostic model to provide a three-dimensional field of the meteorological parameter under investigation (e.g., the wind vector)

2. use of representativeness concepts to provide a quantitative evaluation of the "representativeness" of the diagnostic model outputs in each cell (e.g., the outputs in cells that contain a monitoring station will generally be more representative than those in cells without monitoring stations)

3. definition of an analytical methodology to translate the representativeness computed above into the definition of $\mathbf{H}_k$ and $\mathbf{R}$ in Eq. 3-4

Also, as an additional important contribution, if the representativeness is computed using the gradient concepts illustrated in Appendix B, a prognostic meteorological model can be used to provide an estimate of these gradients and, therefore, a quantitative evaluation of the representativeness of the monitoring data.

### 4.4 A Numerical Algorithm

From the previous discussions, it is clear that general algorithms are difficult to define and that, to be successful, a Kalman filter forecasting algorithm requires the following development steps for mesoscale meteorological forecasting:

1. choice of the meteorological prognostic model

2. simplification of the prognostic model into a linear form and derivation of the linear transition matrix $\mathbf{F}$ to be used in Eq. 3-3

3. evaluation of the input matrix $\mathbf{G}$ and the covariance matrix $\mathbf{Q}$ in Eq. 3-3, which represent model inaccuracies (both analytical and numerical, plus the uncertainties on initial and boundary conditions)

4. analysis of available measurements that can be collected on a real-time basis, and possible use of a diagnostic model to provide a three-dimensional "measurement" field

5. evaluation of spatial and temporal representativeness of measurement data (e.g., using the gradients provided by a prognostic model)

6. quantification of representativeness by estimating $\mathbf{H}_k$ and $\mathbf{R}$ in Eq. 3-4

After completing the above steps, the application of the Kalman filter can be attempted. For example, the general computer-oriented recursive form provided by Zannetti and Switzer (1979) and presented in Figure 4-1, can be used. (Symbols in this notation are slightly different from those used in this report; see the original paper, enclosed as Appendix C, for the correct definitions of the variables.) A programming outline of this method (written in APL language) is also illustrated in Figure 4-2.

A. Initial conditions

$T=0,\ X \leftarrow \underset{\sim}{\mu}_{\underset{\sim}{x}}(0),\ VX=\underset{\sim}{V}_{\underset{\sim}{x}}(0)$

B. Matrices definitions

$FI_1=\underset{\sim}{\Phi}(T+1,T|T),\ FI_2=\underset{\sim}{\Phi}(T+2,T+1|T),\ldots,FI_p=\underset{\sim}{\Phi}(T+p,T+p-1|T),$

$GA=\underset{\sim}{\Gamma}(T),\ H_1=\underset{\sim}{H}(T+1|T),\ H_2=\underset{\sim}{H}(T+2|T),\ldots,H_p=\underset{\sim}{H}(T+p|T),$

$VW=\underset{\sim}{V}_{\underset{\sim}{w}}(T+1|T),\ VV=\underset{\sim}{V}_{\underset{\sim}{v}}(T+1|T)$

C. Predicted states

$X_1=FI_1 \cdot X,\ X_2=FI_2 \cdot X_1,\ldots X_p=FI_p \cdot X_{p-1}$

D. Saving

Save $H_1 \cdot X_1,\ H_2 \cdot X_2,\ldots H_p \cdot X_p$ for future comparison with

the measures $\underset{\sim}{z}(T+1),\ \underset{\sim}{z}(T+2),\ldots\underset{\sim}{z}(T+p)$

E. A-priori error covariance matrix

$VX=FI_1 \cdot VX \cdot FI_1^T+GA \cdot VW \cdot GA^T$

FIGURE 4-1. Computed-oriented recursive form of the Kalman filter method (from Zannetti and Switzer, 1979, paper enclosed as Appendix C).

F. Saving

Forcing of the symmetry of VX for numerical stability, And saving of its main diagonal

G. Filter gain matrix

$$K=VX\cdot H_1^T\cdot[H_1\cdot VX\cdot H_1^T+VV]^{-1}$$

H. Process the observation $Z=\underset{\sim}{z}(T+1)$

$$X = X_1+K\cdot[Z-H_1\cdot X_1]$$

I. A-posteriori error covariance matrix with a formula numerically more stable[1] than (7)

$$VX = [I-K\cdot H_1]\cdot VX\cdot[I-K\cdot H_1]^T+ K\cdot VV\cdot K^T$$

J. Saving

Forcing of the symmetry of VX for numerical stability, and saving of its main diagonal

K. Loop

T=T+1, then end if $T>T_{MAX}$, otherwise go to step B.

FIGURE 4-1. (continued)

```
      ∇KMAIN[□]∇
      ∇ JMAX KMAIN P;J;FI;GAM;H;VW;VV;X;VX;Z;XF;XZ;K
[1]   ⍝
[2]   ⍝    "KMAIN" : MAIN PROGRAM OF REAL-TIME SIMULATION OF THE
[3]   ⍝              LINEAR DISCRETE KALMAN FILTER.
[4]   ⍝
[5]   ⍝ ********************************
[6]   ⍝ ******   INITIALIZATION   ******
[7]   ⍝ ********************************
[8]    XZSAVE←VXSAVE←0⍴0
[9]    J←0
[10]   FI←P READΔFI J
[11]   GAM←READΔGAM J
[12]   H←P READΔH J+1
[13]   VW←READΔVW J
[14]   VV←READΔVV J+1
[15]   X←READΔMU0
[16]   VX←READΔVX0
[17]   Z←READΔZ⍳P
[18] ⍝ ********************************
[19] ⍝ ******   PREDICTED STATE   ******
[20] ⍝ ********************************
[21] LOOP:XF←FI FOREC X
[22]   XZ←H XZCOMP XF
[23]   SAVEΔXZ XZ
[24] ⍝ ************************************************
[25] ⍝ ******   PREDICTED ERROR COVARIANCE MATRIX   ******
[26] ⍝ ************************************************
[27]   VX←(FI[1;;] BY VX BY TRANS FI[1;;])+GAM BY VW BY TRANS GAM
[28]   VX←FORSIM VX
[29]   SAVEΔVX VX
[30] ⍝ ************************************
[31] ⍝ ******   FILTER GAIN MATRIX    ******
[32] ⍝ ************************************
[33]   K←VX BY(TRANS H[1;;]) BY INV(H[1;;] BY VX BY TRANS H[1;;])+V'
[34] ⍝ ******************************************
[35] ⍝ ******   PROCESS THE OBSERVATION   ******
[36] ⍝ ******************************************
[37]   X←XF[1;]+K BY Z[1;]-XZ[1;]
[38] ⍝ ************************************************
[39] ⍝ ******   NEW ERROR COVARIANCE MATRIX   ******
[40] ⍝ ************************************************
[41]   VX←((IDENT(⍴K)[1])-K BY H[1;;]) BY VX BY TRANS(IDENT(⍴K
[42]   VX←VX+K BY VV BY TRANS K
[43]   VX←FORSIM VX
[44]   SAVEΔVX VX
[45] ⍝ ******************************
[46] ⍝ ******   END OF LOOP   ******
[47] ⍝ ******************************
[48]   →((J+P)>JMAX)/END,0⍴J←J+1
[49]   FI←P READΔFI J
[50]   GAM←READΔGAM J
[51]   H←P READΔH J+1
[52]   VW←READΔVW J
[53]   VV←READΔVV J+1
[54]   Z←1 LSHIFT Z
[55]   Z[P;]←READΔZ 1⍴P+J
[56]   →LOOP
[57] END:'*** NORMAL END ***'
      ∇
```

FIGURE 4-2. Program outline of the algorithm presented in Figure 3-1 (written in APL).

# 5. CONCLUSIONS AND FUTURE RECOMMENDATIONS

This report has presented the numerical and software implementation of a cost-effective segment-puff methodology (the AVACTA II model), which is particularly suitable for simulating, on a real-time basis, atmospheric dispersion phenomena. In addition to this main goal, a second topic was discussed: the use of Kalman filtering techniques to improve the real-time forecasting of prognostic meteorological models.

We recommend the continuation of these efforts along the research directions that were outlined in this report. More precisely, we propose a continuation of research efforts on the following three topics:

1. numerical definition and software implementation of a Kalman filter for a prognostic meteorological model, such as SIGMET

2. linkage between a prognostic meteorological model, such as SIGMET, and the particle model MC-LAGPAR (described in the papers enclosed as Appendices D and E)

3. analysis of the problem of computing concentration fluctuations and their relation with averaging time

These three topics are described further in the sections below.

## 5.1 Kalman Filter Implementation

We propose to apply the methodology outlined in Sections 4-3 and 4-4 using 1) a diagnostic model (e.g., the NOABL model, Phillips and Traci, 1978) to interpolate/extrapolate real-time measurements in a three-dimensional domain, and 2) a prognostic model, such as SIGMET, to provide the deterministic corrector. In this way, the output of the diagnostic model will be used to filter the prognostic model's predictions.

A possible alternative way to the implementation of a Kalman filtering scheme will be explored. This alternative method (Meyers, personal communication) is based on a modification of the Navier-Stokes equations (or equation of motion) as follows

$$\frac{\partial \mathbf{u}}{\partial t} = -\mathbf{u}\cdot\nabla\mathbf{u} - \frac{1}{\rho}\nabla p - \mathbf{g} - 2\boldsymbol{\Omega}\times\mathbf{u} - \boldsymbol{\alpha}\cdot(\mathbf{u}-\mathbf{u}_o) \qquad (5\text{-}1)$$

in which $\mathbf{u}$ is the wind vector, p is the pressure, $\rho$ is the density, $\mathbf{g}$ is the gravity acceleration, $\boldsymbol{\Omega}$ is the angular velocity of the earth's rotation, and the additional last term includes the effect of the measurements $\mathbf{u}_o$ at the monitoring locations and produces a new fictitious acceleration that tends to continuously reduce the difference between the $\mathbf{u}$ values and the measurements $\mathbf{u}_o$. This "implicit" incorporation of measurements into the equation of motion will be investigated, both theoretically and numerically.

## 5.2 Particle Modeling and Its Linkage with Prognostic Meteorological Models

### 5.2.1 Particle Modeling Using Monte-Carlo Techniques

Particle modeling is the most recent and powerful computational tool for the numerical discretization of a physical system. It has been particularly successful in a wide spectrum of applications (Hockney and Eastwood, 1981) that range from the atomic scale (electron flow in semiconductors, molecular dynamics) to the astronomical scale (galaxy dynamics), with other important applications to plasma and turbulent fluid dynamics. In particle models, the transport terms, whose correct numerical treatment is very difficult with Eulerian (grid) models, are handled in a straightforward manner. Particles, in fact, have a Lagrangian nature, since they move following the main flow. For this reason, they are often called Lagrangian particles.

Particle models use a certain number of computational (fictitious) particles to simulate the dynamics of a selected physical parameter (e.g., mass, heat, electrical charge density, etc.). Particle motion can be produced by both deterministic velocities and semi-random pseudo-velocities generated using Monte-

Carlo techniques. In this latter case, the trajectory of a single particle simply represents a realization from an infinite set of possible solutions. Important characteristics of the diffusion process can be inferred, however, from the computation of average particle ensemble properties, which are not affected by the randomness of the pseudo-velocities if enough particles are used.

Three main types of particle models can be defined (Hockney and Eastwood, 1981):

- particle-particle (PP) models, where all interaction forces between particles are computed at each time step

- particle-mesh (PM) models, where forces are computed using a field equation (on a grid) for the potential

- PP-PM (or $P^3M$) models, a hybrid approach, where interparticle forces are split into a short-range component (computed using the PP method) and a slowly varying one (computed, using a grid, by the PM method)

Particle modeling of air pollution dispersion phenomena has recently become the subject of a great deal of investigation (e.g., Diehl et al., 1982; Legg and Raupach, 1982; Ley, 1982; Zannetti and Al-Madani, 1983; this latter paper is enclosed as Appendix D). The dispersion of emitted material can be described by a suitable number of fictitious particles moving, at each time step, according to pseudo-velocities simulating 1) transport, 2) turbulent fluctuations, and 3) molecular diffusion (if not negligible). These pseudo-velocities are not intended to simulate the real trajectory of a specific air parcel, but to provide realistic dynamics of the pollutant motion on an ensemble basis. In these applications, each computational (fictitious) particle represents a certain mass of atmospheric pollutant, either a gas (such as $SO_2$) or particulate matter. Examples of particle simulations are presented in Figure 5-1. They clearly show the unique degree of resolution that this method provides in the numerical representation of the dispersion phenomena. (Here, in the interaction between a plume and an elevated inversion, part of the plume is reflected, part is trapped inside the inversion, and part is able to perforate it).

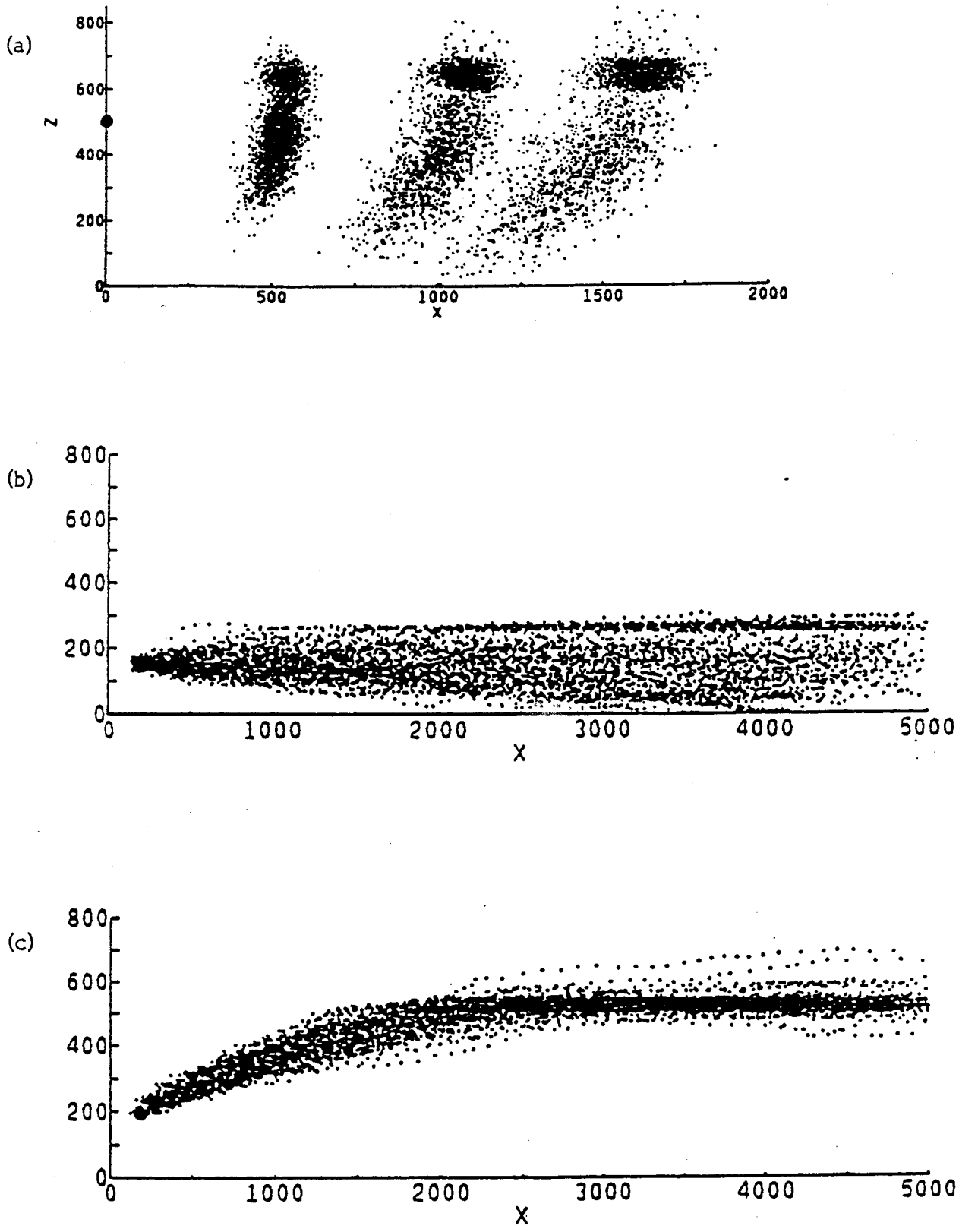


FIGURE 5-1. Qualitative behavior of a) a nonbuoyant puff, b) a nonbuoyant plume, and c) a buoyant plume, interacting with an elevated inversion, as simulated by particle models (from Zannetti and Al-Madani, 1983).

86-69

The very latest developments in air pollution modeling by particle methods (van Dop et al., 1985; Zannetti, 1986; Thomson, 1986; De Baas et al., 1986; Brusasca et al., 1987) have improved our understanding, but also present new problems, both theoretical and practical. In fact, the promising results of all these studies are accompanied by the persisting difficulty of properly evaluating Lagrangian velocity statistics from Eulerian measurements (see Davis, 1982). Nevertheless, particle methods still provide outstanding advantages over other air pollution diffusion modeling techniques, such as Gaussian models and grid models.

Encouraging results for the simulation of unstable, convective conditions have recently been obtained by Brusasca et al. (1987) using the MC-LAGPAR model developed by Zannetti (1986). They consider the effects of convective cells on the dispersion of elevated plumes by adding a vertical velocity w to each particle trajectory. This velocity component is chosen so that 1) the average of w over all the trajectories and heights is zero, 2) updraft particles possess a higher velocity than downdraft particles (about 1.5 higher), and 3) each particle is allowed to jump from an updraft to a downdraft and vice versa with probabilities that depend upon the time scales of the two phenomena.

Figure 5-2 shows the comparison between the ground-level concentrations obtained by MC-LAGPAR with the above assumptions and results of the water-tank experiments by Willis and Deardorff (1981). The ability of MC-LAGPAR to simulate a complex experiment with relatively simple and physically reasonable assumptions is encouraging.

### 5.2.2 The Linkage of MC-LAGPAR With a Prognostic Meteorological Model

We propose a two-phase research project aimed at developing a suitable linkage between the MC-LAGPAR particle model and a prognostic meteorological model, such as SIGMET or other models.

- Phase 1. In this phase, the existing models, a prognostic meteorological model (such as SIGMET or the meteorological models of Bornstein et al., 1985, and Pielke et al., 1983), and the MC-LAGPAR particle

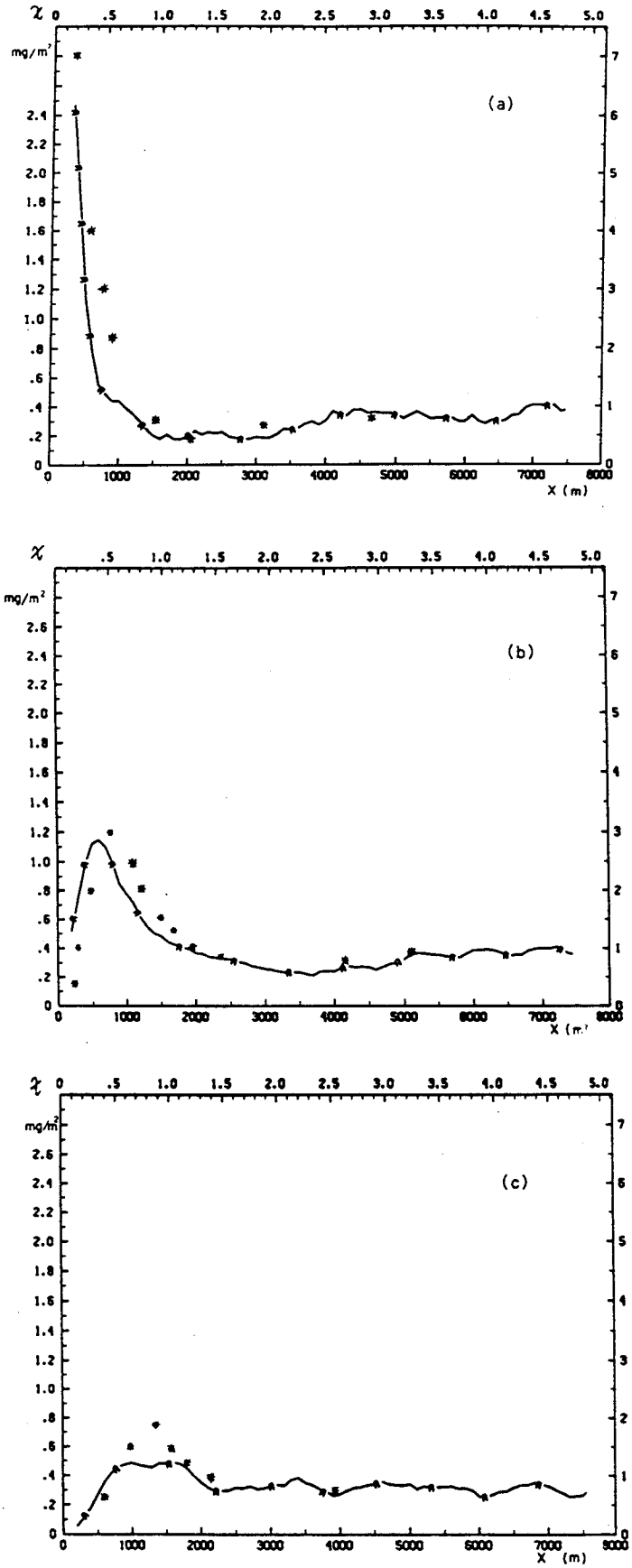


FIGURE 5-2. Ground level concentration from an elevated source in convective conditions. MC-LAGPAR simulations (*) with 3000 particles and water-tank results (continuous curve) with three different source height/mixing height ratios: (a) = 0.067; (b) = 0.24; and (c) = 0.49 (from Brusasca et al., 1986).

model will be used as they are (or with relatively small modifications). We will perform theoretical and numerical investigations and tests aimed at the correct linkage of Eulerian and Lagrangian approaches. This preliminary linkage will be tested against selected data bases (i.e., available tracer experiments).

- Phase 2. Based on the investigations and results of Phase 1, we will implement a new linkage of the selected modeling techniques. It will consist of a modular software product with well-documented routines and will incorporate the modifications and improvements derived from the tests performed during Phase 1. Finally, a new test on a new data base will be made in order to evaluate the performance of the software product with data different from those used to calibrate it. A comprehensive final report will be provided at the end of Phase 2. This report will include a well-documented user's manual describing the developed computer routines.

By linking meteorological and dispersion models, we mean, at minimum, the establishment of a connection between the two that allows the dispersion model to fully use the complex three-dimensional time-varying meteorological information provided by the meteorological model (e.g., the wind field). A real linking process, however, requires the definition and implementation of a theoretical interface between the two models. This interface should properly elaborate the Eulerian output of the meteorological model. This elaboration should not be limited to the analysis of the mean wind field produced by the meteorological model, but should also perform a "translation" of turbulence properties in which the Lagrangian turbulence statistics required by the dispersion model are estimated correctly. Several theoretical and practical difficulties need to be overcome in order to define, implement, test and evaluate this modeling link. The main objective of this project aims at solving these difficulties.

The work to be performed during the two phases described above is discussed in more detail below.

### 5.2.3 Work Plan for Phase 1

Phase 1 research activities will be developed through the following four tasks:

- Task 1. Literature review. We will review the most recent articles in the field of Monte-Carlo particle modeling and Eulerian-Lagrangian representation of atmospheric dispersion phenomena (e.g., van Dop et al., 1985; Thomson, 1986; DeBaas et al., 1986; Etling et al., 1986). The literature review will include the analysis of the important recent developments achieved by using stochastic differential equations (Schuss and Zeev, 1980). As discussed by Melli (1982), Legg and Raupach (1982), and Gifford (1982), Monte-Carlo models are connected with the theory of stochastic differential equations, and each Monte-Carlo scheme can be seen as a particular solution of a system of such equations. Melli (1982) also shows that, starting from the basic equations describing particle motion under the action of both deterministic and stochastic forces, Lagrangian models are finite difference approximations of a set of stochastic differential equations. Additional consideration of this subject is also provided by Melli and Spirito (1983), who show the effects of using random terms different from the usual white noise and indicate the stochastic differential equations capability of representing both Eulerian spatially correlated random fields and Lagrangian time-correlated random particle fluctuations.

  While the main purpose of this literature review is to improve our understanding of Eulerian-Lagrangian relations, we will pay particular attention to the theory of stochastic differential equations and their use to simulate dispersion processes. In particular, we will not limit our literature search to the publications in atmospheric sciences. Research performed in other fields (e.g., hydrology) can provide much insight to our air quality investigations.

o Task 2. Definition of computational algorithms. Based on the literature review in Task 1 and our analysis of the collected material, we will develop a comprehensive theoretical and numerical approach based on a set of computational modules. The analytical and numerical structure of each module will be defined and documented. Among the major problems we expect to investigate are:

- The correct theoretical derivation of the Lagrangian meteorological input required by Monte-Carlo Lagrangian models from meteorological measurements and from the output of an Eulerian meteorological model. We will perform this theoretical derivation based on what we find in the Task 1 literature search and our interpretation of it.

- The treatment not only of the auto-correlation of the wind fluctuations but also of their cross-correlation. Our approach will be based, at least at the beginning, on the review and test of the numerical scheme developed by Zannetti (1986). This new Monte-Carlo method allows the treatment of all three cross-correlation terms in a generic reference system. (Other methods treat only the negative correlation between along-wind and vertical fluctuations and, therefore, need to operate in a special reference system having the x-axis along the main wind direction; this complicates the calculations, which, to be correct, would require a change of the direction of the x-axis at different altitudes.)

- The incorporation of vertical wind velocity fluctuations with a skewed distribution (as in, for example, Baerentsen and Berkowicz, 1984; DeBaas et al., 1986; and Brusasca, et al., 1986). We have recently obtained encouraging results (Brusasca et al., 1986 and 1987) on which we will base our initial approach. Relatively simple Monte-Carlo techniques applied to the vertical velocity w of each particle allow realistic simulation of the behavior of convective cells in unstable atmospheric conditions

(see Figure 5-2). Our approach will involve further investigating and testing this methodology and comparing its outputs with water-tank experiments.

- The problems related to the incorporation of a standard deviation $\sigma_w$ of vertical wind fluctuations that is dependent upon the altitude z. This incorporation has often created numerical simulation problems, with seemingly inaccurate mass accumulation effects in layers with lower $\sigma_w$ (e.g., near the ground). In order to avoid this phenomenon, semi-empirical correction factors have been proposed by Diehl et al. (1982), Wilson et al. (1981), and Legg and Raupach (1982). Some contradictions among these semi-empirical approaches have been investigated by Wilson et al. (1983). In our numerical experiments, we have not found mass accumulation a problem, and our preliminary analyses seem to show that, using a correct random number generator and similarity theory profiles (such as those suggested by Hanna, 1982), ground-level concentrations are qualitatively and quantitatively correct (Brusasca et al., 1986 and 1987). Our approach will be to further test our assumptions in order to fully clarify if and when unrealistic mass accumulation effects can be produced.

o Task 3. Numerical implementation and test. The algorithms defined in Task 2 will be organized into a prototype computer program. This program will be fully modular and will incorporate an available prognostic meteorological model as a separate module. The entire approach will be tested, in both a qualitative and a quantitative way, against suitable available tracer experiments. This test will allow a preliminary verification and evaluation of the linkage developed in Task 2.

### 5.2.4 Work Plan For Phase 2

Phase 2 activities cannot be discussed in the same detail as Phase 1 activities. In fact, Phase 2 studies, approaches and strategies will depend strongly upon Phase 1 results. In general, however, based on our present knowledge, Phase 2 research activities will be developed through the following task :

- o Task 5. Definition and Implementation of a New Theoretical Linkage. This new linkage between advanced meteorological models and particle models will be based on the investigations and results of Phase 1.

- o Task 6. Definition and Implementation of a Modular Software Product. The new linkage defined in Task 5 will be implemented in a software version that will be computationally efficient, well structured and fully modular. Our approach will be to use, as much as possible, modules from existing software and, therefore, to minimize computer programming effort. Most of the programming activity will involve the creation of suitable interfaces between available software modules derived from existing meteorological and particle models. All routines will be written in standard FORTRAN 77 language.

- o Task 7. Model Validation and Testing. The new modeling linkage developed in Task 6 will be tested and validated against suitable tracer experiments. The selected validation days will be different from those used for the Phase 1 calibration/validation exercise. This validation will focus on both the model's ability to simulate the entire concentration field and its capability of properly evaluating maximum ground-level concentration impacts from elevated sources.

- o Task 8. Final Report and User's Manual. A comprehensive final report will be prepared. In order to facilitate the transferability of the software developed during the project, a well-documented user's manual will be also prepared.

### 5.2.5 Expected Difficulties

Several difficulties are expected to be encountered during this research study. Several of them have been mentioned before: for example, the need to correctly link the Eulerian and Lagrangian approaches. This is the key issue in our proposed study and deserves more discussion.

Meteorological models can provide inputs to dispersion models in the form of the average wind field and atmospheric turbulence parameters. In this case, however, the "turbulence" in the dispersion model represents the portion of atmospheric motion that is not explained by the average wind field simulated by the meteorological model. In other words, the more accurate (in space and time) our estimate of the wind field by the meteorological model, the lower the turbulent diffusion intensities in the dispersion models.

In mathematical notation, the wind vector $\mathbf{V}(x, y, z, t)$ can be expressed as

$$\mathbf{V} = \bar{\mathbf{u}} + \mathbf{u}' \qquad (5\text{-}2)$$

in which $\bar{\mathbf{u}}$ represents the large portion of the flow that is resolvable using meteorological models and $\mathbf{u}'$ is the remaining unresolvable component. Clearly, the better the meteorological model, the higher the time- and space-resolution of the term $\bar{\mathbf{u}}$ and the smaller the $\mathbf{u}'$ values.

This interpretation of Eq. 5-2 is very important since it is often used to indicate an intrinsic property of the atmospheric motion (average term plus turbulent fluctuation) instead of the above definition of resolvable and unresolvable component. In our case, the actual performance of the meteorological model, and not the intrinsic properties of the flow, affects the magnitude of $\bar{\mathbf{u}}$ and $\mathbf{u}'$.

This interpretation is a key issue in understanding the turbulent concentration diffusion terms $\langle c'\mathbf{u}' \rangle$, which are often approximated, using K-theory, by

$$\langle c'\mathbf{u}' \rangle = -\mathbf{K} \nabla \langle c \rangle \qquad (5\text{-}3)$$

where **K** is a 3 x 3 turbulent diffusivity tensor. From the previous definition of **u'**, it is clear that the better the meteorological model providing $\bar{\mathbf{u}}$, the lower the $|\langle c'\mathbf{u}'\rangle|$ terms and, consequently, the lower the magnitude of the elements of **K**. In other words, we derive the important conclusion that the eddy diffusion coefficients to be used in a diffusion model are a function of the degree of performance of the meteorological model used to calculate the meteorological input to the dispersion model. Naturally, the same considerations developed above for a K-theory model apply to a Monte-Carlo dispersion model.

The above discussion illuminates a key difficulty of the proposed study, i.e., the necessity of implementing a Lagrangian scheme that describes not atmospheric turbulence per se, but that portion of atmospheric motion that is not explained by the meteorological model. This key issue has not been properly identified, to the best of our knowledge, in past and current model development studies and, therefore, our approach will be to investigate it theoretically and numerically and, we hope, to provide a satisfactory method to handle it.

### 5.3 Analysis and Simulation of Concentration Fluctuations

Several atmospheric dispersion studies (e.g., odor studies and simulations of battlefield scenarios) require the simulation of instantaneous concentrations or semi-instantaneous concentrations (e.g. 15-second averages), or, at least, the probability density function of the concentration in each point of the computational domain for different averaging times. (Clearly, if a model can correctly simulate instantaneous concentrations, the probability density function can always be computed, but not vice versa.)

Several studies (e.g., Hanna, 1984 and 1986) have been performed on the analysis of the properties of concentration fluctuations. We propose to continue these research efforts using particle modeling and Monte-Carlo techniques as a numerical tool to investigate concentration fluctuations and simulate, in a deterministic way, the probability density function of the concentration field.

## 6. REFERENCES


Bach, W.D., Jr. (1984): Aerosol dispersion in the atmospheric surface layer. Boundary-Layer Meteor. 28:409-412.

Baerentsen, J.H., and R. Berkowicz (1984): Monte-Carlo simulation of plume dispersion in the convective boundary layer. Atmos. Environ., 18:701-712.

Bankoff, S.G., and E.L. Hanzevack (1975): The adaptive filtering transport model for prediction and control of pollutant concentration in an urban airshed. Atmos. Environ., 9:793-808.

Benkley, C.W., and A. Bass (1979): Development of mesoscale air quality simulation models. Volume 3. User's Guide to MESOPUFF (Mesoscale Puff) model. EPA 600/7-79-XXX, Research Triangle Park, NC.

Bornstein, R., S. Klotz, R. Street, U. Pechinger, R. Miller (1985): Modeling the polluted coastal urban environment. Electric Power Research Institute final report, Research Project 1630-13, Palo Alto, CA.

Brusasca, G., G. Tinarelli, P. Zannetti and D. Anfossi (1986): Monte-Carlo simulation of plume dispersion in homogeneous and non-homogeneous turbulence. Presented at ENVIROSOFT 86, Newport Beach, California, November.

Brusasca, G., G. Tinarelli, D. Anfossi, and P. Zannetti (1987): Particle modeling simulation of atmospheric dispersion using the MC-LAGPAR. Environ. Software, 2(3):151-158.

Chan, MW., S.J. Head, and S. Machiraju (1979): Development and validation of an air pollution model for complex terrain application. AeroVironment Technical Paper No. 9559 presented at NATO/CCMS Air Pollution Pilot Study, Rome, Italy.

Davis, R.E. (1982): On relating Eulerian and Lagrangian velocity statistics: single particles in homogeneous flows. J. Fluid Mech. 114:1-26.

DeBaas, A.F., H. van Dop and F.T.M. Nieuwstadt (1986): An application of the Langevin equation for inhomogeneous conditions to dispersion in a convective boundary layer. Quart. J. Roy. Meteor. Soc., 112:165-180.

Desalu, A.A., L.A. Gould and F.C. Schweppe (1974): Dynamic estimation of air pollution. IEEE Transactions on Automatic Control AC-19, pp. 904-910.

Diehl, S.R., D.T. Smith and M. Sydor (1982): Random-walk simulation of gradient-transfer processes applied to dispersion of stack emission from coal-fired power plants. J. Appl. Meteor., 21(1):69-83.

Etling, D., J. Preuss and M. Wamser (1986): Application of a random walk model to turbulent diffusion in complex terrain. Atmos. Environ., 20(4):741-747.

Gifford, F.A. (1981): Horizontal diffusion in the atmosphere: A Lagrangian-dynamical theory. Atmos. Environ., 16:505-512.

Hales, J.M., D.C. Powell, and T.D. Fox (1977): STRAM -- an air pollution model incorporating non-linear chemistry, variable trajectories, and plume segment diffusion. EPA 450/3-77-012. Research Triangle Park, NC.

Hanna, S.R. (1986): Spectra of concentration fluctuations: the two time scales of a meandering plume. Atmos. Environ., 20(6):1131-1137.

Hanna, S.R. (1984): The exponential probability density function and concentration fluctuations in smoke plumes. Boundary-Layer Met., 29:361-375.

Hanna, S.R. (1982): Applications in air pollution modeling. From Atmospheric Turbulence and Air Pollution Modeling, Nieuwstadt and van Dop, Eds. Dordrecht, Holland: Reidel.

Hanna, S.R., G.A. Briggs and R.P. Hosker, Jr. (1982): Handbook on Atmospheric Diffusion. Prepared for Office of Health and Environmental Research, Office of Energy Research, U.S. Department of Energy.

Hino, M. (1974): Prediction of atmospheric pollution by Kalman filtering. Proc., Symp. on Modeling for Prediction and Control of Air Pollution.

Hockney, R.W., and J.W. Eastwood (1981): Computer Simulations Using Particles. New York: McGraw-Hill.

Kalman, R.E. (1960): A new approach to linear filtering and prediction problems. J. Basic Eng., pp. 35-108.

Lamb, R.G. (1969): An air pollution model of Los Angeles. M.S. thesis, University of California, Los Angeles (see Lamb, R.G., and M. Neiburger, 1971: An interim version of a generalized urban diffusion model. Atmos. Environ. 5:239-264).

Legg, B.J., and M.R. Raupach (1982): Markov-chain simulation of particle dispersion in inhomogeneous flows: The mean drift velocity induced by a gradient in Eulerian velocity variance. Boundary Layer Meteor., 24:3-13.

Ley, A.J. (1982): A random walk simulation of two-dimensional turbulent diffusion in the neutral surface layer. Atmos. Environ. 16:2799-2808.

Ludwig, F.L., L.S. Gasiorek, and R.E. Ruff (1977): Simplification of a Gaussian puff model for real-time minicomputer use. Atmos. Environ., 11:431-436.

Melli, P. (1982): Lagrangian modeling of dispersion in the planetary boundary layer of particulate released by a line source. Proc. 13th International Technical Meeting on Air Pollution Modeling and Its Application, Ile des Embiez, France, September.

Melli, P., and A. Spirito (1983): Atmospheric diffusion modelling by stochastic differential equations. 14th International Technical Meeting on Air Pollution Modeling and Its Application, Copenhagen, Denmark, September.

Melli, P., P. Bolzern, G. Fronza and A. Spirito (1981): Real-time control of sulphur dioxide emissions from an industrial area. Atmos. Environ., 15(5):653-666.

Nappo, C.J. (1983): Methods of estimating meteorological representativeness. Fifth Symposium on Meteorological Observations and Instrumentation, Toronto, Ontario, Canada, April.

Nappo, C.J., et al. (1982): The workshop on the representativeness of meteorological observations, June 1981, Boulder, Colorado. Bull. Am. Meteor. Soc., 63 (7):761-764.

Ohmstede, W.D., and E.B. Stenmark (1980): A model for characterizing transport and diffusion of air pollution in the battlefield environment. Reprinted from the Volume of Conference Papers: Second Joint Conference on Applications of Air Pollution Meteorology and Second Conference on Industrial Meteorology, New Orleans, LA, March. Published by the American Meteorological Society, Boston, MA.

Phillips, G.T., and R.M. Traci (1978): A preliminary user guide for the NOABL objective analysis code. SAI Report No. SAI-78-769-LJ; U.S. Department of Energy Report RLO/2440-77-10.

Pielke, R.A., R.T. McNider, M. Segal and Y. Mahrer (1983): The use of a mesoscale numerical model for evaluations of pollutant transport and diffusion in coastal regions and over irregular terrain. Bull. Am. Meteor. Soc., 64:243-249.

Plackett, R.L. (1950): Biometrika, 37:149.

Roberts, J.J., E.S. Croke, and A.S. Kennedy (1970): An urban atmospheric dispersion model. Proc., Symposium on Multiple-Source Urban Diffusion Models. Air Pollution Control Office Publ. No. AP-86, pp. 6.1-6.72.

Sawaragi, Y., T. Soeda, T. Yoshimura, S. Oh, Y. Chujo and H. Ishihara (1976): The predictions of air pollution levels by nonphysical models based on Kalman filtering method. J. Dynamic Sys., Measurement and Control, 98 (12):375-386.

Schuss, Z. (1980): Theory and Applications of Stochastic Differential Equations. New York: John Wiley and Sons.

Sheih, C.M. (1978): A puff pollutant dispersion model with wind shear and dynamic plume rise. Atmos. Environ., 12:1933-1938.

Thomson, D.J. (1986): On the relative dispersion of two particles in homogeneous stationary turbulence and the implications for the size of concentration fluctuations at large times. Quart. J. Roy. Meteor. Soc., 112:890-894.

Tran, K.T., and R.C. Sklarew (1979): User guide to impact: An integrated model for plumes and atmospheric chemistry in complex terrain. Form & Substance, Inc., Westlake Village, CA.

U.S Army Research Office (1983): Program Guide, July 1983. Research Triangle Park, NC 27709.

U.S. Army Research Office (1985): Broad Agency Announcement.

U.S. Environmental Protection Agency (1978): Guideline on air quality models. EPA-450/2-78-025, OAQPS No. 1.2-080.

van Dop, H., F.T.M. Nieuwstadt and J.C.R. Hunt (1985): Random walk models for particle displacements in inhomogeneous unsteady turbulent flows. Phys. Fluids, 28(6):1639-1653.

Wiener, N. (1949): The Extrapolation, Interpolation and Smoothing of Stationary Time Series. New York: John Wiley.

Willis, G.E., and J.W. Deardorff (1981): A laboratory study of dispersion from a source in the middle of the convectively mixed layer. Atmos. Environ. 15:109-117.

Wilson, J.D., B.J. Legg and D.J. Thomson (1983): Calculation of particle trajectories in the presence of a gradient in turbulent-velocity variance. Boundary Layer Meteor., 27:163-169.

Wilson, J.D., G.W. Thurtell and G.E. Kidd (1981): Numerical simulation of particle trajectories in inhomogeneous turbulence, III: Comparison of predictions with experimental data for the atmospheric surface layer. Boundary Layer Meteor., 12:423-441.

Young, P. (1974): Recursive approaches to time series analysis. The Inst. of Math. and its Applic., pp. 209-224.

Zannetti, P., and P. Switzer (1979): The Kalman filtering method and its application to air pollution episode forecasting. Presented at the APCA Specialty Conference on Quality Assurance in Air Pollution Measurement, New Orleans, LA, March.

Zannetti, P. (1981): An improved puff algorithm for plume dispersion simulation. J. Applied Met., 20(10):1203-1211.

Zannetti, P., and N. Al-Madani (1983): Numerical simulations of Lagrangian particle diffusion by Monte-Carlo techniques. Presented at the VIth World Congress on Air Quality (IUAPPA), Paris, France, May.

Zannetti, P. (1986): Monte-Carlo simulation of auto- and cross-correlated turbulent velocity fluctuations (MC-LAGPAR II Model). Environ. Software, 1(1):26-30.

Zannetti, P. (1986): A new mixed segment-puff approach for dispersion modeling. Atmos. Environ., 20 (6):1121-1130.

Zannetti, P., G. Carboni, and R. Lewis (1986): AVACTA II -- User's Guide, Release 3. AeroVironment document AV-OM-85/520.

# APPENDIX A

"A New Mixed Segment-Puff Approach for Dispersion Modeling"
by P. Zannetti

*Atmospheric Environment* Vol. 20, No. 6, pp. 1121–1130, 1986.
Printed in Great Britain.

0004–6981/86 $3.00 + 0.00
Pergamon Journals Ltd.

# A NEW MIXED SEGMENT-PUFF APPROACH FOR DISPERSION MODELING

PAOLO ZANNETTI*
AeroVironment Inc., 825 Myrtle Avenue, Monrovia, CA 91016, U.S.A.

(*First received* 22 *July* 1985 *and received for publication* 19 *November* 1985)

**Abstract**—This paper presents a new mixed methodology for realistic and cost-effective simulation of short-term air quality dispersion phenomena using the Gaussian formula. The method can be applied to short-range, intermediate and, especially, long-range transport simulations. Pollutant dynamics are described by the temporal evolution of plume elements, treated as segments or puffs according to their size. While the segments provide a numerically fast simulation during transport conditions, the puffs allow a proper simulation of calm or low-wind situations.

The methodology is incorporated into a computer package (AVACTA II, Release 3) that gives the user large flexibility in defining the computational domain, the three-dimensional meteorological and emission input, the receptor locations, and in selecting plume rise and sigma formulas. AVACTA II provides both pollutant concentration fields and dry/wet deposition patterns. The model uses linear chemistry and is applicable to any two-species reaction chain (e.g., $SO_2$ and $SO_4^{2-}$) where this approximation is reasonable and an appropriate reaction rate is available.

*Key word index*: Air pollution, Gaussian model, puff model, long-range transport, Lagrangian modeling.

## 1. INTRODUCTION AND OVERVIEW

The development of air quality modeling techniques in the last 20 years has been quite remarkable. With the parallel growth in computational capabilities, it has been possible to define and implement extremely advanced simulation techniques. Nevertheless, in spite of the above improvements and expansions, it has been found that often the more complex methodologies possess only a theoretical (or potential) capability of better representing the complexities of the real world. In fact, recent important model validation studies, such as the Electric Power Research Institute (EPRI) Plume Model Validation and Development (PMV&D) Study (for example, see Liu and Moore, 1984), show that when models are applied in an operational, 'hands off' manner:

1. short-term modeling simulations are substantially inaccurate with errors of a factor of two in more than 50% of the cases;
2. the more complex modeling approaches do not provide a substantial improvement in reproducing reality, compared with the more simple ones.

This behaviour has been recently confirmed by several studies presented at the Department of Energy/American Meteorological Society Model Evaluation Workshop (Kiawah Island, SC, October 1984) in which model outputs have been evaluated against three reliable tracer experiment data bases: MATS (Mesoscale Atmospheric Transport Studies, by the Savannah River Laboratory), PMV&D (Plume Model Validation and Development study, by the Electric Power Research Institute), and ASCOT (Atmospheric Studies in Complex Terrain, by the U.S. Department of Energy).

These results indicate the need of additional air pollution modeling effort for improving the present simulation capabilities and allowing the models to reach that level of performance that is expected from them, especially for regulatory applications since air pollution dispersion models are the only tool for inferring a quantitative deterministic relation between anthropogenic pollutant emissions and ambient concentrations. Future model development efforts should aim at (1) the development and application of more complex and sophisticated methodologies, generally requiring more advanced meteorological information; e.g., particle methods (Zannetti, 1984) or higher order closure techniques (Lewellen and Teske, 1976); and (2) the improvement of the simulation capabilities of relatively simple current techniques, mainly using the available meteorological information.

The modeling discussion presented in this paper aims at the second objective above, and presents a new methodology which is able to simulate complex dispersion conditions in both transport and calm situations while maintaining the simplicity of the basic Gaussian equation. This method is computationally cost effective and allows a non-stationary, non-homogeneous representation of atmospheric phenomena such as transport, turbulent diffusion, dry and wet deposition, and first-order reaction chemistry. This mixed segment/puff approach provides an improved simulation

* Most of this research was performed by the author in the course of consulting activity in 1984 at the Center for Thermal and Nuclear Research (CRTN) of the National Electric Power Industry (ENEL) in Milan, Italy.

tool for practical applications in both short-range and long-range air pollution dispersion studies, in either flat or complex terrain. This methodology seems particularly useful for simulating long-range transport of sulfur species ($SO_2$, $SO_4^{2-}$). Model validation studies are under development and their results will be presented in successive papers.

The most widely applied air pollution models are based on the Gaussian plume equation (for example, Turner, 1970) which, in its simplest form, describes the average steady-state concentration $\chi(\mu g\ m^{-3})$ produced at the receptor $\mathbf{r} = (x_r, y_r, z_r)$ by a single point source at $\mathbf{s} = (0, 0, z_s)$ as

$$\chi = \frac{10^9 Q}{2\pi u \sigma_h \sigma_z} \exp\left[-\frac{y_r^2}{2\sigma_h^2}\right] \exp\left[-\frac{(z_s + \Delta h - z_r)^2}{2\sigma_z^2}\right] \quad (1)$$

where $Q$ is the pollutant emission rate ($kg\ s^{-1}$), $\Delta h$ is the plume rise (m), $u$ is the average wind speed at $z_s$ ($m\ s^{-1}$), and $\sigma_h^*$ and $\sigma_z$ (m) are the horizontal and vertical plume standard deviations at the downwind distance $d = x_r$ (m). The plume rise $\Delta h$ and the standard deviations $\sigma_h$ and $\sigma_z$ can be evaluated from several semi-empirical formulae requiring meteorological and emission information. The positive $x$-axis is chosen to coincide with the average wind direction at $z_s$. The concentration $\chi$ is assumed equal to zero (or to a background value) for negative values of $x_r$.

Equation (1) is often expanded with (1) partial or total reflection terms at the ground and at the top of the mixing layer; (2) exponential reduction terms, for simulating dry/wet deposition and first-order chemical transformation; and (3) particle settling velocity. Moreover, it can be spatially integrated for simulating segment, area, and volume sources. Finally, Equation (1) can be rewritten in a climatological form (for example, Martin, 1971) for simulating long-term concentration averages using the combined frequency distribution of the major meteorological variables, such as wind speed, wind direction and atmospheric stability.

This steady-state formulation, however, is valid only during transport conditions (for example, $u \geq 1\ m\ s^{-1}$) in fairly stationary and homogeneous situations. In order to remove these limitations, while still maintaining the simplicity of the Gaussian approach, two dynamic methods have been developed:

1. the segmented plume model (for example, Hales *et al.*, 1977; Benkley and Bass, 1980; Chen *et al.*, 1979), which, however, still requires transport conditions;
2. the puff model (for example, Lamb, 1969; Roberts *et al.*, 1970), which can theoretically work in calm or low-wind conditions.

Both methods break the plume into independent elements (segments or puffs) whose initial features and dynamics are a function of local time-varying emissions and meteorological conditions. Therefore, they are able to simulate non-stationary and non-homogeneous dispersion conditions.

Segments are sections of a Gaussian plume. Each segment generates a concentration field which is still basically computed by Equation (1), and represents the contribution of the entire virtual plume passing through that segment, as illustrated in Fig. 1. Therefore, only one segment (the closest) affects the concentration computation at each receptor, although the occurrence of 180° wind direction changes can create particular conditions where the contribution of two segments (that is, two virtual plumes) should be superimposed at some receptors.

Puff models, on the other hand, generate a concentration field $\chi(\mu g\ m^{-3})$, which is always produced by superimposing the contribution of each single puff, given by the basic formula

$$\chi = \frac{10^9 M}{(2\pi)^{3/2}\sigma_h^2 \sigma_z} \exp\left[-\frac{(x_p - x_r)^2}{2\sigma_h^2}\right] \times \exp\left[-\frac{(y_p - y_r)^2}{2\sigma_h^2}\right] \exp\left[-\frac{(z_p - z_r)^2}{2\sigma_z^2}\right] \quad (2)$$

in which $M$ is the mass (kg) of pollutant of the puff whose center is located at $\mathbf{p} = (x_p, y_p, z_p)$ and whose standard deviations (m) are $\sigma_h$ in the horizontal and $\sigma_z$ in the vertical. As with Equation (1), Equation (2) is often expanded with reflection and deposition terms. Note that Equation (2) differs from Equation (1) mainly because the transport term is replaced by an extra horizontal diffusion term with the consequent disappearance of the wind speed $u$. In a puff model, the wind speed affects the concentration computation only by controlling the density of puffs in the region (that is, the lower the wind speed, the closer a puff is to the next one generated by the same source), and not directly through Equation (2). Therefore, at least in theory, a puff model can handle calm or low-wind conditions. This approach represents an advanced and powerful application of the Gaussian formula.

Several studies have discussed in detail the puff modeling approach, improving its application features. In particular, (1) algorithms were proposed and evaluated for incorporating wind shear effects (Sheih, 1978); (2) virtual distance (Ludwig *et al.*, 1977) and virtual age (Zannetti, 1981) computations were defined for correctly evaluating the $\sigma_h$ and $\sigma_z$ dynamics of the puff; (3) puff merging (Ludwig *et al.*, 1977) or puff splitting (Zannetti, 1981) were incorporated for performing cost-effective simulations with relatively large $\Delta t$ (for example, 5–10 min); and (4) an empirical method was derived (Zannetti, 1981) for evaluating the puff's $\sigma_h$ and $\sigma_z$ growth during calm or low-wind conditions as a function of currently available $\sigma$ functions during transport conditions (this method is presented and expanded in Appendix A).

Numerically correct applications of the puff model are computationally more expensive than those using

*Often $\sigma_h$ is referred to as $\sigma_y$.

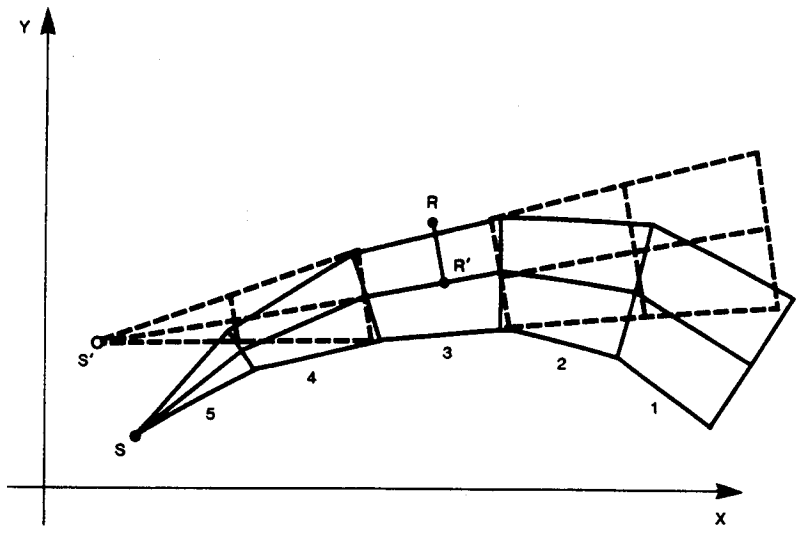


Fig. 1. Computation of the concentration at the receptor $R$ generated by the segmented plume (solid lines). The computation is performed by evaluating the contribution of the virtual plume (dotted lines) from the virtual source $S'$ passing through the closest segment (number 3) to the receptor $R$.

the segmented approach. In fact, a sufficient number of puffs must be generated so that the continuous plume is represented with enough accuracy by the superimposition of several puffs' contributions. For receptors close to the source this may require the generation of a new puff every few seconds. The puff computational cost is justified only when the extra capabilities of the puff approach are required; that is (1) during low-wind conditions which segments cannot handle, and (2) when different sections of the same plume affect a receptor, a situation which is treated in a straightforward way by the puff model, but which requires complex geometrical investigations with the segmented approach. In other cases, for example in common transport conditions, the segmented model is computationally faster and equally accurate.

This paper presents a mixed segment–puff numerical technique aiming at the joint utilization of both approaches, in a way which is both consistent with the physics of the atmospheric dispersion phenomena and computationally efficient. This method is implemented into a new version (Release 3) of the AVACTA II air quality diffusion package. This numerical method is described in section 2, while section 3 presents some details of puff/segment concentration computation. Finally, section 4 summarizes the general features of the AVACTA II computer package. Two appendices are included at the end of the paper. Appendix A describes a methodology for evaluating the $\sigma_h$ and $\sigma_z$ growth during calm or low-wind conditions, while Appendix B presents a preliminary comparison between AVACTA II outputs and (1) concentrations computed using the standard Gaussian steady-state equation; (2) $SF_6$ tracer diffusion experiments.

## 2. THE SEGMENT/PUFF APPROACH

This new approach is a dynamic one, in which each plume is described by a series of 'elements' (segments or puffs) whose characteristics are updated at each 'dispersion' time interval $\Delta t$ (for example, 5–10 min). Meteorological three-dimensional fields (wind and turbulence status) and emission parameters are allowed to change at each 'meteorological' time step $\Delta t_m$ (typically, 30–60 min). The dynamics of each element consist of (1) generation at the source; (2) plume rise; (3) transport by advective wind; (4) diffusion by atmospheric turbulence; (5) ground deposition, dry and wet; and (6) chemical transformation, creating secondary pollutant from a fraction of the primary pollutant. The type of element (segment or puff) does not affect its dynamics, but only the computation of the concentration field, which is discussed in section 3.

Each element is characterized by the following time-varying parameters (see the example in Fig. 2) evaluated at its final central point B:

| | |
|---|---|
| $\mathbf{e} = (x_e, y_e, z_e)$ | coordinates (m) of the point B; |
| $h_e$ | elevation (m) of B above the ground (in flat terrain $h_e = z_e$); |
| $M_1, M_2$ | masses of primary and secondary pollutant (kg); |
| $\sigma_h, \sigma_{z1}, \sigma_{z2}$ | standard deviations (m) of the Gaussian concentration distribution: horizontal, vertical below B, and vertical above B, respectively. |

The characteristics of each element's initial central point $A$ at time $t$ are equal to those, at the same time $t$,

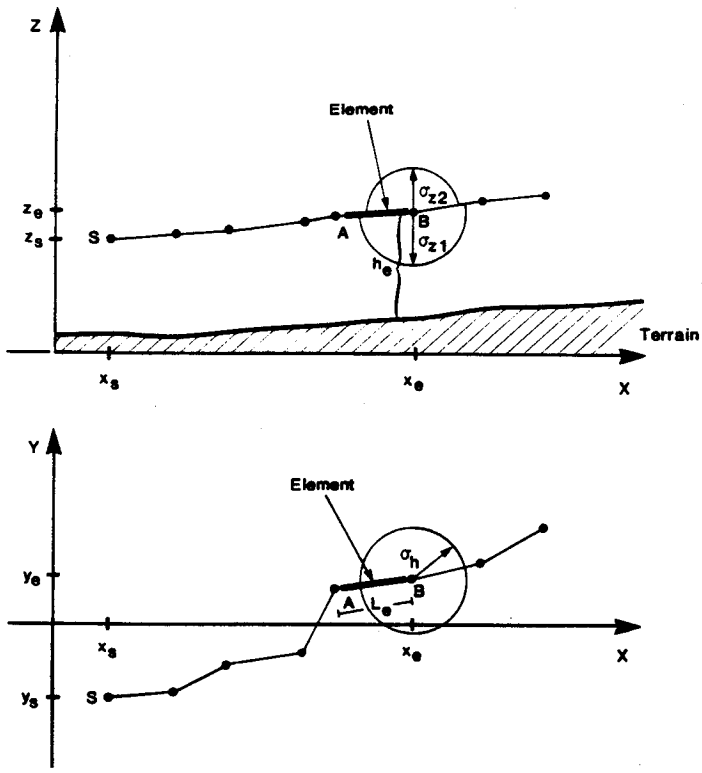


Fig. 2. Chain of elements from the source $S$ at time $t$. The time-varying parameters of a selected element in the chain are illustrated.

of the final central point of the element successively emitted from the same source.

### 2.1. *Generation of plume elements*

At each time interval $\Delta t$, a new element is added to the element 'chain' from each source. The parameters defining each new element have the following initial values: the central final point is set at the source's exit point plus the vertical plume rise $\Delta h$; $M_1 = Q_1 \Delta t$, $M_2 = Q_2 \Delta t$, where $Q_1$ and $Q_2$ are the current emission rates of primary and secondary pollutants (generally $Q_2 = 0$); and $\sigma_h$, $\sigma_{z1}$ and $\sigma_{z2}$ represent the initial $\sigma$s of the plume (for example, 0.369 multiplied by the source exit diameter may be chosen for $\sigma_h$, and $\Delta h/3.16$ for $\sigma_{z1}$ and $\sigma_{z2}$).

### 2.2. *Transport*

At each time interval $\Delta t$, the central final point of each existing element is advected according to the current wind vector $\mathbf{u} = (u_x, u_y, u_z)$ averaged over the volume covered by the element size (i.e. $\pm 2\sigma$), as follows

$$\mathbf{e}^{(\text{new})} = \mathbf{e}^{(\text{old})} + \mathbf{u}\,\Delta t. \tag{3}$$

However, if the horizontal transport term

$$u_h = (u_x^2 + u_y^2)^{1/2} \tag{4}$$

is less than a critical value $u_{min}$ (for example, $u_{min} = 1\ \text{m s}^{-1}$), $u_x$ and $u_y$ are forced to zero since it is assumed that such small terms represent more local intermittent effects than actual transport. In this case, however, a large horizontal diffusion may be produced by the large wind direction fluctuations typically encountered during these low wind speed situations (see the next section).

Moreover, the computerized version of this algorithm includes special user-supplied controls on $z_e$ for avoiding unreasonably large variations of $h_e$, either in complex terrain simulations or during situations characterized by large $u_z$ values. In fact, the program's user can optionally keep the relative variation of $h_e$, at each computational time step, within fixed limits.

### 2.3. *Diffusion*

During each $\Delta t$ the element's $\sigma$s are increased based on the virtual distance/age concept (Ludwig *et al.*, 1977; Zannetti, 1981) which operates for either $\sigma_h$, $\sigma_{z1}$ or $\sigma_{z2}$, according to the following scheme, whose semi-empirical justification is presented in Appendix A,

1. select the current $\sigma$ function $\sigma = \sigma(d)$ for the element ($d$ is the downwind distance) according to the current local meteorology at the element's location; that is, the average atmospheric turbulent status* in the volume covered by the element size;

*The atmospheric turbulence status is often simply represented by a 'stability' class, a discrete number.

2. evaluate the virtual distance $d_v$ such as

$$\sigma^{(old)} = \sigma(d_v) \quad (5)$$

where $\sigma^{(old)}$ is the current $\sigma$ value for the element. The computation in Equation (5) is straightforward for some $\sigma$ formulas (for example, power laws), but requires iterative procedures for others;

3. if $u_h < u_{min}$ force $u_h = u_{min}$;
4. increment $\sigma$ by

$$\sigma^{(new)} = \sigma(d_v + u_h \Delta t). \quad (6)$$

The above dynamics of the $\sigma$s depend upon the choice of the $\sigma$ function and the current atmospheric turbulence status at the element's location. A separate turbulence status can be considered for the computation of horizontal ($\sigma_h$) and vertical ($\sigma_{z1}$, $\sigma_{z2}$) increments, if a proper meteorological input is available. For example, the temperature vertical gradient might provide an evaluation of the 'vertical' turbulence status, while the horizontal wind direction fluctuation intensity provides a good estimate of the 'horizontal' turbulence status. (It must be pointed out that, without the measurement of the horizontal wind direction fluctuation, the estimate of the 'horizontal' turbulence status may be quite wrong and provide horizontal diffusion rates that are much lower than the actual ones.) Different values of the vertical turbulence status above and below the element center generate different dynamics for $\sigma_{z1}$ and $\sigma_{z2}$.

In the software implementation of the above diffusion algorithms, several options are provided to the user for computing the dynamics of the $\sigma$s (e.g., the growth of $\sigma_{z1}$ and $\sigma_{z2}$ may be restricted after the plume becomes well mixed through the boundary layer).

### 2.4. *Dry and wet deposition*

Both dry and wet deposition for the primary and secondary pollutants are simulated by first-order reaction schemes and are computed during each $\Delta t$ (s) by an exponential reduction of the pollutant mass (kg)

$$M_i^{(new)} = M_i^{(old)} \exp[-P_{i,j}\Delta t/360{,}000] \quad (7)$$

where $i$ indicates the primary ($i = 1$) or the secondary ($i = 2$) pollutant, $j$ indicates dry ($j = 1$) or wet ($j = 2$) deposition, and $P_{i,j}$ is the corresponding percentage of reduction per hour ($\%\,h^{-1}$). All mass differences $M_i^{(old)} - M_i^{(new)}$ are deposited and accumulated on the ground.

If the two $P_{i,1}$ are not directly specified as input values, they can be obtained from the deposition velocity values as

$$P_{i,1} = 360{,}000\, V_i/\Delta z_e \quad (8)$$

where $V_i$ are the current deposition velocities ($m\,s^{-1}$) at element's location, and $\Delta z_e = (2\sigma_{z1} + 2\sigma_{z2})$ is the vertical thickness (m) of the element. Equation (8) applies only when the plume has reached the ground (that is, $2\sigma_{z1} \geqslant h_e$), otherwise $P_{i,1} = 0$.

If the two $P_{i,2}$ are not directly specified as input values, they can be obtained (Draxler and Heffter, 1981) from precipitation data as

$$P_{i,2} = S_i P_r/(10 T_p) \quad (9)$$

where $S_i$ are the pollutant scavenging ratios, $P_r$ is the current average precipitation rate at element's location ($mm\,h^{-1}$), and $T_p$ is the thickness (m) of the precipitation layer.

In the software implementation of the above deposition algorithm the parameters $P_{i,j}$ and the precipitation rate $P_r$ are allowed to vary with time and space.

### 2.5. *Chemical transformation*

During each $\Delta t$ (s), a first-order chemical reaction scheme is adopted, in which the chemical transformation term reduces the mass $M_1$ of primary pollutant and increases the mass $M_2$ of secondary pollutant in each element according to

$$M_1^{(new)} = M_1^{(old)} \exp(-k\Delta t/360{,}000) \quad (10a)$$

$$M_2^{(new)} = M_2^{(old)} + (w_2/w_1) M_1^{(old)} \times [1 - \exp(-k\Delta t/360{,}000)] \quad (10b)$$

where $k$ is the current chemical transformation factor at the element location expressed as a percentage of reduction per hour ($\%\,h^{-1}$), and $w_i$ are the pollutant molecular weights ($i = 1, 2$).

## 3. CONCENTRATION COMPUTATION

As discussed in the previous section, plume element dynamics can be computed independently from the type of element (segment or puff). The element type however is a key factor in computing the plume concentration field during each $\Delta t$. The criterion for identifying the type of element is the ratio between its length $L_e$ (the horizontal distance between $A$ and $B$ in Fig. 2) and $\sigma_h$. For a segment

$$L_e/\sigma_h > 2 \quad (11a)$$

and, for a puff,

$$L_e/\sigma_h \leqslant 2 \quad (11b)$$

where the center of the puff is located in the middle between $A$ and $B$. Since $\sigma_h$ continues to grow with time, all segments will eventually become puffs.

The above algorithm assures that, when segments are transformed into puffs, the distance between two consecutive puffs will not be greater than $2\sigma_h$, which is the condition required (Ludwig *et al.*, 1977) for a series of puffs to provide an almost perfect representation of a continuous plume. In calm or low wind speed conditions, $L_e = 0$ and puffs are generated directly from the source.

The above scheme allows a realistic and computationally efficient representation of calm, transport and transitional cases. For example, puffs can accumulate for a few hours in the region near the source during calm conditions, and then be subsequently

advected downwind when the stagnation breaks up. The concentration at each receptor point $R$ due to a certain source $S$ must account for the contribution of all elements generated from $S$; specifically, the sum of the contributions of all existing puffs plus the contribution of the closest segment. This allows a proper dynamic representation of both calm and transport conditions, including the previously mentioned situation in which, due to a 180° change in wind direction, two sections of the same plume may affect the same receptor. In this latter case, in fact, we can generally assume that the elements of the oldest section of the plume have already become puffs, thus allowing both sections of the plume to contribute to the concentration computation at that receptor.

### 3.1. *Puff contribution*

The concentration contribution of a single puff at a receptor $R$ during each $\Delta t$ is basically computed by Equation (2), which allows the computation of the primary pollutant concentration $\chi_1$ (or the secondary one $\chi_2$) from the current values of the puff's variables $M_1$ (or $M_2$), $\sigma_h$, $\sigma_{z1}$ (or $\sigma_{z2}$ if $R$ is above the center of the puff), evaluated by interpolation at the center of the puff, that is the point between its initial and final central points. (It must be remembered that only if the puff has been generated during calm or low-wind conditions, that is, with $u_h = 0$, will its final and initial points coincide.) In the example of Fig. 2, the selected element is indeed a puff since $L_e < 2\sigma_h$, and its central point $\mathbf{p} = (x_p, y_p, z_p)$ is located in the middle between $A$ and $B$.

### 3.2. *Segment contribution*

Because of the condition defined in Equation (11a) each segment has sufficient length $L_e$ to assure that horizontal 'stream-wise' diffusion (that is, diffusion along the length of the segment) can be neglected in comparison with the transport term. This is one of the basic assumptions for Equation (1), which is used as the numerical algorithm for computing the concentration field due to a plume segment. This computation requires the identification of the segment closest to the receptor $R$ and the utilization of the segment's variables for computing, using basically Equation (1), the concentration field generated by the equivalent plume passing through the segment, as illustrated in Fig. 1. The parameters in Equation (1) are evaluated in the following way:

1. segment's variables ($M_1$, $M_2$, $\sigma_h$, $\sigma_{z1}$, $\sigma_{z2}$) are interpolated at the point $R'$ (see Fig. 1), the closest point to $R$ along the segment centerline;
2. $Q$ is evaluated as a virtual current emission rate; that is, $Q = M_1/\Delta t$ (or $M_2/\Delta t$);
3. $u$ is evaluated as a virtual current wind speed; that is, $u = L_e/\Delta t$ (however, $u$ is forced to be $\geqslant u_{min}$ to avoid unrealistic 'convergence' effects);
4. $\sigma_{z2}$ is used instead of $\sigma_{z1}$ if the receptor $R$ is above the point $R'$.

Naturally, only the closest segment is used since its contribution surrogates that of the entire segmented portion of the plume.

### 3.3. *The treatment of the segment–puff transition*

The concentration computation described in the previous section allows the incorporation of all the

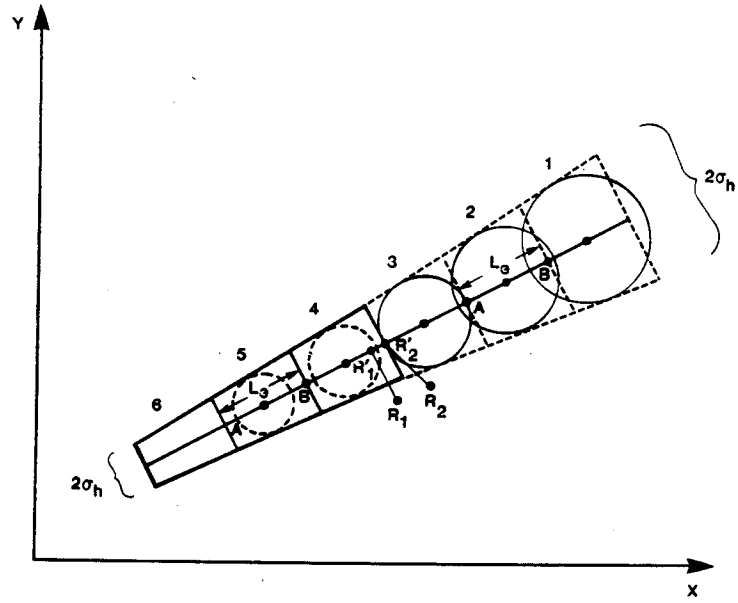


Fig. 3. Chain of elements and special treatment of the transition segment–puff. The contribution of the puffs 2 and 3 is eliminated for computing the concentration in $R_1$. The two segments 4 and 5 are transformed into puffs for computing the concentration in $R_2$.

advantages of both the puff and the segmented approach. Numerical problems, however, arise when the receptor is close to the point in the plume at which segments grow into puffs. In this case (see Fig. 3), care must be taken to avoid an inappropriate overevaluation of the concentration, since the concentration produced by the closest segment surrogates the effect of both the preceeding segments (elements 4, 5 and 6) and the following puffs (elements 1, 2 and 3).

The correct numerical treatment of this case requires the following operations for computing the concentration field:

1. if, during $\Delta t$, a segment becomes a puff (or vice versa), the element is treated as a puff;
2. in the case of receptor $R_1$ in Fig. 3, the contribution of the two puffs preceeding or following the closest segment is eliminated (unless the puffs have $L_e \leqslant \sigma_h/5$, which practically means that they have been generated in calm conditions; in this latter case their contribution is not eliminated);
3. in the case of receptor $R_2$ in Fig. 3, the closest segment and the segment eventually adjacent to it are treated as puffs.

Numerical tests have been performed which have shown that the above algorithms produce a 'smooth' concentration field, in which segment–puff transitions do not reduce the accuracy of the simulation.

### 3.4. *Splitting of elements*

The breaking of a plume into elements allows the evaluation of their dynamics as a function of the local time-varying meteorological conditions. In particular, during each $\Delta t$, the final central point of each element moves from an old to a new position. The horizontal

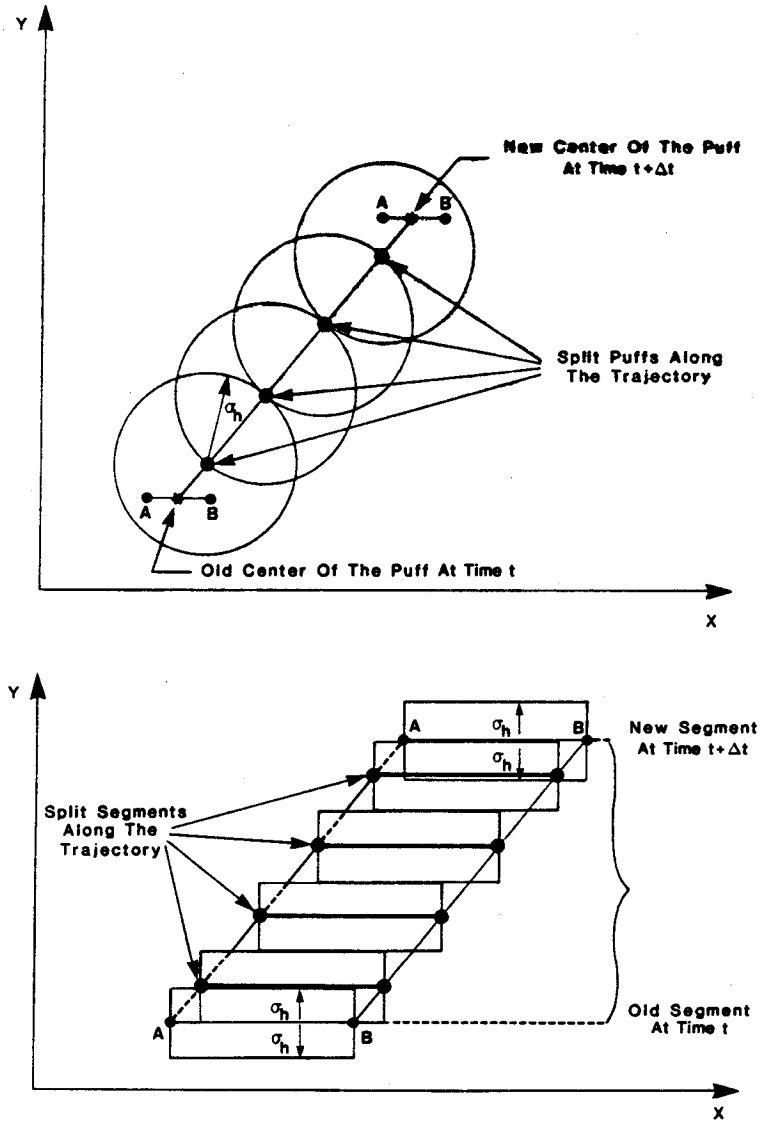


Fig. 4. Splitting process for a puff (above) and a segment (below). *A* and *B* again represent the initial and final central point of the element.

component of this advective displacement is

$$\Delta \mathbf{d}_h = \mathbf{u}_h \Delta t \quad (12)$$

where $\mathbf{u}_h = (u_x, u_y)$ is the current local horizontal wind vector.

Large $|\Delta \mathbf{d}_h|$, due to an increase in wind speed or associated to a change in wind direction, may affect the elements' ability to represent the continuous plume by reducing resolution. The splitting technique, which was originally proposed for puff modeling simulations (Zannetti, 1981), is here incorporated for both puffs and segments and is illustrated in Fig. 4. This splitting generates, when required, a sufficient number of fictitious elements along the element's trajectory during $\Delta t$ to maintain sufficient resolution. The splitting of an element's trajectory is performed for computing its concentration contribution at receptor $R$ when (1) the receptor $R$ is affected by that element, and (2) for puffs, when $|\Delta \mathbf{d}_h| > \sigma_h$ and, for segments, when $|\Delta \mathbf{d}_t| > \sigma_h$, where $\Delta \mathbf{d}_t$ is the component of $\Delta \mathbf{d}_h$ that is transverse to the segment's centerline.

In this splitting computation the masses $M_1$ and $M_2$ of the element are equally distributed among the split elements along the trajectory from the old position to the new one.

## 4. THE AVACTA II COMPUTER PACKAGE

The methodology described in the previous sections has been incorporated into a computer program by expanding and re-structuring the Gaussian segmented package AVACTA II (Chan and Tombach, 1978; Zannetti *et al.*, 1981). The new version (Release 3) of the AVACTA II code incorporates the presented algorithms and, moreover, gives the user large flexibility in (1) defining the computational domain, the three-dimensional meteorological and emission input, and the receptor locations; and (2) selecting plume rise formulae, the $\sigma$ functions and other options. Without explicit user's specifications, standard default values and assumptions are used.

The program is mainly designed for simulating air quality impact from point sources. However, due to its capability of treating sources with an initial $\sigma_h, \sigma_{z1}, \sigma_{z2}$, AVACTA II can also be correctly used for area and volume sources.

A full description of the AVACTA II software can be found in the user's manual (Zannetti *et al.*, 1985b). The major user's options currently implemented in AVACTA II allow the following:

a. selection of one of the following plume rise formulae:
   1. Briggs (Stern, 1976)
   2. CONCAWE (Stern, 1976)
   3. Lucas-Moore (Moore, 1974)
   4. $\Delta h$ subroutine provided by the user;
b. selection of one of the following $\sigma_z$ functions:
   1. Pasquill–Gifford–Turner (in the functional form specified by Green *et al.*, 1980)
   2. Brookhaven (Stern, 1976)
   3. Briggs, open country or urban (Gifford, 1976)
   4. LO-LOCAT (MacCready *et al.*, 1974)
   5. $\sigma_z$ interpolated from user's values specified at fixed downwind distances (100 m, 1 km, 10 km, 100 km) and for each stability
   6. $\sigma_z$ subroutine provided by the user;
c. selection of a $\sigma_h$ function, independently from the $\sigma_z$ choice (same selection as for $\sigma_h$, with the additional $\sigma_h$ function from Irwin, 1979);
d. selection of different reflection assumptions; for example, partial reflection, total reflection with the Yamartino (1977) method, etc.;
e. direct specification of the meteorological input or the optional utilization of a special module (WEST module; Fabrick *et al.*, 1977) for evaluating, from meteorological measurements, a three-dimensional non-divergent wind field in either flat or complex terrain;
f. optional automatic generation of receptors on a user's specified grid (in rectangular or polar coordinates);
g. control of the element's vertical motion for avoiding unrealistic displacements, especially in complex terrain conditions.

The output of AVACTA II provides a full set of statistics of the concentration time series simulated at the receptor points (for both the primary and the secondary pollutants), and the dry deposition and wet deposition fields on a user selected grid. These statistics comprise hourly concentration values, 3-h and 24-h running concentration averages, and hourly, 3-h and 24-h total highest and highest–second-highest concentrations.

*Acknowledgements*—The author is grateful to the Center for Thermal and Nuclear Research (CRTN) of the National Electric Power Industry (ENEL) in Milan, Italy for their partial support of this study. Dr Gabriele Carboni, of CRTN-ENEL, provided important help and support, especially for the implementation of the model computer code and its user's manual. Appreciation is extended to Ms Roberta Lewis and Dr Ivar Tombach, of AeroVironment Inc., for their editorial review and useful discussions, and to Ms Barbara McMurray for typing the manuscript. The contribution of Cathedral Bluffs Shale Oil Company (Grand Junction, CO) to the early development of AVACTA II is gratefully acknowledged.

## REFERENCES

Benkley C. W. and Bass A. (1980) Development of mesoscale air quality simulation models, Vol. 3. User's Guide to MESOPUFF (Mesoscale Puff) model. EPA 600/7-80-058, U.S. Environment Protection Agency, Research Triangle Park, NC.

Chan M. W., Head S. J. and Machiraju S. (1979) Development and validation of an air pollution model for complex terrain application. Paper presented at NATO/CCMS Air Pollution Pilot Study, Rome, Italy. AeroVironment Technical Paper No. 9559.

Chan M. W. and Tombach I. H. (1978) AVACTA—air pollution model for complex terrain applications. AeroVironment Inc., Pasadena, CA. Rep. AV-M-8213.

Draxler R. R. and Heffter J. L. (1981) Workbook for estimating the climatology of regional–continental scale atmospheric dispersion and deposition over the United States. NOAA Technical Memorandum ERL ARL-96.

Fabrick A., Sklarew R. and Wilson J. (1977) Point source model evaluation and development study. Science Applications Inc. Report for the California Air Resources, Board and California Energy Resources Conservation and Development Commission, under Contract A5-058-87.

Gifford F. A. (1976) Turbulent diffusion-typing schemes: a review. *Nuclear Safety* **17**, 68–86.

Green A. E. S., Singhal R. P. and Venkateswar R. (1980) Analytic extensions of the Gaussian plume model. *J. APCA* **30**, 773–000.

Hales J. M., Powell D. C. and Fox T. D. (1977) STRAM—an air pollution model incorporating non-linear chemistry, variable trajectories, and plume segment diffusion. EPA 450/3-77-012. Environmental Protection Agency, Research Triangle Park, NC.

Irwin J. S. (1979) Estimating plume dispersion—a recommended generalized scheme. *Fourth Symposium on Turbulence, Diffusion and Air Pollution.* AMS, Reno, NV, January.

Lamb R. G. (1969) An air pollution model of Los Angeles. M.S. thesis, University of California, Los Angeles, [see Lamb R. G. and Neiburger M. (1971) An interim version of a generalized urban diffusion model. *Atmospheric Environment* **5**, 239–264].

Lewellen W. S. and Teske M. (1976) Second-order closure modeling of diffusion in the atmospheric boundary layer. *Boundary-Layer Met.* **10**, 69–90.

Liu M.-K. and Moore G. E. (1984) Diagnostic validation of plume models at a Plains site. EPRI Final Report, EA-3077, January.

Ludwig F. L., Gasiorek L. S. and Ruff R. E. (1977) Simplification of a Gaussian puff model for real-time minicomputer use. *Atmospheric Environment* **11**, 431–436.

MacCready P. B., Baboolal L. B. and Lissaman P. B. S. (1974) Diffusion and turbulence aloft over complex terrain. Preprint volume, *AMS Symposium on Atmospheric Diffusion and Air Pollution*, Santa Barbara, CA.

Martin D. O. (1971) An urban diffusion model for estimating long-term average values of air quality. *J. APCA* **21**, 16–23.

Moore D. J. (1974) A comparison of the trajectories of rising buoyant plumes with theoretical–empirical models. *Atmospheric Environment* **8**, 441–457.

Roberts J. J., Croke E. S. and Kennedy A. S. (1970) An urban atmospheric dispersion model. *Symposium on Multiple-Source Urban Diffusion Models.* Air Pollut. Control Office Publ. No. AP-86, pp. 6.1–6.72 (available from the author).

Sheih C. M. (1978) A puff pollutant dispersion model with wind shear and dynamic plume rise. *Atmospheric Environment* **12**, 1933–1938.

Stern A. C. (Ed.) (1976) *Air Pollution*, Vol. I. Academic Press, New York.

Turner D. B. (1970) Workbook for atmospheric diffusion estimates. EPA Rep. AP-26 (NTIS PB 191-482).

Yamartino R. J. (1977) A new method of computing pollutant concentration in the presence of limited vertical mixing. *J. APCA* **25**, 467–468.

Zannetti P. (1981) An improved puff algorithm for plume dispersion simulation. *J. appl. Met.* **20**, 1203–1211.

Zannetti P. (1984) New Monte Carlo scheme for simulating Lagrangian particle diffusion with wind shear effects. *Appl. Math. Modeling* **8**, 188–192.

Zannetti P., Carboni G. and Lewis R. (1985a) AVACTA II: User's Guide—Release 3. AeroVironment Inc. Technical Report 85/520.

Zannetti, P., Carboni G. and Ceriani A. (1985b) AVACTA II model simulations of worst-case air pollution scenarios in northern Italy. Paper presented at the NATO-CCMS *Fifteenth International Technical Meeting (ITM) on Air Pollution Modeling and Its Application*, St. Louis, MO.

Zannetti P., Perun V. S. and Chan M. W. (1981) AVACTA II: User's Guide—Release 1. AeroVironment Inc., Pasadena, CA. Technical Report AV-FR-81/598.

## APPENDIX A

Let us assume that the dynamics of $\sigma$ (for either $\sigma_h$, $\sigma_{z1}$, or $\sigma_{z2}$) are represented by a power law of the downwind distance; that is

$$\sigma(d) = a\,d^b \tag{A.1}$$

where the coefficients $a$ and $b$ depend upon the atmospheric turbulence status. Equation (A.1) is valid only during transport conditions (that is, $u_h \geqslant u_{min}$), and the current value $\sigma^{(old)}$ of $\sigma$ for a given element at time $t$ is a function of each different turbulence status that was encountered by the element along its trajectory.

If $a$ and $b$ represent the current values (at time $t$) of the coefficients at the element's location, $\sigma^{(old)}$ can be expressed by

$$\sigma^{(old)} = a\,d_v^b \tag{A.2}$$

where $d_v$ is the 'virtual' downwind distance. More precisely, $d_v$ is the distance that the element would have travelled to have the same $\sigma^{(old)}$ at time $t$ if the atmospheric turbulence status had been stationary and homogeneous (that is, constant $a$ and $b$) along the entire trajectory.

Equation (A.2) gives

$$d_v = (\sigma^{(old)}/a)^{1/b} \tag{A.3}$$

which allows the derivation of the new value of $\sigma$ at time $t + \Delta t$ by

$$\sigma^{(new)} = a(d_v + u_h \Delta t)^b. \tag{A.4}$$

For calm conditions ($u_h \leqslant u_{min}$), the above formulation is not correct. In this situation, however, it can be correctly assumed that the dynamics of $\sigma$ are represented by a power law of time, that is

$$\sigma(t) = a'\,t^{b'} \tag{A.5}$$

where the new coefficients $a'$, $b'$ depend again upon the atmospheric turbulence status. Similar to transport case, if $a'$ and $b'$ are the current values (at time $t$) of the coefficients, the current value $\sigma^{(old)}$ of $\sigma$ can be expressed by

$$\sigma^{(old)} = a'\,t_v^{b'} \tag{A.6}$$

where $t_v$ is the 'virtual' age of the element. More exactly, $t_v$ is the length of time that the element would have existed to have the same $\sigma^{(old)}$ at time $t$, if the atmospheric turbulence status had been stationary and homogeneous (that is, constant $a'$ and $b'$) during the element's entire life.

Equation (A.6) gives

$$t_v = (\sigma^{(old)}/a')^{1/b'} \tag{A.7}$$

allowing the evaluation of the new $\sigma$ at time $t + \Delta t$ by

$$\sigma^{(new)} = a'(t_v + \Delta t)^{b'}. \tag{A.8}$$

Available tracer experiments provide values of $a$, $b$ for each turbulence status, thus allowing the application of Equations (A.3) and (A.4) for computing the dynamics of $\sigma$s during each time step $\Delta t$ characterized by transport conditions. Little or no experimental information is, however, available for calm conditions to evaluate $a'$ and $b'$ for each turbulence status.

To circumvent this lack of information, we analyze the special case of stationary and homogeneous turbulence conditions with $u_h = u_{min}$. In this case, both Equations (A.2) and (A.6) are valid, which gives

$$\sigma^{(old)} = a d_v^b = a' t_v^{b'}. \tag{A.9}$$

But, in this special case, $d_v$ and $t_v$ are the actual current downwind distance and age of the element, and therefore

$$d_v = u_{min} t_v \tag{A.10}$$

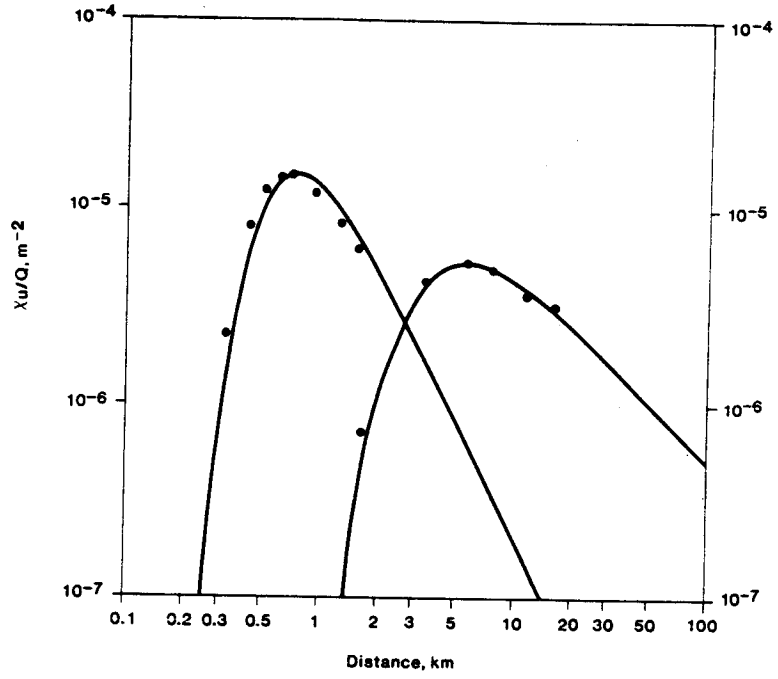


Fig. B.1. Comparison of AVACTA II outputs (dots) with standard Gaussian model results (curves from Turner, 1970). The two curves refer to the *B* stability (left) and *E* stability (right) class.

which, substituted in Equation (A.9), gives

$$a' = a u_{\min}^{b} \tag{A.11}$$

and

$$b' = b \tag{A.12}$$

which allow the evaluation of the coefficients $a'$ and $b'$ from the known coefficients $a$ and $b$, for each corresponding atmospheric turbulent status.

Let us now focus on the element's dynamics at time $t$, independently from the possible non-stationary and non-homogeneous turbulence conditions that have characterized its dynamics before $t$. The element's $\sigma$ dynamics are described by Equation (A.4) in transport conditions and by Equation (A.8) in low-wind conditions. By substituting Equations (A.7), (A.11), and (A.12) in the low-wind Equation (A.8) and remembering (A.3), we can rewrite (A.8) as

$$\sigma^{(\text{new})} = a(d_v + u_{\min}\Delta t)^{b} \tag{A.13}$$

which allows us to conclude that both transport and low-wind conditions can be simply treated by Equation (A.4) (which uses the known parameters $a$ and $b$) by simply forcing $u_h = u_{\min}$ in low-wind conditions. The correct application of the method, however, requires the identification of the appropriate value for the transitional wind speed $u_{\min}$.

The four-step scheme presented in section 2.3 is a generalization of the above computations, using a general $\sigma(d)$ function, not necessarily expressed as a power law.

## APPENDIX B

A full validation exercise is currently in progress, in which AVACTA II outputs will be compared with the data collected during several tracer diffusion experiments. This appendix presents some preliminary semi-quantitative evaluation of AVACTA II performance.

The model has been compared with standard Gaussian steady-state techniques and the AVACTA II capability of reproducing well, in stationary and homogeneous conditions, the output of standard Gaussian packages has been verified. An example of this comparison is illustrated in Fig. B.1.

Some preliminary AVACTA II simulations have been performed during two stagnant episodic conditions in Northern Italy (see Zannetti *et al.*, 1985b for a more detailed discussion). During the first episode (22 January 1982), a 3-h elevated $SF_6$ release was performed in the Turbigo area and ambient concentrations (30-min averages) were collected from 34 $SF_6$ ground-level monitors. AVACTA II showed some capability of evaluating (about half of the time) the maximum $SF_6$ concentration impact within a factor of two (but not necessarily at the same location where the maximum was measured). During the second episode (4–5 November 1981), AVACTA II was used to simulate the $SO_2$ ground-level impact from the emissions generated by the Turbigo power plant. The model performance was similar, but with a tendency to underpredict horizontal diffusion and overpredict concentration impacts.

While the above evaluation seems promising, these results confirm the difficulties in simulating stagnant, episodic conditions and the need of more modeling calibration effort.

## APPENDIX B

"A Note on the Problems Related to the Evaluation and Validation of Air Quality Models Using Field Measurements"

(AV-M-86/525)

AV-M-86/525

# A NOTE ON THE PROBLEMS RELATED TO THE EVALUATION AND VALIDATION OF AIR QUALITY MODELS USING FIELD MEASUREMENTS

By

Paolo Zannetti

AeroVironment Inc.
825 Myrtle Avenue
Monrovia, California 91016

August 1986

In the past, scientists involved in air pollution studies have generally accepted the following hypotheses:

1. Air quality dispersion models give a simplified representation of reality, while field measurements, when not affected by large measurement errors, provide a direct assessment of the real world.

2. Air quality dispersion models must be compared with field data in order to evaluate their degree of performance.

3. The most important justification of the use of modeling techniques is given by their ability to represent conditions (e.g., the impact of future emissions) that cannot be evaluated by direct monitoring of environmental parameters.

4. Only models that have been successfully compared with field data can be used to provide reliable environmental assessments.

The purpose of this note is to justify and illustrate the author's opinion that, in many practical applications, the above statements can be wrong or misleading.

Let us call $c(x,y,z,t)$ the actual time- and space-varying concentration field in a certain region(*). Dispersion models provide two types of information:

either

1. The concentration field $\hat{c}_1(x_i, y_i, z_i, t, \Delta t)$ at user-specified receptor points $(x_i, y_i, z_i)$, where $\hat{c}_1$ represent the average concentration during the time interval $(t - \Delta t/2, t + \Delta t/2)$

or

*The same considerations apply to other parameters, such as deposition or visibility impairment.

2. The concentration field $\hat{c}_2(x_i, y_i, z_i, \Delta V_i, t, \Delta t)$ at user-specified receptor cells of volume $\Delta V_i$ centered around the points $(x_i, y_i, z_i)$, where $\hat{c}_2$ represent the average concentration in the volume $\Delta V_i$ during the time interval $(t - \Delta t/2, t + \Delta t/2)$

For example, Gaussian models give $\hat{c}_1$, while grid models give $\hat{c}_2$.

Monitoring at selected measurement points $(x_i, y_i, z_i)$ provides concentration data $c'(x_i, y_i, z_i, t, \Delta t)$ that represent the average concentration during the time interval $(t - \Delta t/2, t + \Delta t/2)$.

Comparison of measurement data c' with model outputs $\hat{c}_1$ or $\hat{c}_2$ encounters several problems:

1. The comparison of point measurements c' with volume-average simulations $\hat{c}_2$

2. The definition of performance evaluation criteria based on the statistical comparison of c' with $\hat{c}_1$ or $\hat{c}_2$ and the physical interpretation of this comparison

Both these problems can cause misleading results and require careful consideration of the following facts:

1. The measurements c', even when the measurement errors are negligible, represent a partial description of the actual three-dimensional field c

2. Model outputs $\hat{c}_1$ or $\hat{c}_2$ generally cover the entire computational domain and, in particular, areas where measurements are not available

3. The real question in model validation is "how good is a model in representing c?" and not "how good is a model in representing c'?"

Let us quantify the above remarks by introducing the concept of horizontal length scale of c, where c now represents the actual time- and space-varying ground-level concentration field during time intervals of length $\Delta t$; i.e., $c(x,y,t,\Delta t)$. It is

$$\left| \frac{\partial\, c(x,y,t,\Delta t)}{\partial\, x} \right| = \frac{c(x,y,t,\Delta t)}{L_x(x,y,t,\Delta t)} \tag{1}$$

$$\left| \frac{\partial\, c(x,y,t,\Delta t)}{\partial\, y} \right| = \frac{c(x,y,t,\Delta t)}{L_y(x,y,t,\Delta t)} \tag{2}$$

which shows that the horizontal length scale ($L_x$ or $L_y$) is a function of space (x,y), time (t), orientation (x or y), and time interval ($\Delta t$). If spatial isotropy is assumed,

$$L_x(x,y,t,\Delta t) = L_y(x,y,t,\Delta t) = L_h(x,y,t,\Delta t) \tag{3a}$$

where $L_h$ is the horizontal length scale. Moreover, if stationary conditions are assumed,

$$L_h(x,y,t,\Delta t) = L_h(x,y,\Delta t) \tag{3b}$$

If stationary and homogeneous conditions are assumed,

$$L_h(x,y,t,\Delta t) = L_h(\Delta t). \tag{3c}$$

The larger the interval $\Delta t$, the smoother the concentration c, and the larger the length scale $L_h$. $L_h$ is generally smaller in the regions of maximum impacts, which are characterized by high spatial concentration gradients. Often, especially for small $\Delta t$, hypotheses (3b) and (3c) are not applicable.

The physical meaning of the length scale is illustrated below. If c has an exponential concentration distribution along x, i.e.,

$$c(x,t,\Delta t) = c_o \exp(-ax), \tag{4}$$

then

$$L_x = 1/a. \tag{5}$$

If c has a Gaussian concentration distribution along y, i.e.,

$$c(y,t,\Delta t) = c_o \exp\left[-\frac{1}{2}\left(\frac{y}{\sigma_y}\right)^2\right], \tag{6}$$

then

$$L_y \simeq \sigma_y \tag{7}$$

(actually, $L_y = \sigma_y^2/|y|$; therefore, $L_y = 0.3 - 0.5\ \sigma_y$ at the tail of the distribution, $L_y = \infty$ for $y = 0$, and $L_y = \sigma_y$ for $y = \pm\ \sigma_y$).

The above examples indicate that if the concentration field $c(x,y,t,\Delta t)$ is measured by a network of monitoring points, the measurements $c'(x,y,t,\Delta t)$ will represent a correct description of the main features of the field $c(x,y,t,\Delta t)$ only if the distance between monitoring points is less than the horizontal scale length of $c(x,y,t,\Delta t)$(*). If this condition is not met most of the time, the monitoring network simply does not provide enough information about the field c and its data can provide wrong or misleading results in model validation exercises.

(*)This condition can be stated in a less restrictive way. In practice, we require the distance between monitoring points to be less than $L_h$ only in those areas affected by significant impact or areas of particular environmental importance (e.g., ecologically sensitive regions). Some lack of spatial resolution in areas surely affected by low impacts can be tolerated.

This unfortunate situation happened in several short-range tracer experiments, when

1. The plume trajectory missed the monitoring station area, or

2. The plume horizontal size was smaller than expected and concentrations were measured only at one or two receptors at a certain downwind distance.

Tracer experiments give immediate evidence of the above cases when data are useless. Unfortunately, the same does not apply for other field experiment activities in which the determination of the actual length scale of the measured variables is not straightforward, and, therefore, data can be collected without realizing their possible lack of physical content.

On the positive side of the issue, since the length scale always increases with $\Delta t$, a network that is often useless for $\Delta t$ = 1 hour, may be quite appropriate for $\Delta t$ = three months. Also, length scales are a function of the type of parameter under examination. Primary pollutants (such as $SO_2$), have small length scales near their sources, while secondary pollutants (such as $O_3$) have larger length scales. Dry deposition of secondary pollutants (such as $SO_4^=$) has large length scales, while total wet deposition of any pollutant has small ones, due to the large spatial variation of the precipitation rates. (Relative wet deposition, i.e., wet deposition amounts per unit of rainfall, should have larger length scales, probably comparable with the dry deposition ones of the same pollutants.)

Let us move from the semi-theoretical considerations presented above to some specific cases. Figure 1 illustrates a case (unfortunately quite typical) in which the monitoring spatial resolution is insufficient. What can be done? Very little, except using a larger $\Delta t$ (which will increase $L_h$). However, if we confine our model evaluation to the dotted region in Figure 1, which possesses a satisfactory monitoring density, our statistical comparisons with model outputs can be meaningful (this may be quite appropriate if we know, for example, that the maximum concentration impact is <u>always</u> within the dotted region).

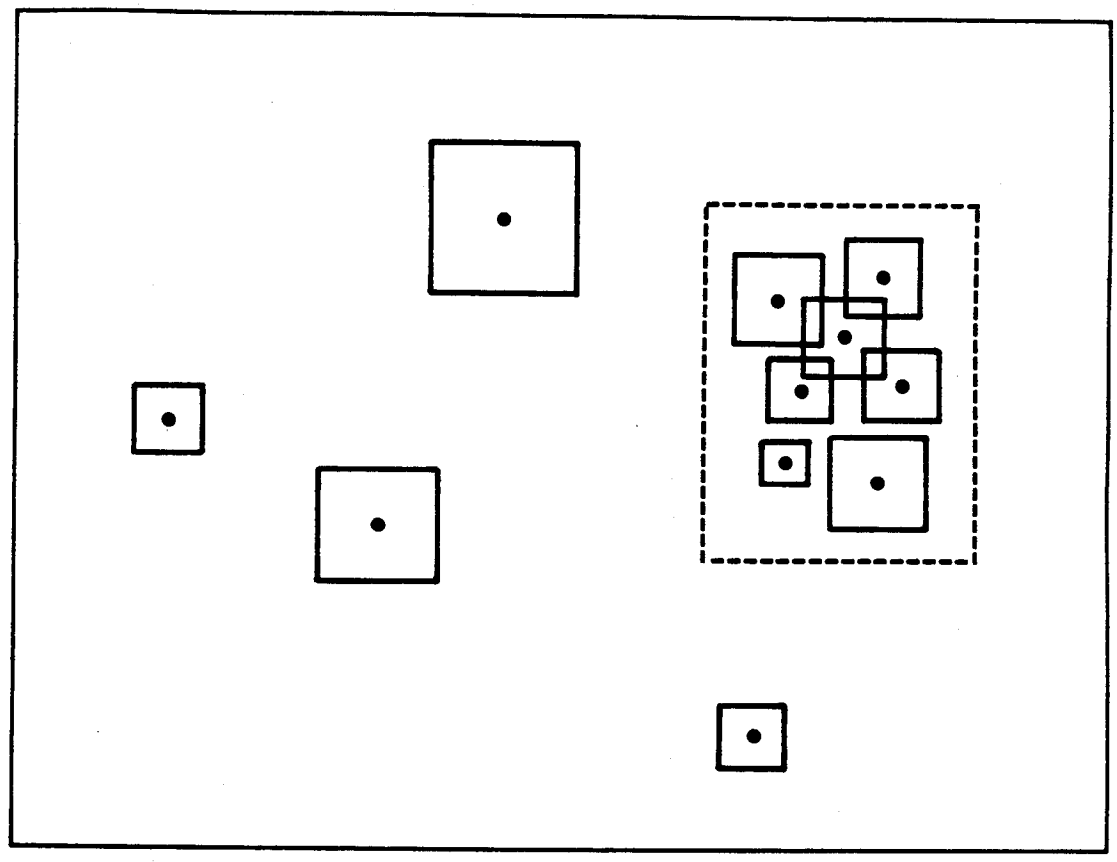

FIGURE 1. Monitoring points and their associated $L_h$ x $L_h$ region for the c(x,y) field at a certain time t for a certain averaging time $\Delta t$.

The point that we try to make is that the data $c'(x,y,t,\Delta t)$ measured by the monitoring network (such as the one depicted in Figure 1) are generally unable to provide reliable information on the spatial variability of the concentration $c(x,y,t,\Delta t)$. We can compare this situation with a tracer experiment in which only a couple of ground-level receptors monitor non-zero plume concentrations. If we are sure that the receptors are below the center of the plume, we can, perhaps, evaluate the maximum concentration impact (at that downwind distance), but, otherwise, the measurements are practically useless. (During a tracer experiment this conclusion is immediate; other monitoring situations can provide similar questionable data, but in a less evident fashion.)

But how can we evaluate $L_h$ in Figure 1? The best way is by intensive experiments of limited duration in which additional monitoring stations are deployed around the existing ones. This can give some estimates, under different meteorological conditions and averaging times, of the gradients required in Equations (1) and (2).

But these data are seldom available. Therefore, $L_h$ can be determined only by assuming some theoretical spatial distributions of c or by comparing with more intensive data collected in similar regions. The length scale $L_h$ can also be evaluated by a model providing the field $\hat{c}_1$. Even though the model is not perfect (our objective is actually to evaluate its performance) we may assume that its average <u>computed</u> concentration length scales are acceptable for our purposes. (Model outputs $\hat{c}_2$ cannot be used for evaluating $L_h$, since they are spatial averages.)

But why is it incorrect to compare model outputs with monitoring data in Figure 1? After all, if the model is good, its outputs should agree with the measurements, independently of the spatial significance of these measurements. The fact of the matter is that, if we have a case such as the one depicted in Figure 1, the measurements c' are only a very partial representation of the features of the actual field c. In this case, a successful comparison between model outputs and measurements does not necessarily imply that the model is good, and, vice versa, an unsuccessful comparison does not necessarily mean that the model is

wrong. In other words, the model is evaluated only locally, in the receptor areas $L_h \times L_h$ centered on the monitoring points, and the "unevaluated" portion of the model is so large that one should question the validity of any evaluation/calibration results.

Also, in situations such as the one illustrated in Figure 1, instead of immediately comparing model outputs $\hat{c}$ with measurements c', one may ask a priori what providing the best total information on the actual field c is: the modeling outputs $\hat{c}_1$ (or $\hat{c}_2$) or the measurements c'? Certainly c' is more reliable near the monitoring points. But what about the total information content that one can derive from $\hat{c}$ or c'? In other words, if c' is not a sufficient representation of c, what is the physical meaning of comparing $\hat{c}$ with c'?

Let us use, as a paradox, the example of a tracer experiment in which the wind is blowing from south and the receptors monitoring the tracer are located east of the release point. Clearly, the tracer plume misses the monitoring area. What is providing the highest information content on the physics of the phenomenon? The model (that we suppose not validated) is saying that the concentration impacts $\hat{c}$ are expected north of the release point. We know that model predictions can easily be wrong by an order of magnitude (for short-term averages) and by a factor of two (for long-term averages). But the information content of the monitoring data c' is clearly even less than that.

Again, during tracer experiments critical situations (such as the plume missing the receptors) are evident to everyone. We believe that similar situations in model evaluation exercises can frequently happen without detection. We, therefore, question the validity of several model evaluation exercises and we believe that situations can easily occur where the total information content provided by a non-validated model is (potentially) superior to that provided by monitoring data.(*)

(*) The consideration of the full three-dimensional field $c(x,y,z,t,\Delta t)$ instead of only the ground-level field $c(x,y,t,\Delta t)$ may further enhance the validity of this statement.

Let us discuss an example which can illustrate the above considerations. We have recently analyzed the results of a regional modeling study (air quality and visibility) in the Southwest United States. Model outputs ($SO_4^=$, light extinction, particle light scattering and wet sulfur deposition), in the form of annual averages, were compared with available monitoring data. The comparisons, which seemed reasonably successful, all had something in common: model outputs were not compared with measurements in locations of maximum impact, since these data were not available. The situation is schematically illustrated in Figure 2. Can we say, in this case, that the model is successfully validated? We do not think so. Can we say that the present monitoring data are more reliable than model outputs in assessing the real world? Probably not. Which gives, on a global basis, the most reliable information: model outputs or measurements? Probably model outputs, at least at the present time.

A different, but related problem, is given by the comparison between model outputs $\hat{c}_2$ on large grid cells of sizes $\Delta x$, $\Delta y$ (for example 80 km x 80 km) with point measurements. Again, in order to evaluate the validity of this comparison, the length scale $L_h$ of the actual field c needs to be evaluated. Then, four basic situations can be encountered, as illustrated in Figure 3:

Case (a): (not illustrated) If no monitoring station regions ($L_h$x $L_h$) are covering a grid cell, the model outputs $\hat{c}_2$ in that cell cannot be validated.

Case (b): If only one monitoring station region is covering a grid cell, and $L_h << \Delta x$ or $\Delta y$, the model outputs $\hat{c}_2$ in that cell cannot be validated.

Case (c): If most or all of a cell is covered by one or more monitoring station regions with $L_h > \Delta x$ and $\Delta y$, geometrical interpolation techniques can be used to infer a "measured" c' value for that cell, to be compared with model outputs $\hat{c}_2$.

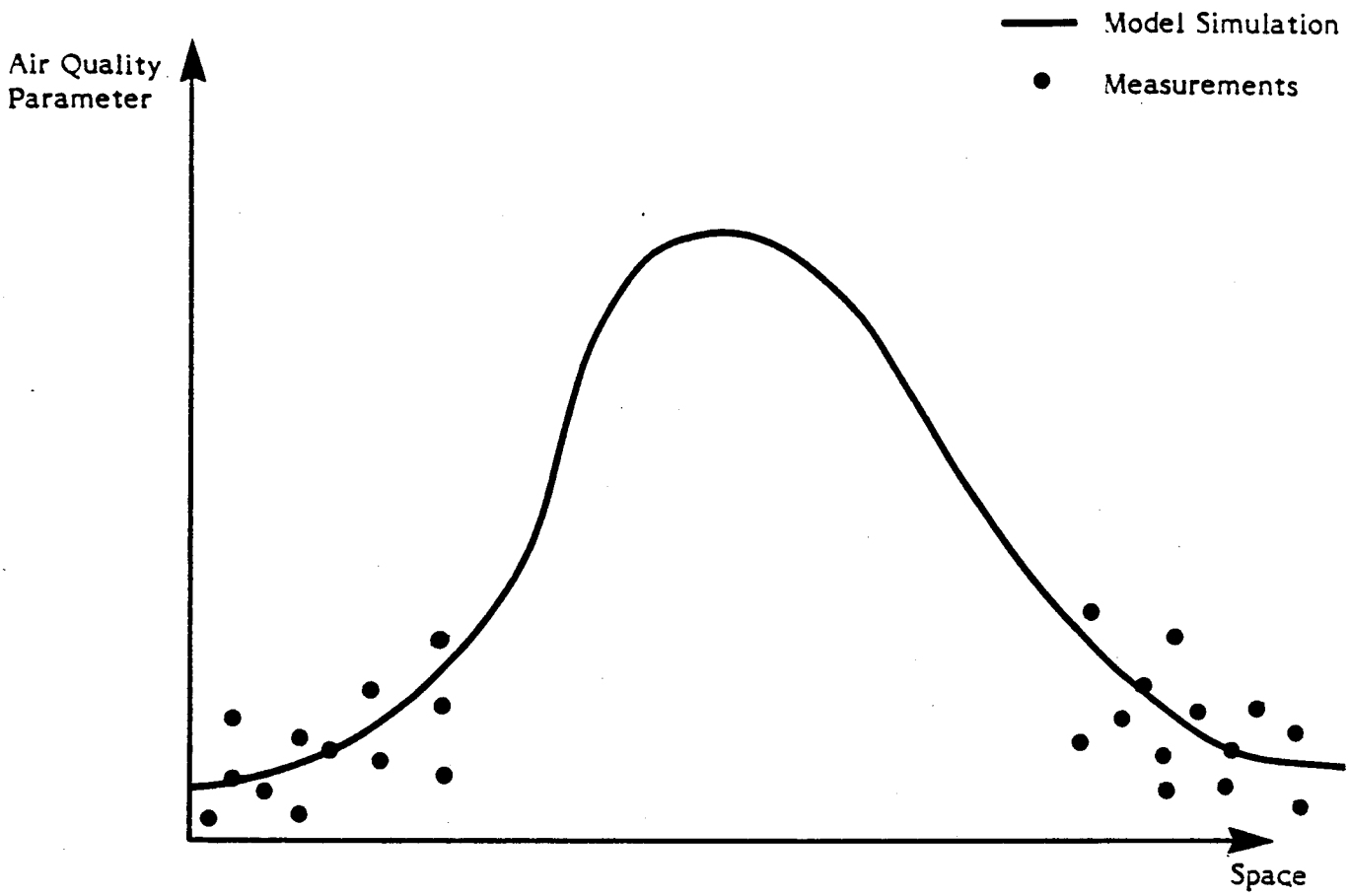


FIGURE 2. Schematic illustration of the range of simulation values and corresponding measurements.

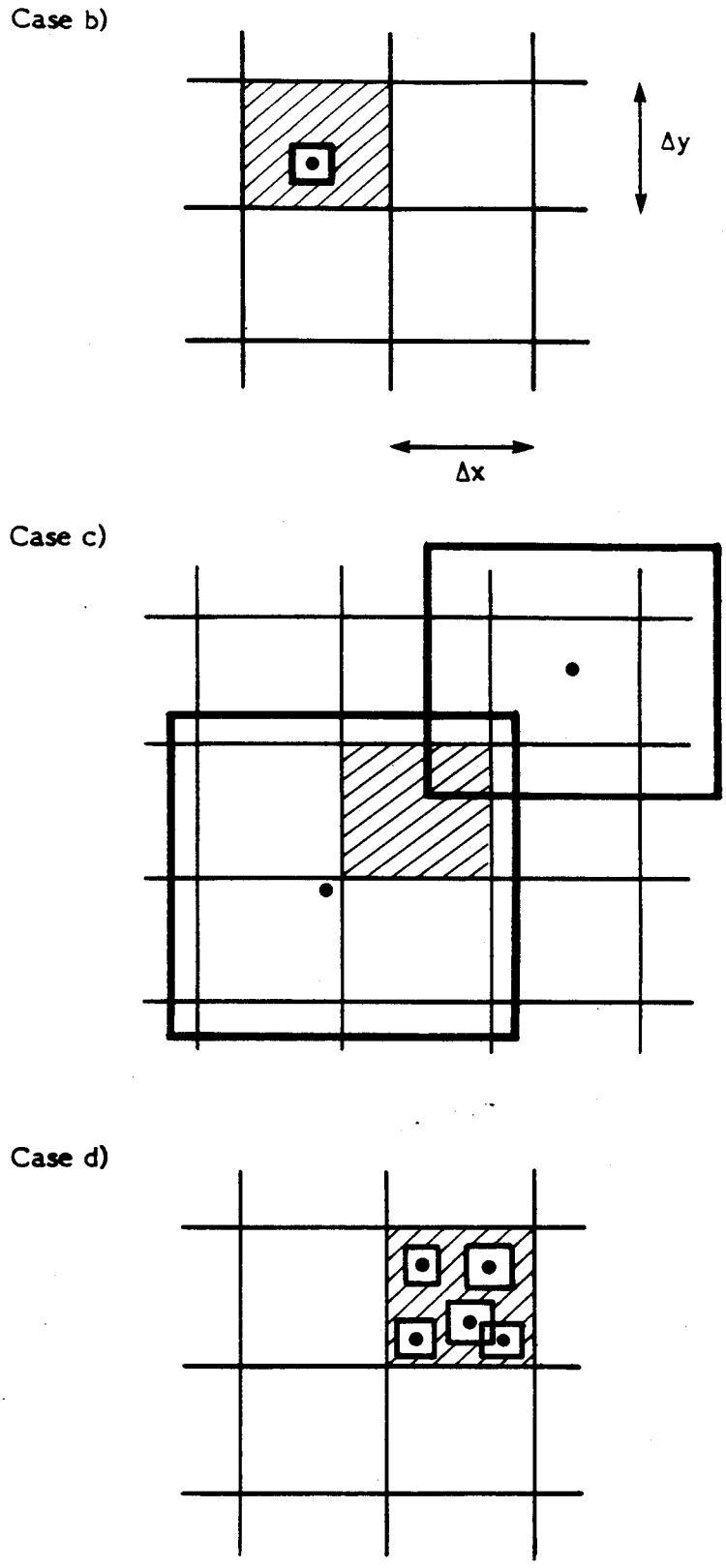


FIGURE 3. Monitoring points and their associated $L_h$ x $L_h$ region with respect to a superimposed grid network for model simulations. Each cell of the grid has Δx x Δy.

87-147

Case (d): If most or all of a cell is covered by several monitoring station regions with $L_h < \Delta x$ and $\Delta y$, geometrical averaging techniques can be used to infer a "measured" c' value for that cell, to be compared with model outputs $\hat{c}_2$.

Again, cases (a) and (b) may be quite frequent in past and current model validation exercises, and statistical evaluation results can be worng or misleading.

In conclusion, we want to emphasize that the major objective of any air quality model performance evaluation should be the estimate the model's ability to represent the actual concentration field c satisfactorily. Since c is not known, we must use a partial representation of it given by the field measurements c'. We believe, based on the previous considerations and our air quality experience, that:

1. Often the results of validation/calibration studies are wrong or misleading, due to the poor spatial resolution of the monitoring stations

2. In several circumstances, the three-or two-dimensional depiction of the concentration c by the measurements c' can be so limited that serious questions should be raised about the validity of any comparison between model outputs $\hat{c}$ and measurements c'. In these cases, the total information content of the model outputs $\hat{c}$ may be greater than the information provided by the measurements c'. In other words it may be <u>theoretically wrong</u> to base our judgment of model performance on the comparison with field data c'.

# APPENDIX C

"The Kalman Filtering Method and Its Application to Air Pollution Episode Forecasting"

IBM PALO ALTO SCIENTIFIC CENTER REPORT NO. G320-3381

April 1979

# THE KALMAN FILTERING METHOD AND ITS APPLICATION TO AIR POLLUTION EPISODE FORECASTING

Paolo Zannetti[+]

Paul Switzer[o]

IBM Corporation
Palo Alto Scientific Center
1530 Page Mill Road
Palo Alto, California 94304

[+]IBM Scientific Center, Venezia, Italy

[o]Stanford University, Stanford, California

Abstract

This paper presents an application of the Kalman filtering method to multi-station air pollution modeling in order to obtain a useful real-time predictor of concentration levels, especially during episode situations. Special attention has been paid to avoiding certain high dimensionality problems of the Kalman filter while still retaining some of the deterministic "physical" information of the transport and diffusion phenomena. Moreover, a method is proposed to forecast future state values using only a probabilistic knowledge of future state-transition matrices, which is the most common situation in air pollution real-time forecasting with probabilistic meteorological input. Specifically, the method is applied to $SO_2$ and meteorological data (Summer 1975) supplied by the RAMS network (Environmental Protection Agency's Regional Air Pollution Study) installed in the St. Louis Missouri area. The results of the proposed methodology are compared with those supplied by single-station predictors.

## 1. Introduction

Kalman filters are a class of linear minimum-error-variance sequential state estimation algorithms. They have been used in many applied fields and, in particular, in navigation space guidance and orbit determination[1] and in hydrology[2]. The linear discrete version of this methodology can be used for forecasting problems where the transition mechanism of a discrete system is described by the discrete "message model"

$$\underset{\sim}{x}(t+1) = \underset{\sim}{\Phi}(t+1,t)\underset{\sim}{x}(t) + \underset{\sim}{\Gamma}(t)\underset{\sim}{w}(t+1) \tag{1}$$

In this equation, $\underset{\sim}{\Phi}(t+1,t)$ is the state-transition matrix from t to t+1, $\underset{\sim}{x}(t)$ is the state vector at time t, $\underset{\sim}{w}(t+1)$ is a zero-mean white noise stochastic process with covariance matrix $\underset{\sim}{V}_{\underset{\sim}{w}}(t+1)$, and $\underset{\sim}{\Gamma}(t)$ is the noise transition matrix. The dimension of $\underset{\sim}{w}$ is not necessarily equal to that of $\underset{\sim}{x}$.

In the general theory, the state $\underset{\sim}{x}(t)$ is not observed directly. Instead, observations have the form of an "observation model"

$$\underset{\sim}{z}(t) = \underset{\sim}{H}(t)\underset{\sim}{x}(t) + \underset{\sim}{v}(t) \tag{2}$$

where $\underset{\sim}{z}(t)$ is the observation vector at time t [generally of dimension less than that of $\underset{\sim}{x}(t)$], $\underset{\sim}{v}(t)$ is a zero mean white noise measurement error process with covariance matrix $\underset{\sim}{V}_{\underset{\sim}{v}}(t)$, and $\underset{\sim}{H}(t)$ is an appropriate coefficient matrix. Starting from the general problem of (1) and (2), the Kalman filtering method allows a recursive on-line estimation at time t of $\underset{\sim}{x}(t+k)$, k=1,2,... by considering only the effect of the most recent observation $\underset{\sim}{z}(t)$, instead of resolving at each time the entire problem by the classical least square regression technique.

Recently this method has been used in air pollution problems in order to obtain more accurate predicted values in episode forecasting and control. This can be done by considering $\underset{\sim}{x}(t)$ as the vector of concentrations of a pollutant at the grid points[3] (or at the monitoring points[4]) of the study area. The state vector $\underset{\sim}{x}(t)$ might also be extended to include some additional adaptive parameters[3] but we do not make use of this extension here. Then the transition matrix $\underset{\sim}{\Phi}$ becomes either the matrix of the spatial discretization (K-model) of the transport and diffusion equation[3] (including time-dependent emission and meteorological inputs), or a multiple regression matrix[4]. Model inaccuracies and emissions and meteorology input errors are

included in the system noise process $\underset{\sim}{w}(t)$.

A very important problem arises in the application of the Kalman filter to air pollution problems. In fact, it is necessary to avoid the high dimensionality of the resulting Kalman filter equations. For example, when $\underset{\sim}{\Phi}$ is the time-evolution transition matrix of the K-model, a simple spatial grid of 20×20×10 points produces Kalman filter matrices of dimension 4000×4000. Many proposals have been made for the simplification of this problem. In particular, either the Green function can be used[5] to reduce the equation of the K-model to a difference equation of relatively small dimension, or a discrete form of Chandrasekar-type equations can be applied[6] for the same goal. Alternatively, the region can be partitioned into subregions[3] and, if the subvectors of the subregions are not coupled (or weakly coupled), the filter algorithm can be applied separately to each of the subvectors, so reducing the size of the matrices which must be manipulated. Finally, a multiple linear regression model can be used[4] for $\underset{\sim}{\Phi}$, so reducing the dimension of the filter to the number of monitoring stations in the area, losing however the "physical" information of the diffusion phenomenon.

Our proposed method uses for the dimension of the filter the number of monitoring stations, but it incorpo-

rates the meteorological information by having the matrix $\underset{\sim}{\Phi}(t+1,t)$ depend on the meteorological conditions and time-of-day at time t+1. However, meteorological conditions at future times may only be probabilistically estimated at time t. This leads to special methods for the estimation at time t of $\underset{\sim}{\Phi}(t+k,t+k-1)$, k=1,2,... . The entire methodology can be used in an adaptive form by estimating all model parameters on a learning time-period of given fixed length close to the forecasting time.

A general computer-oriented description of the Kalman filter method is presented in Section 2 and in the Appendix. In Section 3 the method is applied to meteorological and $SO_2$ data collected in St. Louis, Missouri. In particular, the results of the method are compared with those obtained with single-station predictors in order to show the forecasting improvement of the methodology we have adopted. Finally, in Section 4, conclusions and future developments are discussed.

## 2. The linear Kalman filter method and the estimation of the $\underset{\sim}{\Phi}$ matrices.

Starting from equation (1) and (2) is possible to develop[1,7] a linear unbiased minimum-error-variance algor-

ithm (Kalman filter) for the estimation of the state of a linear time-varying dynamic system, driven by white noise of zero mean and known variance. Under the further assumptions that $\underset{\sim}{v}$, $\underset{\sim}{w}$ and $\underset{\sim}{x}$ are mutually uncorrelated, the relevant formulas are [$\underset{\sim}{x}(t_2|t_1)$ is the estimate at time $t_1$ of $\underset{\sim}{x}(t_2)$]:

predicted state $$\underset{\sim}{x}(t+1|t) = \underset{\sim}{\Phi}(t+1,t)\underset{\sim}{x}(t|t); \tag{3}$$

predicted error covariance matrix

$$\underset{\sim}{V}_{\underset{\sim}{x}}(t+1|t) = \underset{\sim}{\Phi}(t+1,t)\underset{\sim}{V}_{\underset{\sim}{x}}(t|t)\underset{\sim}{\Phi}^{T}(t+1,t) + \underset{\sim}{\Gamma}(t)\underset{\sim}{V}_{\underset{\sim}{w}}(t+1)\underset{\sim}{\Gamma}^{T}(t); \tag{4}$$

filter gain matrix

$$\underset{\sim}{K}(t+1) = \underset{\sim}{V}_{\underset{\sim}{x}}(t+1|t)\underset{\sim}{H}^{T}(t+1)[\underset{\sim}{H}(t+1)\underset{\sim}{V}_{\underset{\sim}{x}}(t+1|t)\underset{\sim}{H}^{T}(t+1)+\underset{\sim}{V}_{\underset{\sim}{v}}(t+1)]^{-1}; \tag{5}$$

after processing the observation $\underset{\sim}{z}(t+1)$

$$\underset{\sim}{x}(t+1|t+1) = \underset{\sim}{x}(t+1|t) + \underset{\sim}{K}(t+1)[\underset{\sim}{z}(t+1)-\underset{\sim}{H}(t+1)\underset{\sim}{x}(t+1|t)]; \tag{6}$$

new error covariance matrix

$$\underset{\sim}{V}_{\underset{\sim}{x}}(t+1|t+1) = [\underset{\sim}{I}-\underset{\sim}{K}(t+1)\underset{\sim}{H}(t+1)]\underset{\sim}{V}_{\underset{\sim}{x}}(t+1|t); \tag{7}$$

where $\underset{\sim}{V}_{\underset{\sim}{x}}(t_2|t_1)$ is the covariance matrix of the error $\underset{\sim}{x}(t_2)-\underset{\sim}{x}(t_2|t_1)$.

In the Appendix a computer oriented scheme of equations (1-7) is developed. This method uses equation (3) recursively in order to obtain the forecast up to p time-steps ahead. This forecast requires, at each time t, the estimates $\underset{\sim}{\Phi}(t+k,t+k-1|t)$, k=1,2,...p of future state-transition matrices which may be highly time dependent. In air pollution, for example, the state-transition matrix

$\underset{\sim}{\Phi}(t+k,t+k-1)$ should contain all the information at time t about the evolution of meteorology and emissions between t+k-1 and t+k. To solve this problem we propose that, after an analysis of the physical system, a reasonably small number n of system "categories" or "classes" be selected[8,9]. In this way, to each time interval t is associated a system class $\alpha(t)$. According to this categorization, there are n possible state transition matrices $\underset{\sim}{\Phi}_{\alpha}$ which can be selected at each time step. The estimation of the future system classes is done with probabilistic methods, i.e., at each time t we suppose that $\alpha(t+1)$ has a probability distribution depending on the current system class $\alpha(t)$ [and by recursion we may compute the probability distributions for $\alpha(t+k)$, k=1,2,...,p]. Then we propose that the predicted states be obtained by applying (3)recursively, i.e.,

$$\underset{\sim}{x}(t+k|t)=\underset{\sim}{\Phi}(t+k,t+k-1|t)\underset{\sim}{x}(t+k-1|t),\ k=1,2,\ldots,p \qquad (8)$$

where $\underset{\sim}{\Phi}(t+k,t+k-1|t)$ is the average of the $\underset{\sim}{\Phi}_{\alpha}$ matrices weighted by their corresponding probabilities. A practical application of this method is developed in the next section.

## 3. An application of the Kalman filter to $SO_2$ forecasting

The methodology of the previous section has been applied to hourly meteorological and $SO_2$ data. The period of analysis is Summer 1975 (2208 hourly time periods) and the data was supplied by three monitoring stations of the RAMS network (Environmental Protection Agency's Regional Air Pollution Study) installed in St. Louis, Missouri (Figure 1). The following time series have been used: three $SO_2$ time series, (Station 3, industrial area; Station 5, commercial area; Station 13, suburban area) wind speed (Station 3), wind direction (Station 3), temperature vertical gradient (Station 5), and hour of the day. All these, except $SO_2$, have been categorized as follows:

- wind speed, 3 classes ($\leq$2m/s, >2m/s and $\leq$6m/s, >6m/s);
- wind direction, 8 classes
  (N-NE,NE-E,E-SE,SE-S,S-SW,SW-W,W-NW,NW-N);
- temperature vertical gradient, 3 classes based on the variable $s = \frac{\Delta T}{\Delta z} + \frac{1^{o}C}{100m}$ ($s<-0.005$ unstable, $s\geq-0.005$ and $s\leq0.005$ neutral, $s>0.005$ stable); and
- hour of the day, 5 classes (night, transition, low

insolation, average, high) according to Table I*.

According to the scheme of Table II, 18 different meteorological classes have been defined, where each class shows an occurrence of at least 30 hourly cases. Moreover, by combining these 18 meteorological classes with the 5 hour-type classes, 57 combined classes have been defined in Table III (each of at least 20 hourly cases). This distinction is necessary because, at each time t, the future hour-type is exactly known, while the forecasting of future meteorological classes must be done probabilistically.

The probabilities associated with the 18 meteorological classes at time t+1, given we are in combined class $\alpha(t)$ at time t, are estimated from the relative frequencies in the data and are shown in Table IV. Since the hour class is known, in this way we get probabilities for each combined class $\alpha'(t+1)$, given each combined class $\alpha(t)$ at time t. These probabilities are denoted by $q^1_{\alpha\alpha'}$, and $\sum_{\alpha'=1}^{57} q^1_{\alpha\alpha'}=1$ for any $\alpha$. The corresponding probabilities for k steps ahead are denoted $q^k_{\alpha\alpha'}$. Assuming a first-order Markov chain, they are obtained recursively by

---

*Personal communication from Dr. L.J. Shieh, IBM Scientific Center, Palo Alto, CA.

$$q^{h+1}_{\alpha\alpha'} = \sum_{\alpha''=1}^{57} q^{h}_{\alpha\alpha''} q^{1}_{\alpha''\alpha'} \quad ,h=1,\ldots,k-1 \tag{9}$$

The transition matrix estimates, given the system state $\alpha(t)$ at time t, are then (p=8)

$$\underset{\sim}{\Phi}(t+k,t+k-1|t) = \sum_{\alpha'=1}^{57} \underset{\sim}{\Phi}_{\alpha'} q^{k}_{\alpha\alpha'} \quad ,k=1,\ldots,8 \tag{10}$$

The general program scheme, described in the Appendix, has been applied to our data in the following way. The state vector $\underset{\sim}{x}(t)$ has four components given by the three $SO_2$ hourly concentrations measured for the time t in ppm at the three selected stations, and a forth component which is identically 1 as required for the easier application of multiple regression methods. For each of the 57 meteorological-time-of-day categories $\alpha$, we have in Table V a 4×4 state-transition matrix $\underset{\sim}{\Phi}_{\alpha}$ which is estimated by multiple regression methods. A simplified version of the general methodology (1-7) has been used in which, for computational purposes, the covariance $\hat{V}_{\underset{\sim\sim}{\Gamma w}}$ of $\underset{\sim\sim}{\Gamma w}$, expressed in $ppm^2$ and estimated from the data, has been completely ascribed to $\underset{\sim}{w}$ by setting

$$\underset{\sim}{V}_{\underset{\sim}{w}} = \hat{\underset{\sim}{V}}_{\underset{\sim\sim}{\Gamma w}} = \begin{pmatrix} 2.436\ 10^{-5} & 6.495\ 10^{-6} & 2.656\ 10^{-6} \\ 6.495\ 10^{-6} & 5.160\ 10^{-5} & -2.626\ 10^{-6} \\ 2.656\ 10^{-6} & -2.626\ 10^{-6} & 2.561\ 10^{-4} \end{pmatrix}, \quad \underset{\sim\sim}{\Gamma} = \begin{pmatrix} 1 & 0 & 0 \\ 0 & 1 & 0 \\ 0 & 0 & 1 \\ 0 & 0 & 0 \end{pmatrix} \tag{11}$$

This estimate, $\hat{\underset{\sim}{V}}_{\underset{\sim\sim}{\Gamma w}}$, has been calculated using the error series $\underset{\sim}{x}(t+1) - \underset{\sim}{\Phi}_{\alpha(t+1)} \underset{\sim}{x}(t)$ during the analyzed period

(Summer 1975), where the $\underset{\sim}{x}$ are known because the observations $\underset{\sim}{z}(t)$ have been taken without error ($\underset{\sim}{v}=\underset{\sim}{0}$). Moreover, in our formulation, we have $H=\Gamma^T$. In this simplified version of the general model the forecasting results are the same as those obtained by applying the usual multiple regression model alone. At time t=0 we start with the initial conditions $\underset{\sim}{\mu}_{\underset{\sim}{x}}(0)=\underset{\sim}{0}$ and $\underset{\sim}{V}_{\underset{\sim}{x}}(0)=2\underset{\sim}{V}_{\underset{\sim}{w}}$. The model has been applied to the same data set (Summer 75) used for model parameter estimation (fitting application).

In addition to the probabilistic treatment we also calculated a "best" predictor based on exact knowledge of the future meteorological classes. This provides the upper bound performance of our Kalman filter method. We may expect that the real-time performance of the predictor scheme might be close to the "upper bound" performance if an expert meteorologist can supply a realistic forecast (up to 8 hours ahead) of the meteorological classes which is superior to the conditioned probability forecast.

Figures 2-4 show the results obtained in our case study. Figure 2 refers to Station 3 and shows, respectively, the root mean square error of the predicted $SO_2$ concentrations and the correlation coefficient of our computations. These are compared with similar calculations obtained with the persistence concentration model and a

single-station fitting predictor defined in another paper[9].

This latter predictor has been defined in the following way. For any given combined class $\alpha$ ($\alpha$=1,2,...,57) let $\underset{\sim}{T}^0_\alpha \equiv \{t_1, t_2, \ldots\}$ be the collection of hourly periods during which that condition $\alpha$ obtained. Define $\mu^0_\alpha$ and $\sigma^0_\alpha$ to be the mean and the standard deviation of the observed $SO_2$ hourly concentrations at time $\underset{\sim}{T}^0_\alpha$. Similarly define $\underset{\sim}{T}^k_\alpha \equiv \{t_1+k, t_2+k, \ldots\}$ and let $\mu^k_\alpha$, $\sigma^k_\alpha$ be the mean and standard deviation of the observed $SO_2$ hourly concentrations at times $\underset{\sim}{T}^k_\alpha$. Finally, define $\rho^k_\alpha$ to be the lag k autocorrelation between the $SO_2$ concentrations at times $\underset{\sim}{T}^0_\alpha$ and those at times $\underset{\sim}{T}^k_\alpha$. With these 5×n parameters (in our case 285) for each k, we apply the following k-hours-ahead predictor:

$$\frac{c(t+k|t) - \mu^k_{\alpha(t)}}{\sigma^k_{\alpha(t)}} = \rho^k_{\alpha(t)} \frac{c(t) - \mu^0_{\alpha(t)}}{\sigma^0_{\alpha(t)}} \qquad (12)$$

that allows the concentration estimation $c(t+k|t)$ on the basis of the observed combined class $\alpha(t)$ and $SO_2$ concentration $c(t)$ at time t. In the case where $c(t)$ and $c(t+k)$ are modeled to have a joint normal distribution in each condition class, then this predictor is equivalent to the conditional mean of $c(t+k)$ given the data at time t. The predictor may also be regarded as an AR(1) model conditioned on the meteorological-time-of-day class.

The single-station predictor (12) nearly always performs less well than the upper bound of our current Kalman multi-station method. Only for extended forecasts does this single-station model appear to perform somewhat better because separate parameters were estimated for each prediction lag instead of the recursive parameter estimation used here. Figure 3 refers to Station 5 and Figure 4 to Station 13 (similar to Figure 2).

## 4. Conclusions

A presentation of the linear Kalman filter method has been made, with particular emphasis on application to air pollution prediction problems and to computer programming. A case study has been developed, which shows the usefulness of the general approach. This method may be improved in order to better fit the air pollution data by using a sequential correlated noise model

$$\underset{\sim}{w}(t+1) = \underset{\sim\sim}{\Psi}\underset{\sim}{w}(t) + \underset{\sim}{\varepsilon}(t+1) \qquad (13)$$

A substantial improvement in forecasting performance might be expected if $SO_2$ emission data are considered in the definition of the general classes. Moreover, further

improvement may be expected by better taking into account, in the definition of matrices $\underset{\sim}{\Phi}$, the physics of the diffusion phenomena.

Acknowledgements

We thank Dr. Piero Sguazzero and Dr. Danny Shieh of the IBM Scientific Centers of Venice, Italy and Palo Alto, California for useful discussions. This work has been developed in connection with STAAP project (Statistical Techniques Applied to Air Pollution): a collaboration between the Palo Alto and Venice IBM Scientific Centers and the Department of Statistics of Stanford University.

References

1. A. H. Jazwinski, Stochastic Processes and Filtering Theory, Academic Press, New York, 1970.

2. E. Todini, "Using a desk-top computer for a on-line flood warning system", IBM J. Res. Develop., 22(5): p 464 (1978).

3. S. G. Bankoff and E. L. Hanzevack, "The adaptive-filtering transport model for prediction and control of pollutant concentration in an urban airshed", Atmos. Environ., 9:p 793 (1975).

4. Y. Sawaragi, T. Soeda, T. Yoshimura, S. Ohe, Y. Chujo and H. Ishihara, "The predictions of air pollution levels by nonphysical models based on Kalman filtering method", J. Dynamic Syst., Meas. and Contr. 98(12): p 375 (1976).

5. M. Hino, "Prediction of atmospheric pollution by Kalman-filtering", Proc. Symp. on Modeling for Prediction and Control of Air Pollution (1974).

6. A. A. Desalu, L. A. Gould and F. C. Schweppe, "Dynamic estimation of air pollution", IEEE Trans. Automat. Contr., AC19(6): p 904 (1974).

7. A. P. Sage and J. L. Melsa, Estimation Theory with Applications to Communications and Control, McGraw-Hill, New York. 1971, p 529.

8. G. Finzi, G. Fronza, S. Rinaldi and A. Spirito, "Prediction and real-time control of $SO_2$ pollution from a power plant", Proceedings of the 71st Annual Meeting of the APCA, Houston, June 25-30, 1978.

9. P. Zannetti and P. Switzer, "Some problems on validation and testing of numerical air pollution models", to be presented at the 4th Symposium on Turbulence, Diffusion and Air Pollution, Reno, Nevada, January 15-18, 1979.

## APPENDIX

It can be useful to rewrite all the method (1-7) in a computer oriented recursive form referred to a forecasting performed from 1 to p time steps ahead:

A. Initial conditions

$$T=0,\ X \leftarrow \underset{\sim}{\mu}_{\underset{\sim}{x}}(0),\ VX=\underset{\sim}{V}_{\underset{\sim}{x}}(0)$$

B. Matrices definitions

$$FI_1=\underset{\sim}{\Phi}(T+1,T|T),\ FI_2=\underset{\sim}{\Phi}(T+2,T+1|T),\ldots,FI_p=\underset{\sim}{\Phi}(T+p,T+p-1|T),$$

$$GA=\underset{\sim}{\Gamma}(T),\ H_1=\underset{\sim}{H}(T+1|T),\ H_2=\underset{\sim}{H}(T+2|T),\ldots,H_p=\underset{\sim}{H}(T+p|T),$$

$$VW=\underset{\sim}{V}_{\underset{\sim}{w}}(T+1|T),\ VV=\underset{\sim}{V}_{\underset{\sim}{v}}(T+1|T)$$

C. Predicted states

$$X_1=FI_1 \cdot X,\ X_2=FI_2 \cdot X_1,\ldots X_p=FI_p \cdot X_{p-1}$$

D. Saving

Save $H_1 \cdot X_1,\ H_2 \cdot X_2,\ldots H_p \cdot X_p$ for future comparison with the measures $\underset{\sim}{z}(T+1),\ \underset{\sim}{z}(T+2),\ldots\underset{\sim}{z}(T+p)$

E. A-priori error covariance matrix

$$VX=FI_1 \cdot VX \cdot FI_1^T+GA \cdot VW \cdot GA^T$$

F. Saving

Forcing of the symmetry of VX for numerical stability, And saving of its main diagonal

G. Filter gain matrix

$$K=VX\bullet H_1^T\bullet[H_1\bullet VX\bullet H_1^T+VV]^{-1}$$

H. Process the observation $Z=\underset{\sim}{z}(T+1)$

$$X = X_1+K\bullet[Z-H_1\bullet X_1]$$

I. A-posteriori error covariance matrix with a formula numerically more stable[1] than (7)

$$VX = [I-K\bullet H_1]\bullet VX\bullet[I-K\bullet H_1]^T+ K\bullet VV\bullet K^T$$

J. Saving

Forcing of the symmetry of VX for numerical stability, and saving of its main diagonal

K. Loop

T=T+1, then end if $T>T_{MAX}$, otherwise go to step B.

For a more complete documentation on this subject, the APL version of the main program of the algorithm is included in this Appendix. This main program calls other APL functions whose role is easily understandable by their names.

```
      ∇KMAIN[□]∇
      ∇ JMAX KMAIN P;J;FI;GAM;H;VW;VV;X;VX;Z;XF;XZ;K
[1]   ⍝
[2]   ⍝    "KMAIN" : MAIN PROGRAM OF REAL-TIME SIMULATION OF THE
[3]   ⍝              LINEAR DISCRETE KALMAN FILTER.
[4]   ⍝
[5]   ⍝ ********************************
[6]   ⍝ ******   INITIALIZATION   ******
[7]   ⍝ ********************************
[8]    XZSAVE←VXSAVE←0ρ0
[9]    J←0
[10]   FI←P READΔFI J
[11]   GAM←READΔGAM J
[12]   H←P READΔH J+1
[13]   VW←READΔVW J
[14]   VV←READΔVV J+1
[15]   X←READΔMU0
[16]   VX←READΔVX0
[17]   Z←READΔZ⍳P
[18]  ⍝ ********************************
[19]  ⍝ ******   PREDICTED STATE   ******
[20]  ⍝ ********************************
[21]  LOOP:XF←FI FOREC X
[22]   XZ←H XZCOMP XF
[23]   SAVEΔXZ XZ
[24]  ⍝ ************************************************
[25]  ⍝ ******   PREDICTED ERROR COVARIANCE MATRIX   ******
[26]  ⍝ ************************************************
[27]   VX←(FI[1;;] BY VX BY TRANS FI[1;;])+GAM BY VW BY TRANS GAM
[28]   VX←FORSIM VX
[29]   SAVEΔVX VX
[30]  ⍝ ************************************
[31]  ⍝ ******   FILTER GAIN MATRIX    ******
[32]  ⍝ ************************************
[33]   K←VX BY(TRANS H[1;;]) BY INV(H[1;;] BY VX BY TRANS H[1;;])+VV
[34]  ⍝ ******************************************
[35]  ⍝ ******   PROCESS THE OBSERVATION   ******
[36]  ⍝ ******************************************
[37]   X←XF[1;]+K BY Z[1;]-XZ[1;]
[38]  ⍝ ************************************************
[39]  ⍝ ******   NEW ERROR COVARIANCE MATRIX   ******
[40]  ⍝ ************************************************
[41]   VX←((IDENT(ρK)[1])-K BY H[1;;]) BY VX BY TRANS(IDENT(ρK)[1])-K BY H[1;;]
[42]   VX←VX+K BY VV BY TRANS K
[43]   VX←FORSIM VX
[44]   SAVEΔVX VX
[45]  ⍝ ******************************
[46]  ⍝ ******   END OF LOOP   ******
[47]  ⍝ ******************************
[48]   →((J+P)>JMAX)/END,0ρJ←J+1
[49]   FI←P READΔFI J
[50]   GAM←READΔGAM J
[51]   H←P READΔH J+1
[52]   VW←READΔVW J
[53]   VV←READΔVV J+1
[54]   Z←1 LSHIFT Z
[55]   Z[P;]←READΔZ 1ρP+J
[56]   →LOOP
[57]  END:'*** NORMAL END ***'
      ∇
```

| month | | day-hour | | | | | | | | | | | | | | | | | | | | | | | |
|---|---|---|---|---|---|---|---|---|---|---|---|---|---|---|---|---|---|---|---|---|---|---|---|---|---|
| | | 1 | 2 | 3 | 4 | 5 | 6 | 7 | 8 | 9 | 10 | 11 | 12 | 13 | 14 | 15 | 16 | 17 | 18 | 19 | 20 | 21 | 22 | 23 | 24 |
| june | 75 | 1 | 1 | 1 | 1 | 1 | 2 | 2 | 3 | 4 | 5 | 5 | 5 | 5 | 5 | 5 | 4 | 3 | 3 | 2 | 2 | 2 | 1 | 1 | 1 |
| july | 75 | 1 | 1 | 1 | 1 | 1 | 2 | 2 | 3 | 4 | 4 | 5 | 5 | 5 | 5 | 5 | 4 | 3 | 3 | 2 | 2 | 2 | 1 | 1 | 1 |
| august | 75 | 1 | 1 | 1 | 1 | 1 | 2 | 2 | 3 | 4 | 4 | 5 | 5 | 5 | 5 | 4 | 4 | 3 | 3 | 2 | 2 | 1 | 1 | 1 | 1 |

Table I. Determination of the hour-of-day classes (insolation) based on the month and the hour of the day.

| Met Cl. | WD | Stab. | WS | Met Cl. | WD | Stab. | WS | Met Cl. | WD | Stab. | WS |
|---|---|---|---|---|---|---|---|---|---|---|---|
| 1 | N-NE | S,N | All | 7 | E-SE | I | All | 13 | S-SW | I | >6m/s |
| 2 | N-NE | I | All | 8 | SE-S | S,N | All | 14 | SW-W | All | All |
| 3 | N-NE | S,N | All | 9 | SE-S | I | ≤6m/s | 15 | W-NW | All | All |
| 4 | N-NE | I | ≤2m/s | 10 | SE-S | I | >6m/s | 16 | NW-N | S,N | All |
| 5 | N-NE | I | >2m/s | 11 | S-SW | S,N | All | 17 | NW-N | I | ≤6m/s |
| 6 | E-SE | S,N | All | 12 | S-SW | I | ≤6m/s | 18 | NW-N | I | >6m/s |

Table II. Definition of the meteorological classes as a function of wind direction, stability (I=unstable, N=neutral, S=stable), and wind speed conditions.

| Comb. Class | Meteo Class | hour-type Class | Comb. Class | Meteo Class | hour-type Class | Comb. Class | Meteo Class | hour-type Class |
|---|---|---|---|---|---|---|---|---|
| 1 | 1 | All | 20 | 7 | 5 | 39 | 13 | 4 |
| 2 | 2 | 1 | 21 | 8 | 1 | 40 | 13 | 5 |
| 3 | 2 | 2 | 22 | 8 | 2-3-4-5 | 41 | 14 | 1 |
| 4 | 2 | 3 | 23 | 9 | 1 | 42 | 14 | 2 |
| 5 | 2 | 4 | 24 | 9 | 2 | 43 | 14 | 3 |
| 6 | 2 | 5 | 25 | 9 | 3 | 44 | 14 | 4 |
| 7 | 3 | All | 26 | 9 | 4 | 45 | 14 | 5 |
| 8 | 4 | All | 27 | 9 | 5 | 46 | 15 | 1 |
| 9 | 5 | 1 | 28 | 10 | All | 47 | 15 | 2 |
| 10 | 5 | 2 | 29 | 11 | 1 | 48 | 15 | 3 |
| 11 | 5 | 3 | 30 | 11 | 2-3-4-5 | 49 | 15 | 4 |
| 12 | 5 | 4 | 31 | 12 | 1 | 50 | 15 | 5 |
| 13 | 5 | 5 | 32 | 12 | 2 | 51 | 16 | All |
| 14 | 6 | 1 | 33 | 12 | 3 | 52 | 17 | 1 |
| 15 | 6 | 2-3-4-5 | 34 | 12 | 4 | 53 | 17 | 2 |
| 16 | 7 | 1 | 35 | 12 | 5 | 54 | 17 | 3 |
| 17 | 7 | 2 | 36 | 13 | 1 | 55 | 17 | 4 |
| 18 | 7 | 3 | 37 | 13 | 2 | 56 | 17 | 5 |
| 19 | 7 | 4 | 38 | 13 | 3 | 57 | 18 | All |

Table III

Definition of the 57 combined classes on the basis of the 18 different meteorological classes and the 5 hour-of day classes.

| Comb. Class | Meteorological Class at time t+1 | | | | | | | | | | | | | | | | | |
|---|---|---|---|---|---|---|---|---|---|---|---|---|---|---|---|---|---|---|
| α at time t | 1 | 2 | 3 | 4 | 5 | 6 | 7 | 8 | 9 | 10 | 11 | 12 | 13 | 14 | 15 | 16 | 17 | 18 |
| 1 | .50 | .12 | .09 | .00 | .00 | .03 | .00 | .03 | .03 | .00 | .00 | .00 | .00 | .00 | .03 | .15 | .03 | .00 |
| 2 | .09 | .56 | .03 | .06 | .09 | .00 | .06 | .00 | .00 | .00 | .03 | .03 | .00 | .00 | .00 | .03 | .03 | .00 |
| 3 | .11 | .74 | .03 | .03 | .05 | .00 | .00 | .00 | .00 | .00 | .00 | .00 | .00 | .00 | .00 | .00 | .05 | .00 |
| 4 | .00 | .57 | .00 | .17 | .17 | .00 | .00 | .00 | .04 | .00 | .00 | .00 | .00 | .00 | .00 | .00 | .00 | .04 |
| 5 | .00 | .65 | .00 | .04 | .15 | .00 | .08 | .00 | .00 | .00 | .00 | .00 | .00 | .00 | .00 | .00 | .04 | .04 |
| 6 | .00 | .57 | .00 | .00 | .25 | .00 | .04 | .00 | .00 | .00 | .00 | .04 | .00 | .00 | .00 | .00 | .11 | .00 |
| 7 | .08 | .00 | .50 | .10 | .08 | .18 | .04 | .02 | .00 | .00 | .00 | .00 | .00 | .00 | .00 | .00 | .00 | .00 |
| 8 | .00 | .27 | .07 | .20 | .17 | .03 | .20 | .00 | .03 | .00 | .00 | .00 | .00 | .00 | .00 | .00 | .03 | .00 |
| 9 | .00 | .07 | .17 | .00 | .57 | .03 | .17 | .00 | .00 | .00 | .00 | .00 | .00 | .00 | .00 | .00 | .00 | .00 |
| 10 | .00 | .04 | .07 | .00 | .57 | .04 | .25 | .04 | .00 | .00 | .00 | .00 | .00 | .00 | .00 | .00 | .00 | .00 |
| 11 | .00 | .09 | .00 | .00 | .73 | .00 | .14 | .00 | .00 | .00 | .00 | .05 | .00 | .00 | .00 | .00 | .00 | .00 |
| 12 | .00 | .12 | .00 | .00 | .53 | .00 | .35 | .00 | .00 | .00 | .00 | .00 | .00 | .00 | .00 | .00 | .00 | .00 |
| 13 | .00 | .04 | .00 | .04 | .74 | .00 | .06 | .00 | .04 | .02 | .00 | .02 | .00 | .02 | .00 | .00 | .00 | .00 |
| 14 | .02 | .00 | .06 | .00 | .00 | .55 | .08 | .18 | .04 | .00 | .04 | .00 | .00 | .00 | .00 | .00 | .02 | .00 |
| 15 | .00 | .03 | .05 | .00 | .00 | .46 | .08 | .27 | .03 | .00 | .03 | .03 | .00 | .00 | .00 | .03 | .00 | .00 |
| 16 | .00 | .05 | .03 | .05 | .05 | .11 | .57 | .03 | .08 | .00 | .03 | .00 | .00 | .00 | .00 | .00 | .00 | .00 |
| 17 | .00 | .05 | .00 | .05 | .05 | .15 | .60 | .05 | .05 | .00 | .00 | .00 | .00 | .00 | .00 | .00 | .00 | .00 |
| 18 | .00 | .00 | .00 | .05 | .20 | .05 | .40 | .00 | .25 | .00 | .00 | .00 | .00 | .00 | .05 | .00 | .00 | .00 |
| 19 | .00 | .04 | .00 | .04 | .11 | .00 | .46 | .04 | .21 | .04 | .00 | .04 | .04 | .00 | .00 | .00 | .00 | .00 |
| 20 | .00 | .00 | .00 | .02 | .09 | .02 | .67 | .00 | .14 | .02 | .00 | .00 | .00 | .00 | .00 | .00 | .02 | .00 |
| 21 | .00 | .00 | .02 | .00 | .00 | .05 | .01 | .49 | .07 | .00 | .28 | .07 | .01 | .00 | .00 | .01 | .00 | .00 |
| 22 | .00 | .00 | .00 | .00 | .00 | .04 | .01 | .50 | .16 | .01 | .14 | .11 | .00 | .00 | .01 | .00 | .00 | .00 |
| 23 | .00 | .00 | .00 | .00 | .05 | .05 | .11 | .05 | .26 | .05 | .26 | .16 | .00 | .00 | .00 | .00 | .00 | .00 |
| 24 | .00 | .05 | .00 | .00 | .00 | .05 | .00 | .10 | .40 | .00 | .00 | .40 | .00 | .00 | .00 | .00 | .00 | .00 |
| 25 | .00 | .00 | .00 | .00 | .00 | .07 | .07 | .33 | .40 | .00 | .00 | .07 | .07 | .00 | .00 | .00 | .00 | .00 |
| 26 | .00 | .00 | .00 | .00 | .00 | .00 | .08 | .04 | .48 | .12 | .00 | .24 | .04 | .00 | .00 | .00 | .00 | .00 |
| 27 | .00 | .00 | .00 | .00 | .00 | .00 | .30 | .00 | .37 | .10 | .00 | .20 | .00 | .00 | .00 | .00 | .03 | .00 |
| 28 | .00 | .00 | .00 | .00 | .00 | .00 | .03 | .11 | .14 | .40 | .03 | .09 | .14 | .03 | .03 | .00 | .00 | .00 |
| 29 | .00 | .00 | .01 | .00 | .00 | .02 | .00 | .17 | .00 | .00 | .64 | .06 | .04 | .05 | .01 | .00 | .00 | .00 |
| 30 | .00 | .00 | .00 | .00 | .00 | .00 | .00 | .12 | .00 | .00 | .35 | .41 | .03 | .06 | .03 | .00 | .00 | .00 |
| 31 | .00 | .00 | .00 | .00 | .00 | .00 | .00 | .03 | .04 | .00 | .24 | .54 | .04 | .06 | .00 | .03 | .01 | .00 |
| 32 | .00 | .00 | .00 | .00 | .00 | .00 | .02 | .06 | .04 | .00 | .08 | .63 | .06 | .06 | .04 | .00 | .00 | .00 |
| 33 | .00 | .03 | .00 | .00 | .00 | .00 | .00 | .05 | .03 | .00 | .03 | .56 | .13 | .15 | .03 | .00 | .00 | .00 |
| 34 | .00 | .02 | .00 | .00 | .00 | .00 | .02 | .00 | .11 | .02 | .00 | .49 | .17 | .11 | .00 | .02 | .04 | .00 |
| 35 | .02 | .00 | .00 | .00 | .03 | .00 | .00 | .02 | .14 | .00 | .00 | .61 | .12 | .05 | .00 | .00 | .03 | .00 |
| 36 | .00 | .00 | .00 | .00 | .00 | .00 | .00 | .00 | .00 | .04 | .19 | .15 | .52 | .11 | .00 | .00 | .00 | .00 |
| 37 | .00 | .00 | .00 | .00 | .00 | .00 | .00 | .06 | .00 | .00 | .06 | .19 | .69 | .00 | .00 | .00 | .00 | .00 |
| 38 | .00 | .00 | .00 | .00 | .00 | .00 | .00 | .04 | .00 | .04 | .00 | .17 | .71 | .04 | .00 | .00 | .00 | .00 |
| 39 | .00 | .00 | .00 | .00 | .00 | .00 | .00 | .00 | .00 | .18 | .00 | .05 | .68 | .09 | .00 | .00 | .00 | .00 |
| 40 | .00 | .00 | .00 | .00 | .00 | .00 | .00 | .00 | .02 | .06 | .00 | .10 | .72 | .10 | .00 | .00 | .00 | .00 |
| 41 | .00 | .00 | .00 | .00 | .00 | .03 | .00 | .00 | .00 | .00 | .09 | .09 | .00 | .59 | .18 | .00 | .00 | .03 |
| 42 | .00 | .03 | .00 | .00 | .00 | .09 | .03 | .00 | .00 | .00 | .00 | .09 | .00 | .55 | .18 | .03 | .00 | .00 |
| 43 | .00 | .00 | .00 | .00 | .00 | .06 | .00 | .00 | .00 | .00 | .00 | .06 | .06 | .69 | .13 | .00 | .00 | .00 |
| 44 | .00 | .04 | .00 | .00 | .00 | .00 | .00 | .00 | .00 | .00 | .04 | .15 | .00 | .52 | .19 | .00 | .07 | .00 |
| 45 | .00 | .02 | .00 | .00 | .02 | .00 | .00 | .00 | .00 | .00 | .00 | .16 | .02 | .63 | .12 | .00 | .02 | .00 |
| 46 | .00 | .00 | .00 | .00 | .00 | .00 | .00 | .00 | .00 | .00 | .05 | .03 | .00 | .13 | .66 | .11 | .03 | .00 |
| 47 | .00 | .00 | .00 | .04 | .04 | .00 | .00 | .08 | .00 | .00 | .00 | .08 | .00 | .04 | .58 | .00 | .15 | .00 |
| 48 | .00 | .00 | .00 | .00 | .00 | .00 | .00 | .00 | .04 | .00 | .00 | .00 | .00 | .19 | .59 | .00 | .19 | .00 |
| 49 | .00 | .00 | .00 | .00 | .04 | .00 | .00 | .00 | .00 | .00 | .00 | .04 | .00 | .08 | .60 | .00 | .20 | .04 |
| 50 | .00 | .00 | .00 | .02 | .02 | .00 | .00 | .00 | .00 | .00 | .00 | .05 | .00 | .12 | .67 | .00 | .09 | .02 |
| 51 | .06 | .04 | .00 | .00 | .00 | .00 | .00 | .00 | .00 | .00 | .00 | .00 | .00 | .02 | .11 | .51 | .26 | .00 |
| 52 | .02 | .05 | .00 | .00 | .00 | .00 | .00 | .00 | .00 | .00 | .00 | .00 | .00 | .00 | .05 | .11 | .77 | .00 |
| 53 | .00 | .15 | .00 | .00 | .00 | .00 | .00 | .00 | .00 | .00 | .00 | .00 | .00 | .03 | .09 | .06 | .68 | .00 |
| 54 | .00 | .13 | .03 | .00 | .03 | .00 | .00 | .00 | .06 | .00 | .00 | .00 | .00 | .00 | .06 | .00 | .68 | .00 |
| 55 | .00 | .05 | .00 | .00 | .00 | .00 | .00 | .00 | .00 | .00 | .00 | .00 | .00 | .00 | .08 | .00 | .82 | .05 |
| 56 | .00 | .08 | .00 | .01 | .00 | .00 | .00 | .00 | .00 | .00 | .00 | .01 | .00 | .00 | .08 | .00 | .72 | .08 |
| 57 | .00 | .09 | .00 | .00 | .00 | .00 | .00 | .00 | .00 | .00 | .00 | .00 | .00 | .00 | .09 | .00 | .20 | .63 |

Table IV. Estimates of the probabilities, for each combined class at time t, of occurrence at time t+1 of the 18 meteorological classes.

| Comb. Cl. α | $\underset{\sim}{\Phi}_\alpha$ Elements | | | | | | | | | | | |
|---|---|---|---|---|---|---|---|---|---|---|---|---|
| | (1,1) | (1,2) | (1,3) | (1,4) | (2,1) | (2,2) | (2,3) | (2,4) | (3,1) | (3,2) | (3,3) | (3,4) |
| 1 | .902 | .018 | -.005 | .001 | .650 | .515 | -.081 | .008 | .063 | -.015 | 1.167 | -.001 |
| 2 | 1.433 | -.118 | -.049 | .003 | .560 | .713 | -.075 | .005 | -.019 | -.092 | .762 | .004 |
| 3 | .795 | .131 | -.018 | .001 | 1.272 | .648 | .068 | -.002 | .087 | -.182 | .677 | .005 |
| 4 | 1.211 | .301 | -.040 | -.003 | .144 | 1.155 | -.008 | -.003 | .835 | -.314 | .673 | .025 |
| 5 | .846 | -.038 | -.055 | .004 | -.401 | 1.037 | .014 | .004 | .145 | .136 | .927 | .011 |
| 6 | .787 | .007 | .031 | .002 | .170 | .807 | -.072 | .004 | -.604 | .293 | .577 | .006 |
| 7 | .441 | -.000 | -.002 | .001 | -1.159 | .946 | -.054 | .006 | -.136 | .142 | .877 | -.001 |
| 8 | 1.111 | .027 | .034 | -.000 | .830 | .501 | .605 | -.001 | -.349 | .229 | .584 | .003 |
| 9 | .601 | .001 | .001 | .001 | .111 | .833 | .015 | .004 | 2.196 | -.082 | .733 | -.002 |
| 10 | 1.169 | -.009 | -.014 | -.000 | -1.928 | .978 | .052 | .011 | 2.175 | -.013 | .596 | -.005 |
| 11 | .878 | -.039 | -.032 | .001 | -.028 | .511 | -.022 | .004 | 3.169 | .216 | .794 | -.006 |
| 12 | .657 | -.010 | .012 | .001 | .250 | .612 | .033 | .005 | 1.341 | -.113 | .886 | -.001 |
| 13 | .761 | -.056 | .010 | .002 | .050 | .291 | .027 | .015 | .969 | -.039 | .910 | -.006 |
| 14 | .769 | .001 | .004 | .001 | .241 | .603 | -.033 | .003 | -.269 | -.010 | .798 | .002 |
| 15 | .594 | .036 | .006 | .001 | -.399 | 1.136 | -.061 | .001 | -.111 | -.089 | .623 | .006 |
| 16 | .166 | .000 | .164 | .001 | -.170 | .658 | .106 | .005 | .195 | .003 | 2.008 | -.005 |
| 17 | .361 | -.006 | .056 | .001 | .124 | .804 | -.562 | .018 | -1.043 | .038 | 1.474 | -.000 |
| 18 | .285 | .002 | .090 | .002 | 1.493 | .714 | -.047 | -.002 | -.369 | .072 | .931 | .002 |
| 19 | .896 | -.042 | -.045 | .002 | .015 | .627 | -.069 | .004 | .633 | -.306 | .683 | .008 |
| 20 | .879 | .066 | .070 | -.002 | .511 | .748 | -.013 | .000 | .547 | .061 | .774 | -.002 |
| 21 | .493 | .052 | -.002 | .002 | -.036 | .316 | -.002 | .002 | 2.433 | -.224 | .793 | -.003 |
| 22 | .687 | .083 | .001 | .001 | .013 | .278 | -.009 | .002 | .987 | -.029 | .908 | -.002 |
| 23 | .339 | .057 | .019 | .002 | -.002 | .382 | .005 | .001 | -.139 | .228 | 1.138 | .002 |
| 24 | 1.187 | -.191 | .101 | -.000 | .416 | .657 | .008 | -.001 | -.298 | -.520 | 1.078 | .007 |
| 25 | 1.012 | -.155 | -.055 | .004 | -.009 | .691 | .013 | .002 | 1.120 | -.289 | .510 | .005 |
| 26 | .873 | .067 | -.007 | .001 | -.025 | .986 | -.023 | .001 | -.146 | -.019 | .680 | .013 |
| 27 | .940 | .002 | -.059 | .002 | -.022 | .749 | -.070 | .006 | .046 | .082 | .838 | .003 |
| 28 | .283 | .084 | -.000 | .001 | -.057 | .936 | .044 | -.001 | .060 | .021 | .274 | .004 |
| 29 | .698 | .106 | .010 | .002 | .065 | .682 | .003 | .001 | .167 | -.796 | .831 | .005 |
| 30 | 1.002 | .260 | -.010 | -.001 | .090 | .640 | -.004 | .001 | -.054 | -.080 | .466 | .003 |
| 31 | 1.209 | .242 | .002 | -.001 | .019 | .760 | -.008 | .001 | -.773 | .035 | .669 | .010 |
| 32 | .828 | -.018 | -.006 | .003 | .161 | .483 | -.003 | .002 | .106 | -.377 | 1.104 | .001 |
| 33 | 1.322 | -.499 | .051 | .002 | .915 | -.056 | .042 | -.001 | .925 | -.598 | .842 | .000 |
| 34 | .949 | -.070 | .039 | .002 | .135 | .603 | -.008 | .002 | -.081 | -.025 | .757 | .011 |
| 35 | .701 | -.049 | -.042 | .006 | .061 | .617 | .015 | .001 | -.151 | .382 | .865 | .004 |
| 36 | .744 | -.135 | -.018 | .003 | -.007 | .749 | -.037 | .002 | -.817 | -1.033 | .364 | .020 |
| 37 | 1.002 | -.543 | .065 | .003 | .005 | .214 | .027 | .002 | -.178 | -.190 | .274 | .007 |
| 38 | .585 | .022 | .142 | .001 | .158 | .355 | -.037 | .002 | .247 | -.010 | .923 | -.001 |
| 39 | .630 | .011 | .043 | .001 | .110 | .487 | .053 | .001 | -.655 | -.109 | .361 | .009 |
| 40 | .632 | -.012 | -.041 | .003 | -.242 | 1.024 | -.062 | .003 | .024 | -.094 | .417 | .004 |
| 41 | .628 | .261 | .088 | .000 | -.043 | 1.114 | .194 | -.001 | .023 | .096 | 1.088 | -.001 |
| 42 | .617 | .162 | .060 | .001 | -.022 | .478 | .006 | .002 | -.139 | .174 | .366 | .004 |
| 43 | .446 | .604 | .329 | -.002 | .144 | .232 | .008 | .001 | -.017 | .014 | .889 | .000 |
| 44 | .307 | .062 | .252 | .003 | .036 | 1.009 | .202 | -.001 | -.046 | .148 | .307 | .006 |
| 45 | .844 | .203 | -.151 | .002 | -.074 | .792 | -.088 | .003 | .039 | .576 | 1.087 | -.002 |
| 46 | 1.016 | -.381 | .133 | .000 | .039 | .653 | .063 | .001 | .027 | .051 | .366 | .002 |
| 47 | .336 | -.165 | .004 | .005 | -.002 | .026 | -.005 | .003 | -.029 | -.034 | .133 | .003 |
| 48 | .840 | .657 | .216 | -.002 | .001 | .790 | .567 | -.000 | -.042 | -.008 | .569 | .002 |
| 49 | 1.945 | .575 | .019 | -.005 | .038 | .643 | .007 | .000 | .184 | .403 | .116 | .000 |
| 50 | .701 | -.139 | .039 | .003 | .011 | .869 | -.017 | .000 | .130 | .028 | .179 | .002 |
| 51 | .744 | .198 | -.012 | -.001 | -.251 | .939 | -.004 | .002 | -.013 | .002 | 1.319 | -.001 |
| 52 | .402 | -.002 | .006 | .002 | -.715 | 1.343 | -.008 | .003 | .093 | -.040 | .175 | .003 |
| 53 | .420 | -.014 | -.013 | .003 | -.405 | .758 | -.052 | .006 | -.079 | .149 | .387 | .002 |
| 54 | 1.170 | .572 | -.143 | -.003 | .357 | 1.032 | -.091 | -.001 | -.507 | .393 | .856 | .003 |
| 55 | .503 | .180 | -.037 | .003 | .156 | .550 | .090 | .002 | .056 | .122 | .899 | .001 |
| 56 | .772 | .041 | -.011 | .001 | -.111 | .670 | .122 | .002 | .167 | .447 | .861 | -.002 |
| 57 | .315 | -.040 | -.007 | .003 | -.002 | .811 | -.011 | .001 | .029 | -.826 | .264 | .009 |

Table V. $\underset{\sim}{\Phi}_\alpha$ transition matrices for each combined class α. The fourth row of each matrix is identically 0 0 0 1.

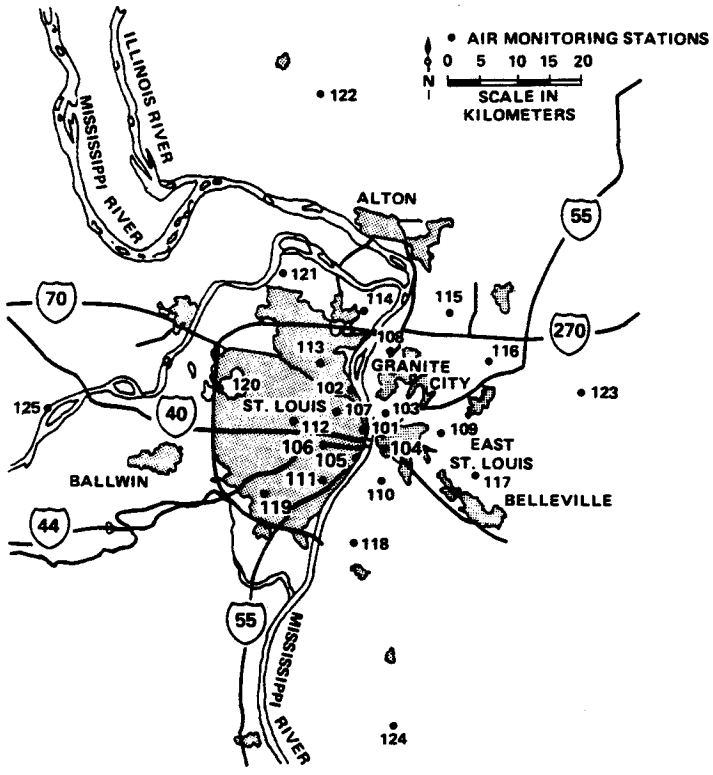


Figure 1. RAMS network installed in St. Louis Missouri (Environmental Protection Agency's Regional Air Pollution Study).

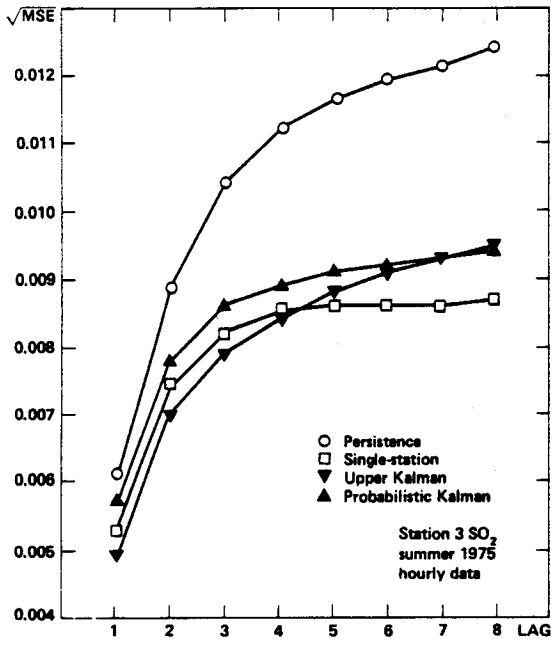


Fig. 2a

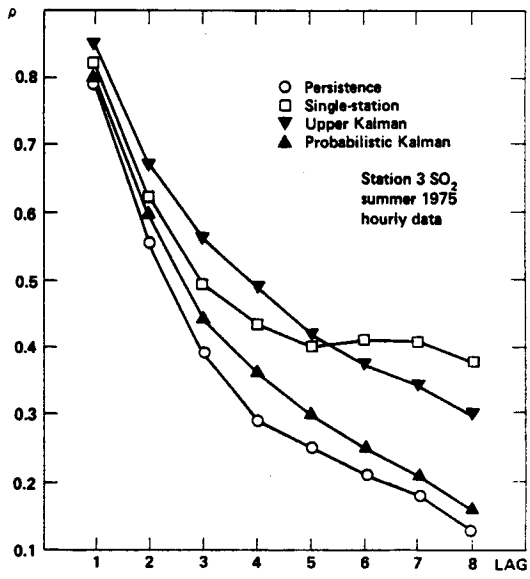


Fig. 2b

Figure 2 Root mean square error (a) and correlation coefficient (b) between measured and forecasted data, for different forecasting lags, of the following models: concentration persistence (0), single-station predictor (□), Kalman filter upper bound (▼) and probabilistic bound (▲). Data of Station 3.

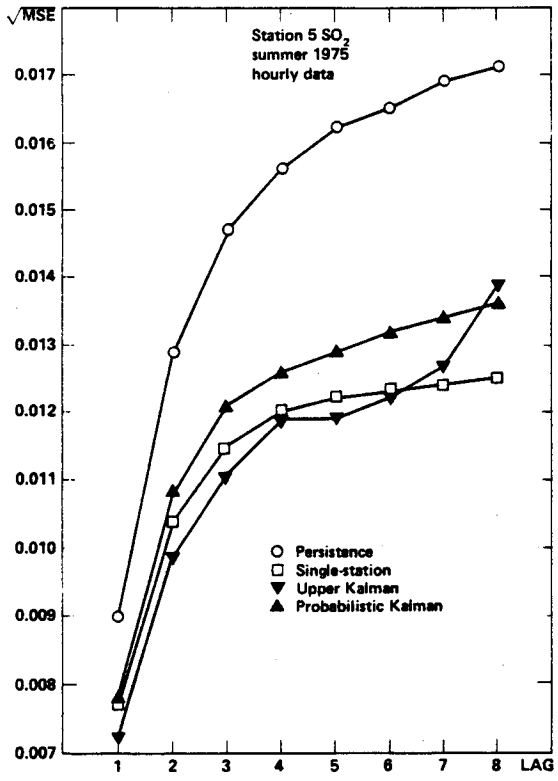


Fig. 3a

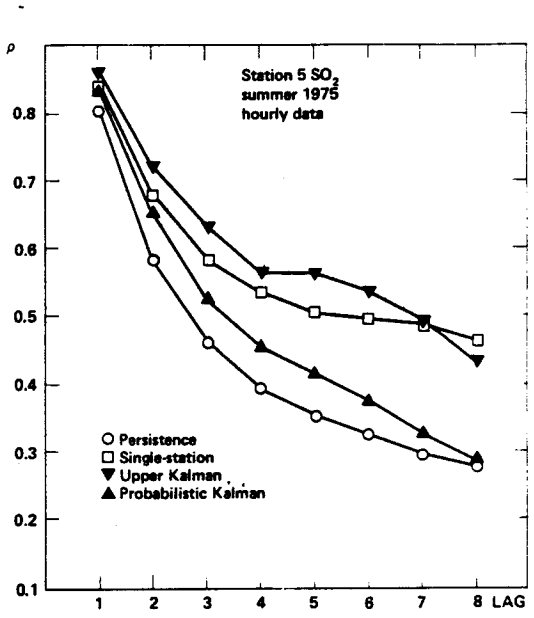


Fig. 3b

Figure 3 Same as Figure 2 for Station 5.

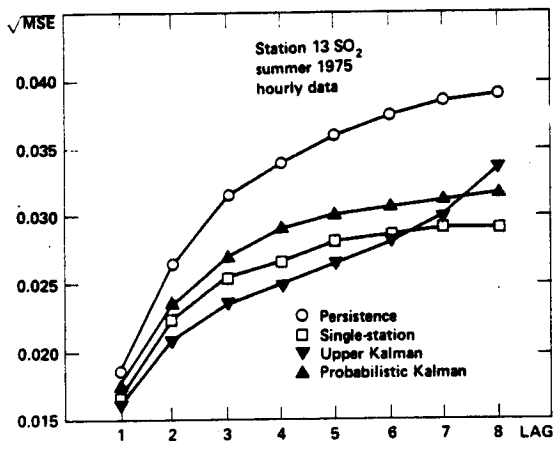


Fig. 4a

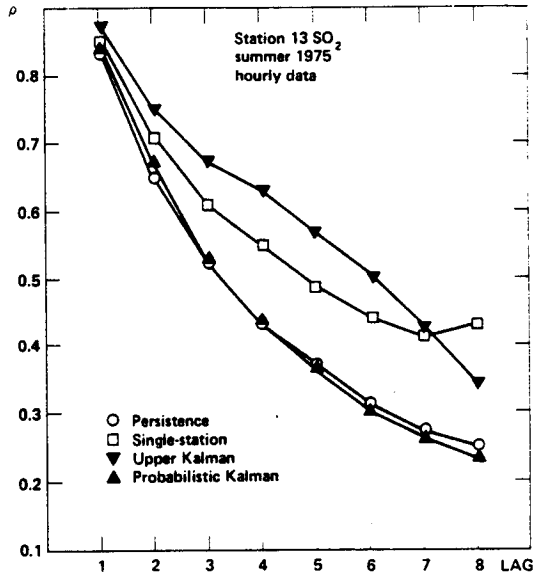


Fig. 4a

Figure 4 Same as Figure 2 for Station 13.

# SCIENTIFIC CENTER REPORT INDEXING INFORMATION

| | | | |
|---|---|---|---|
| 1. AUTHOR(S) : P. Zannetti and P. Switzer | | | 9. SUBJECT INDEX TERMS 16 Mathematics |
| 2. TITLE : The Kalman Filtering Method and its Application to Air Pollution Episode Forecasting | | | |
| 3. ORIGINATING DEPARTMENT Palo Alto Scientific Center | | | |
| 4. REPORT NUMBER G320-3381 | | | |
| 5a. NUMBER OF PAGES 27 | 5b. NUMBER OF REFERENCES 9 | | |
| 6a. DATE COMPLETED January 1979 | 6b. DATE OF INITIAL PRINTING April 1979 | 6c. DATE OF LAST PRINTING | |


7. ABSTRACT :

This paper presents an application of the Kalman filtering method to multi-station air pollution modeling in order to obtain a useful real-time predictor of concentration levels, especially during episode situations. Special attention has been paid to avoiding certain high dimensionality problems of the Kalman filter while still retaining some of the deterministic "physical" information of the transport and diffusion phenomena. Moreover, a method is proposed to forecast future state values using only a probabilistic knowledge of future state-transition matrices, which is the most common situation in air pollution real-time forecasting with probabilistic meteorological input. Specifically, the method is applied to $SO_2$ and meteorological data (Summer 1975) supplied by the RAMS network (Environmental Protection Agency's Regional Air Pollution Study) installed in the St. Louis Missouri area. The results of the proposed methodology are compared with those supplied by single-station predictors.


8. REMARKS : This paper is a more extended version of the article (same title) accepted for presentation at the APCA Speciality Conference "Quality assurance in air pollution measurement", March 11-14, 1979, Grand Hotel, New Orleans, LA.

# APPENDIX D

"Simulation of Transformation, Buoyancy and Removal Processes by Lagrangian Particle Methods"

14th International Technical Meeting on Air Pollution Modeling and its Application. Copenhagen, Denmark, 27-30 September, 1983.

# SIMULATION OF TRANSFORMATION, BUOYANCY AND REMOVAL PROCESSES BY LAGRANGIAN PARTICLE METHODS

Paolo Zannetti(*) and Nazik Al-Madani

Environmental and Earth Sciences Division
Kuwait Institute for Scientific Research
P.O.Box 24885, Safat, KUWAIT

## INTRODUCTION AND SUMMARY

Particle methods (Hockney and Eastwood, 1981) are the most recent and advanced numerical tools for computer modeling of dynamic systems. They seem particularly successful in simulating turbulent fluid dynamics, due to their capability of incorporating semi-random components. Particle modeling of air pollution diffusion phenomena has recently become the subject of a great deal of investigation (e.g., Diehl et al., 1982; Legg and Raupach, 1982; Ley, 1982, Zannetti and Al-Madani, 1983). The promising results of these studies are, however, accompanied by the persisting difficulty of properly evaluating Lagrangian velocity statistics from Eulerian measurements (see Davis, 1982). Nevertheless, particle methods provide outstanding advantages over other air pollution diffusion modeling techniques, such as Gaussian models and grid models, as discussed below.

Atmospheric diffusion processes are characterized by turbulent eddies in which the motion of different air parcels is strongly auto-and cross-correlated. With simulation particles, the computer modeling of these eddies would, therefore, require the expensive computation of the interactions between each particle and its surrounding ones. A different approach can be followed if only ensemble averages need to be computed. In this case, in fact, each simulation particle can move independently from the others and its motion can be very realistically simulated by semi-random

(*) On leave of absence from AeroVironment Inc., 145 Vista Ave., Pasadena, CA 91107, USA.

fluctuations generated by computer Monte-Carlo techniques. These Lagrangian simulations with stochastic components seem extremely useful for at least reproducing such phenomena, as atmospheric turbulent diffusion, whose physical mechanism is too complex to be simulated by deterministic techniques.

A need exists to incorporate suitable numerical tools for the simulation of atmospheric phenomena besides turbulence into the Lagrangian particle methods. Therefore, this paper, after a few introductory remarks, discusses the definition and the computer implementation of special algorithms for the simulation of dynamic plume rise, chemical decay, and deposition-resuspension effects by particle methods. These algorithms have been incorporated into a prototype computer diffusion code (MC-LAGPAR, written in APL language) whose simulation results for a few test cases are presented and discussed.

## THE MODEL

In the atmospheric boundary layer, the dispersion of emitted gaseous material can be described by a suitable number of fictitious particles moving, at each time step, according to pseudo-velocities simulating (1) transport, (2) turbulent fluctuations, and (3) molecular diffusion (if not negligible). These pseudo-velocities do not intend to simulate the real trajectory of a specific pollutant parcel, but to provide realistic dynamics of the pollutant motion on an ensemble basis.

The pseudo-velocities are decomposed into two terms: the space-dependent average values $\bar{u}_x$, $\bar{u}_y$, $\bar{u}_z$ (which must be provided by a meteorological model or by an interpolation-extrapolation of meteorological measurements), plus the particle-dependent fluctuations. Different Monte-Carlo schemes have been proposed to calculate the fluctuations u', v', and w' of the pseudo-velocities (e.g., Watson and Barr, 1976; Hanna, 1981). To properly simulate the wind shear effects, Zannetti (1981) developed a scheme in which the pseudo-velocity fluctuations are auto-correlated (for all three components) and cross-correlated (between the vertical and along-wind fluctuations):

$$u'(t_2) = \phi_1 u'(t_1) + u''(t_2) \tag{1a}$$

$$v'(t_2) = \phi_2 v'(t_1) + v''(t_2) \tag{1b}$$

$$w'(t_2) = \phi_3 w'(t_1) + \phi_4 u'(t_2) + w''(t_2) \tag{1c}$$

In this scheme, the $\phi$ parameters and the intensities of the purely random components u", v", w" can be inferred from algebraical manipulations of known meteorological input parameters (intensities and correlations of the wind fluctuations).

In addition to transport and diffusion, particle methods can be used in a particularly effective way for providing a realistic treatment of buoyancy, chemical decay and ground deposition-resuspension effects. In the following sections, specific algorithms are proposed for the treatment of these special effects.

Dynamic Plume Rise

Particle methods provide a straightforward treatment of the dynamic plume rise. In fact, each emitted particle, tagged with its emission characteristics, can consume an increment of its initially supplied buoyancy F at each time step $\Delta t$:

$$\Delta F = \frac{\partial F}{\partial t} \Delta t \tag{2}$$

where $\partial F/\partial t$ is a function of meteorology (e.g., wind speed, temperature, stability). Each $\Delta F$ can then provide an additional vertical velocity

$$w_{pr} = f(\Delta F) \tag{3}$$

that moves each particle $w_{pr} \Delta t$ in the vertical direction, effectively simulating a dynamic plume rise.

Alternatively, a simpler computation can be performed rearranging existing semi-empirical plume rise formulas, as shown in the example below.

After the transformation $x = ut$, the TVA plume rise formula (Stern, 1976) can be written

$$\Delta h(t) = cF^{1/3}u^{-1/3}t^{2/3} \tag{4}$$

in which the constant c is

$$c(z) = 1.58 - 0.414 \frac{\partial \theta}{\partial z} \tag{5}$$

$\partial\theta/\partial z$ is the potential temperature gradient ($^{o}C/100$ m), F is the buoyancy ($m^4 s^{-3}$) and u is the wind speed ($ms^{-1}$).

Both c and u vary with z. This suggests an empirical dynamic two-step computation in which the trajectory

$$z(t) = H + \Delta h(t) \tag{6}$$

of each particle is computed by (2nd step)

$$z(t+\Delta t) \simeq z(t) + w_{pr}\,\Delta t \tag{7}$$

where

$$w_{pr} = \left(\frac{dz}{dt}\right)_{t+\Delta t/2} = \left(\frac{d\Delta h}{dt}\right)_{t+\Delta t/2}$$

$$\simeq c\left[z(t+\Delta t/2)\right]F^{1/3}\;\; u\left[z(t+\Delta t/2)\right]^{-1/3}\;\; \frac{2}{3}\,(t+\Delta t/2)^{-1/3} \tag{8}$$

and (1st step)

$$z(t+\Delta t/2) \simeq z(t) + \left(\frac{dz}{dt}\right)_t\;\; \Delta t/2 \tag{9}$$

where

$$\left(\frac{dz}{dt}\right)_t = \left(\frac{d\Delta h}{dt}\right)_t \simeq c\left[z(t)\right]F^{1/3}\;\; u\left[z(t)\right]^{-1/3}\;\; \frac{2}{3}\,t^{-1/3} \tag{10}$$

Emitted particles do not need to be provided with the same buoyancy. Actually, the extra vertical diffusion produced during plume rise will be realistically simulated by releasing particles with a buoyancy defined by

$$F = \bar{F} + F' \tag{11}$$

where $\bar{F}$ is the average value and F' is a random component (particle-dependent) of suitable intensity.

Chemical Decay

An exponential decay, taking into account all removal factors except ground deposition, can be performed at each time step. If the time scale of the phenomenon is $T_c$ (where $T_c$ can be a function

of the type of pollutant and of the meteorology) the probability of removal for each particle at each time step is

$$p_c = 1 - \exp(-\Delta t/T_c) \tag{12}$$

Consequently, $p_c n_p$ particles must be randomly cancelled from the computational domain, where $n_p$ is the current number of active (i.e., not cancelled or deposited) particles.

Ground Deposition-Resuspension

At the end of each time step, all active particle locations need to be tested to single out those particles (say $n_b$) that have been moved below terrain ($z<0$). Some of these $n_b$ particles will be reflected and the rest of them will be deposited on the ground. If $T_d$ is the time constant of this partial deposition process, each of the $n_b$ particles currently below the terrain has a probability of

$$p_d = 1 - \exp(-\Delta t/T_d) \tag{13}$$

to be deposited. Therefore, $p_d n_b$ randomly selected particles (among the previously identified $n_b$) will be deposited and the rest of them ($n_b - p_d n_b$) will be reflected.

Particles deposited on the ground can be resuspended back to the computational domain or permanently absorbed by the ground. If $n_d$ is the current number of deposited particles and $T_s$ is the time scale of the resuspension process, each of the $n_b$ particles has a probability of

$$p_s = 1 - \exp(-\Delta t/T_s) \tag{14}$$

to be resuspended. Therefore, at each time step, $p_s n_d$ particles will be resuspended; but, at the same time, if a particle remains deposited on the ground for a period of time greater than a critical value $T_{dmax}$, the particle will be permanently absorbed.

$T_d$, $T_s$ and $T_{dmax}$ are functions of the meteorology (especially the surface wind speed) and the characteristics of both the pollutant and the ground surface. The proper inference of these values allows

realistic diffusion simulations very difficult to obtain using other modeling techniques.

## THE MC-LAGPAR CODE

A prototype computer code written in APL has been developed that incorporates, among other things, the algorithms previously described. The code simulates the diffusion of a single puff in flat terrain with non-homogeneous non-stationary meteorological conditions. The code is fully grid-free, since the meteorological variables are inputted at selected altitudes and then linearly interpolated at each particle's elevation. In this way, abrupt variations of the meteorological input parameters (causing artificial shear effects) are avoided. Moreover, since the selected altitudes do not need to be equally spaced, any degree of resolution in inputting the meteorological values can be obtained.

The meteorological variables required at each altitude at each time step are:

- the average wind components $\bar{u}_x$, $\bar{u}_y$, $\bar{u}_z$
- the standard deviations $\sigma_{u'}$, $\sigma_{v'}$, and $\sigma_{w'}$ of the pseudo-velocities (u' and v' are the along-wind and the cross-wind components; w' is along z)
- the auto-correlations $r_{u'}$, $r_{v'}$, $r_{w'}$ of the pseudo-velocities
- the cross-correlation $r_{u'w'}$
- the potential temperature gradient $\partial\theta/\partial z$.

In addition to these, $T_c$, $T_d$, $T_s$, $T_{dmax}$ need to be inputted (a single value for the entire domain).

The time increment $\Delta t$ must be carefully chosen. All model parametrizations are independent from $\Delta t$, but nevertheless, abrupt variations of particle elevations should be avoided and w' $\Delta t$ values should be less than the length scale of the vertical variation of the meteorological input. Ten seconds is probably a reasonable upper limit value for $\Delta t$.

## COMPUTER SIMULATIONS

The MC-LAGPAR code has been applied for the simulation of a few test cases to provide a qualitative demonstration of the flexibility and the high degree of resolution of this numerical approach. Each simulation (150 steps of 10 seconds each) generates a puff of 100 particles at the source location. Particle locations (x,z) are

plotted every three time steps thus generating a continuous plume up to a few kilometers downwind of the source. The vertical dimension chosen was twice the horizontal one.

Fig. 1 shows a slightly buoyant plume released at an altitude of 100 m during dispersion conditions of moderate vertical turbulence. The wind speed is 1 $ms^{-1}$ at the ground and 4 $ms^{-1}$ at the top of the domain. The $\sigma_{u'}$ and $\sigma_{v'}$ parameters start with 0.5 $ms^{-1}$ at the ground to 1.0 $ms^{-1}$ at 100m, remaining constant above that level. The $\sigma_{w'}$ parameter has the same behaviour, i.e., from 0.2 $ms^{-1}$ at the ground to 0.5 $ms^{-1}$ at 100m. The autocorrelations $r_{u'}$, $r_{v'}$, and $r_{w'}$, are constant at 0.7, 0.7, and 0.5, respectively. The cross-correlation $r_{u'w'}$ increases from -0.3 at the ground to -0.1 at the top.

Fig. 2 shows the dynamics of an elevated (150m) hot plume during conditions of low vertical turbulence. Meteorological values are similar to the previous simulation, except $\sigma_{w'}$, which now grows from 0.1 $ms^{-1}$ at the ground to 0.35 $ms^{-1}$ at 100m, then decreasing to 0.15 $ms^{-1}$ at the top.

The simulation in Fig. 3 is very similar to the previous one. Now, however, an elevated inversion layer has been added by forcing $\sigma_{w'}$ equal to 0.1 $ms^{-1}$ and $\partial\theta/\partial z$ equal 2 $^{o}C/100m$ between 500m and 550m. Most particles have enough buoyancy to penetrate the inversion layer and be trapped inside. Only a few particles perforate the inversion layer reaching the more turbulent region above. This simulation is characterized by a very unusual result, i.e., the decrease of the plume's $\sigma_z$ with the downwind distance at 2 km from the source.

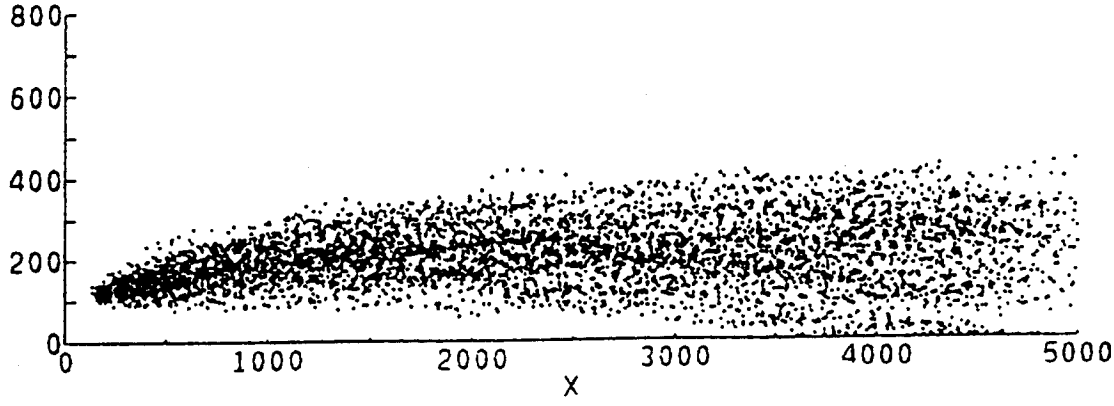


Fig. 1 - Simulation of a slightly buoyant elevated plume with moderate turbulence.

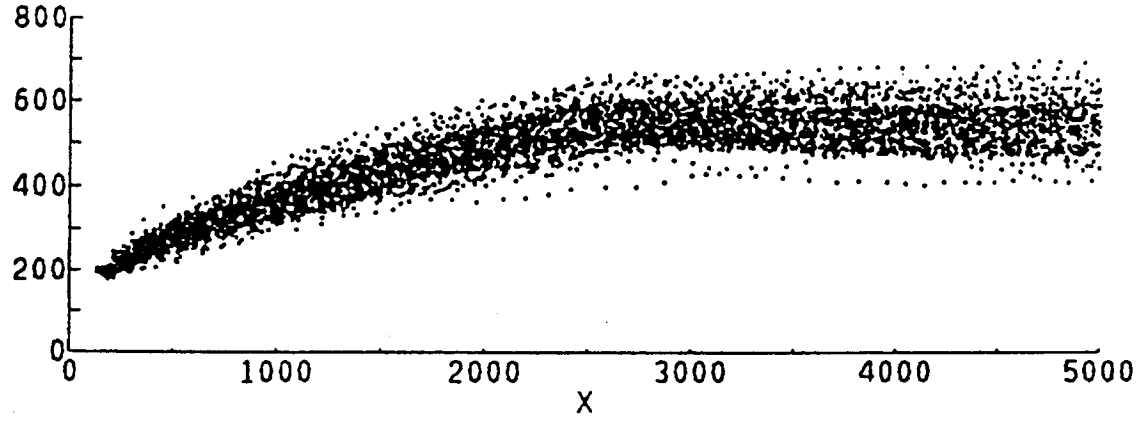


Fig. 2 - Simulation of a hot elevated plume with low turbulence.

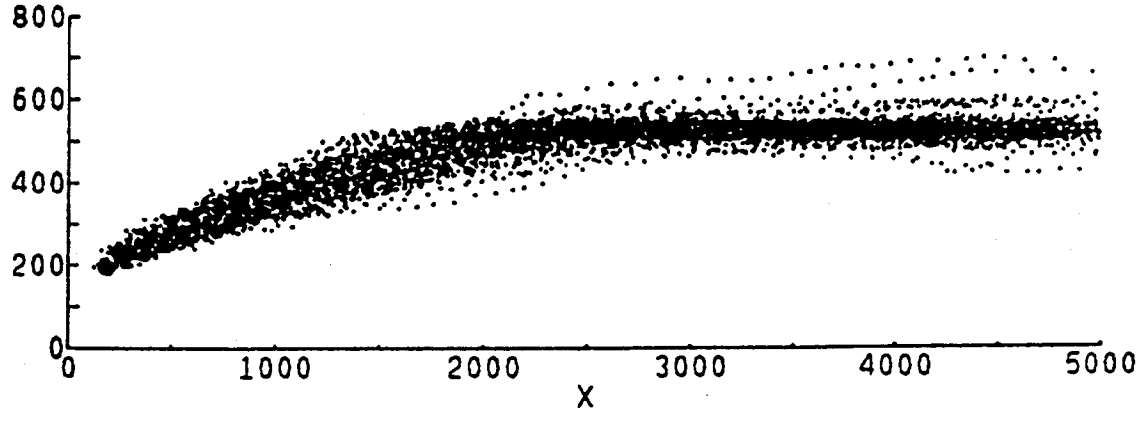


Fig. 3 - Simulation of a hot elevated plume with low turbulence and the presence of an elevated inversion layer between 500 m and 550 m.

Fig. 4 shows the release of a non-buoyant plume in moderate vertical turbulence in which $\sigma_w$, reaches its maximum (0.6 $ms^{-1}$) at 250m, just below an elevated inversion layer between 250 m and 300 m. With a non-buoyant plume, the inversion layer acts more like a reflection barrier for the particles, even though particle trapping effects are still evident.

Finally, Fig. 5 presents a low-level release (at 10 m) with slight buoyancy in moderate vertical turbulence. Deposition-resuspension phenomena are accounted for by $T_d$ = 10 s, $T_{dmax}$ = 50 s and $T_s$ = 1000 s. With these values, 23% of the emitted mass is found permanently deposited on the ground 1500 s from its release.

## CONCLUSIONS

Lagrangian particle methods applied to air pollution dispersion simulations can easily provide a degree of resolution and accuracy not obtainable by other simulation techniques. This method can also incorporate a realistic treatment of such phenomena as buoyancy and deposition-resuspension. This technique can be seen as a very "natural" and effective way of simulating atmospheric dispersion processes. In fact, whereas other modeling techniques operate a questionable discretization of the atmospheric turbulence into "stability" classes or require a meteorological input (e.g., the eddy diffusion coefficients K's) not directly measurable, the particle methods require meteorological input parameters (i.e., the pseudo-velocity statistics) that seem very close to the measurable wind statistics. Nevertheless, much investigation is still required to provide a fully acceptable method of relating Eulerian wind measurements to the required pseudo-velocity (Lagrangian) statistics.

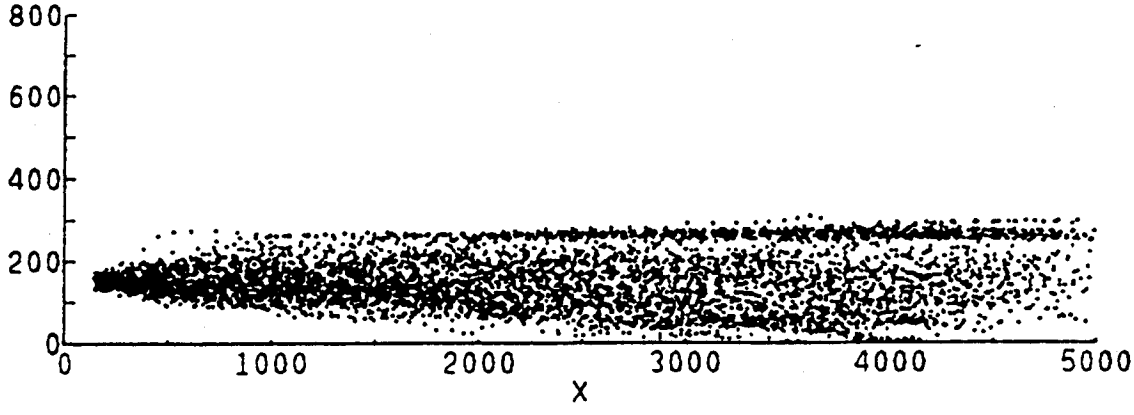


Fig. 4 - Simulation of a non-buoyant plume with moderate turbulence and the presence of an elavated inversion layer between 250 m and 300 m.

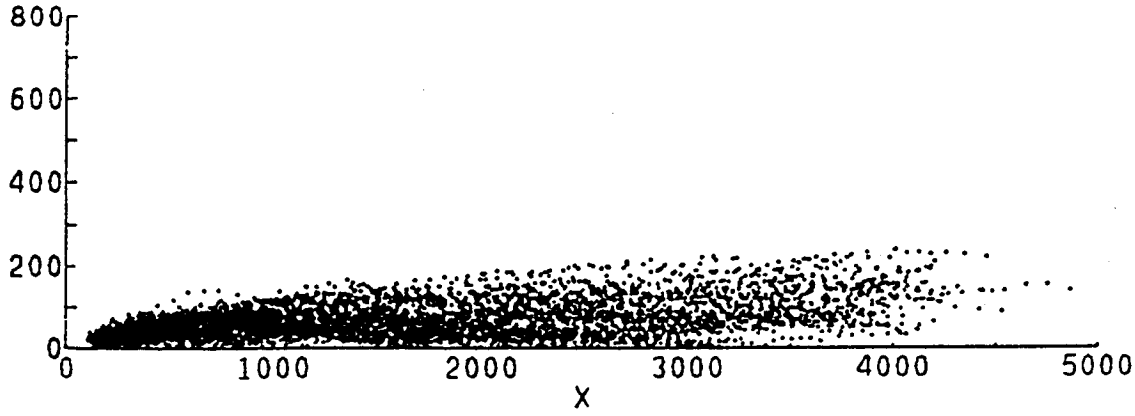


Fig. 5 - Simulation of a low-level release with slight buoyancy, moderate vertical turbulence, and deposition-resuspension effects.

REFERENCES

Davis, R. E., 1982, On Relating Eulerian and Lagrangian Velocity Statistics: Single Particles in Homogeneous Flows. J. Fluid Mech., 114, 1-26.

Diehl, S. R., Smith, D. T., and Sydor, M. 1982, Random-Walk Simulation of Gradient-Transfer Processes Applied to Dispersion of Stack Emission from Coal-Fired Power Plants. Journ. of Appl. Meteor., 21(1), 69-83.

Hanna, S. R., 1981, Lagrangian and Eulerian Time-Scale Relations in the Daytime Boundary Layer. Journ. of Appl. Meteor., 20 (3), 242-249.

Hockney, R. W., and Eastwood, J. W., 1981, Computer Simulations Using Particles. McGraw-Hill, Inc.

Legg, B. J., and Raupach, M. R., 1982, Markov-Chain Simulation of Particle Dispersion in Inhomogeneous Flows: the Mean Drift Velocity Induced by a Gradient in Eulerian Velocity Variance. Boundary-Layer Meteorology, 24, 3-13.

Ley, A. J., 1982, A Random Walk Simulation of Two-Dimensional Turbulent Diffusion in the Neutral Surface Layer. Atmos. Environ., 16(12), 2799-2808.

Stern, A. C., Ed., 1976, Air Pollution. Third Edition. Volume I p. 429-30. Academic Press.

Watson, C. W. and Barr, S., 1976, Monte-Carlo Simulation of the Turbulent Transport of Airborne Contaminants. Los Alamos Scientific Laboratory, Technical Report LA-6103.

Zannetti, P., 1981, Some Aspects of Monte-Carlo Type Modeling of Atmospheric Turbulent Diffusion. 7th Conference on Probability and Statistics in Atmospheric Sciences, AMS. Monterey, CA, Nov. 2-6, 1981.

Zannetti, P., and N. Al-Madani., 1983, Numerical Simulations of Lagrangian Particle Diffusion by Monte-Carlo Techniques. VIth World Congress on Air Quality (IUAPPA). Paris, May 16-20, 1983.

# APPENDIX E

"Particle Modeling Simulation of Atmospheric Dispersion Using the MC-LAGPAR Package"

# Particle Modeling Simulation of Atmospheric Dispersion using the MC-LAGPAR Package

G. Brusasca (1), G. Tinarelli (1), D. Anfossi (2), P. Zannetti (3)

(1) ENEL, Centro di Ricerca Termica e Nucleare, via Rubattino 54, 20134 Milano, Italy
(2) C.N.R. Istituto di Cosmogeofisica, Corso Fiume 4, 10133 Torino, Italy
(3) AeroVironment, Inc., 825 Myrtle Avenue, Monrovia, CA 91016, USA

ABSTRACT

A Monte Carlo model and computer code (MC-LAGPAR) for simulating atmospheric transport and diffusion of plumes are described. The turbulent diffusion is simulated by the semi-random motion of Lagrangian particles. The particles are emitted by a point source and dispersed in a computational domain by pseudo-velocities derived from vertical profiles of meteorological variables.

The MC-LAGPAR code includes the implementation of special algorithms for the simulation of a dynamic plume rise, chemical decay, deposition and resuspension effects. Furthermore, computer-graphics displays have been developed. The model, here used in its two dimensional version, is validated in the well-known case of homogeneous and stationary turbulence. In this case, we compared the concentration fields obtained by our model with those calculated by the known analytical solution. In both computations, the standard deviations of wind velocities are calculated according to the Taylor formulas.

In the nonhomogeneous case, the vertical structure of turbulence is parameterized according to the scheme suggested by Hanna. As an example of the non-homogeneous case, we present numerical simulations in convective (unstable) conditions in which the influence of updraughts and downdraughts is empirically taken into account.

KEYWORDS: Air pollution, Lagrangian modelling, Monte Carlo, Particle Models, Homogeneous and Nonhomogeneous turbulence.

## 1. INTRODUCTION

Atmospheric diffusion processes in the Planetary Boundary Layer (PBL) are strongly affected by phenomena characterized by turbulent eddies of different scales, i.e., semi-random atmospheric motion that is strongly auto- and cross-correlated. The emission of pollutants in the PBL, due to natural and anthropogenic sources, generates concentration fields whose evolution is strongly dependent upon the turbulent properties of the atmosphere.

Deterministic air quality models are an important tool for providing unambiguous source-receptor relationships, i.e., the assessment of the fraction of concentration caused by each source in each receptor area. In particular, only the use of a reliable deterministic simulation model allows the definition and implementation of appropriate and cost-effective emission control strategies in a certain region.

Dispersion models simulate: 1) atmospheric transport; 2) atmospheric turbulent diffusion; 3) chemical and photochemical processes; and 4) ground deposition (dry and/or wet).

Models can be divided into two main categories: Eulerian and Lagrangian models. Eulerian models (e.g., K-theory grid models, Mc Rae et al. [1]) use a fixed reference system, while Lagrangian models (e.g., puff models, Zannetti [2]) either use a reference system that travels with the average atmospheric motion (e.g., a photochemical Lagrangian box model, Drivas et al. [3]) or split the plumes into "elements" and calculate the separate dynamics of each element. This second category (Lagrangian models) seems to be the most appropriate for simulating atmospheric dispersion processes.

The most recent and powerful computational tool for the numerical discretization, in a Lagrangian frame, of a physical system is provided by particle modeling techniques (Hockney and Eastwood [4]). Using particle methods in air pollution applications, emitted polluting material is characterized by "fictitious" computer particles. Each particle is "moved" at each time step by pseudo-velocities, that take into account both the average wind transport and the (seemingly) random turbulent fluctuations of the wind components.

Several air quality studies have applied particles methods (Lamb [5], Lange [6], Hanna [7], De Baas et al. [8], Baerentsen and Berkowicz [9], McNider [10], Pielke et al. [11], Segal et al. [12]). Potentially, the method is superior in both numerical accuracy and physical representativeness. However, much research is still needed to extract, from meteorological measurements (most of them Eulerian ones) the Lagrangian input required to run these models, i.e., the generation scheme of the pseudo-velocities that move each particle at each time step. Most particle models use Monte-Carlo techniques (random number generation methods) to generate the pseudo-velocities.

The approach and formulation of one of the aforesaid models, i.e., MC-LAGPAR (Zannetti [13]) is described in the following section. Then, simulation outputs relative to cases of both homogeneous and nonhomogeneous turbulence are presented and discussed. Finally, conclusive remarks are provided in the last section.



*Paper received on 15 May 1987 and in final form on 10 September 1987.*
*Referees: Prof. Roger Pielke and Dr. Steve Hanna*

## 2. MC-LAGPAR MODEL

The MC-LAGPAR model was originally formulated (Zannetti [14]) to allow the simulation of air parcel motion with both autocorrelation and cross-correlation terms. In particular the method includes the (negative) cross-correlation $\overline{u'w'}$ between the horizontal (along wind) and vertical fluctuations of the wind vector. This term sometimes plays an important role and its inclusion provides better simulation capabilities in comparison with other particle models.

The basic scheme assumes that each particle is moved at each time step $\Delta t$ by a pseudo-velocity $\underline{V}(x,y,z,t,p)$ that is a function of space and time and that is particle dependent. If we assume that the x-axis is chosen along the average wind direction, it is $\underline{V}(\bar{u}+u',v',\bar{w}+w')$ where u', v' and w' are the fluctuations above the average values $\bar{u}$, 0, and $\bar{w}$, which are either known or available as an output of an Eulerian meteorological model. The fluctuations of each particle p are updated at each $\Delta t$ by the following Monte-Carlo scheme:

$$u'(t+\Delta t) = f_1 u'(t) + u''(t+\Delta t) \quad (1)$$

$$v'(t+\Delta t) = f_2 v'(t) + v''(t+\Delta t) \quad (2)$$

$$w'(t+\Delta t) = f_3 w'(t) + f_4 u'(t+\Delta t) + w''(t+\Delta t) \quad (3)$$

where u", v", w" are random values generated by Monte-Carlo methods. If the statistics of the fluctuations u', v', w' are known (i.e., variance, autocorrelation and cross-correlation $\overline{u'w'}$), the parameters $f_1$, $f_2$, $f_3$, $f_4$ and the variances of u", v", w" can be computed, for each particle at each time step, using algebraic manipulations (Zannetti [13]) :

$$f_1 = r_{u'} \quad (4)$$

$$f_2 = r_{v'} \quad (5)$$

$$f_3 = \frac{r_{w'} - f_1 r^2_{u'w'}}{1 - f_1^2 r^2_{u'w'}} \quad (6)$$

$$f_4 = \frac{r_{u'w'} \frac{\sigma_{w'}}{\sigma_{u'}} (1 - f_1 r_{w'})}{(1 - f_1^2 r^2_{u'w'})} \quad (7)$$

$$\sigma^2_{u''} = \sigma^2_{u'} (1 - f_1^2) \quad (8)$$

$$\sigma^2_{v''} = \sigma^2_{v'} (1 - f_2^2) \quad (9)$$

$$\sigma^2_{w''} = \sigma^2_{w'} (1 - f_3^2) - f_4^2 \sigma^2_{u'} - 2 f_1 f_2 f_4 r_{u'w'} \sigma_{u'} \sigma_{w'} \quad (10)$$

The MC-LAGPAR model has been recently expanded (Zannetti [15]) to incorporate all three cross-correlations $\overline{u'v'}$, $\overline{v'w'}$, $\overline{u'w'}$ in a generic (x,y,z) reference system. The simulations presented in this paper have been obtained, however, using the simpler scheme of Eqs. 1-3.

MC-LAGPAR incorporates several optional routines for the treatment of a dynamic plume rise ([16], [17], [18]); chemical decay, ground deposition/absorption/resuspension are taken into account with simple exponential formulas:

$$p_x = 1 - e^{\frac{-\Delta t}{T_x}}$$

where $p_x$ and $T_x$ are the probability and the time scale of removal or deposition or absorption or resuspension effects.

The model can simulate the nonstationary evolution of a single puff release or the behaviour of a continuously emitted plume in stationary conditions. The former case (single puff) is simulated by an instantaneous generation of particles with the same initial velocity fluctuations. It is commonly claimed that this generation allows the representation of relative diffusion, even though this assumption has been recently challenged (Hanna, personal communication). The latter case (continuous plume) is simulated by a continuous generation of particles with initial velocity fluctuations randomly extracted from the velocity distributions at the source heights. This assumption allows a correct simulation of the "ensemble" properties of the plume. In the rest of the paper we focus only on the simulation of a continuous plume, using assumptions that pertain to one-hour averaging times.

Particles hitting the ground are allowed to be reflected. In this case, however, the "memory" w' of the reflected particle is forced to change sign in order to correctly treat the reflection phenomena. A similar condition can be prescribed for the upper boundary.

The current version of the MC-LAGPAR computer code is written in APL. The code performs dispersion simulations in a three dimensional domain with flat terrain and requires emission and meteorological input. The meteorological input is dependent only upon the altitude and must be specified at user-selected elevations. This input is: the average wind components ( $\bar{u}$, $\bar{v}$, $\bar{w}$ ), the variances and autocorrelations of the fluctuations u', v' and w', the cross-correlation $\overline{u'w'}$, and the potential temperature gradient (only to calculate the plume rise). These user-specified values are linearly interpolated at each step to provide the values at each particle's elevation. Meteorological measurements can be used to directly or indirectly evaluate the above meteorological parameters. In particular, a set of suitable algorithms has been proposed (Hanna [19]) that provides the above variances and autocorrelations using the mixing height $h_i$, the Monin-Obukhov length L, the convective velocity scale $w_*$, the friction velocity $u_*$, the roughness length $z_o$, and the Coriolis parameter f ; all parameters can be either directly measured or evaluated from meteorological measurements. In addition, the $T_x$ time scales need to be inputted. Finally, the number of particles n and the time step $\Delta t$ of the simulation must be done.

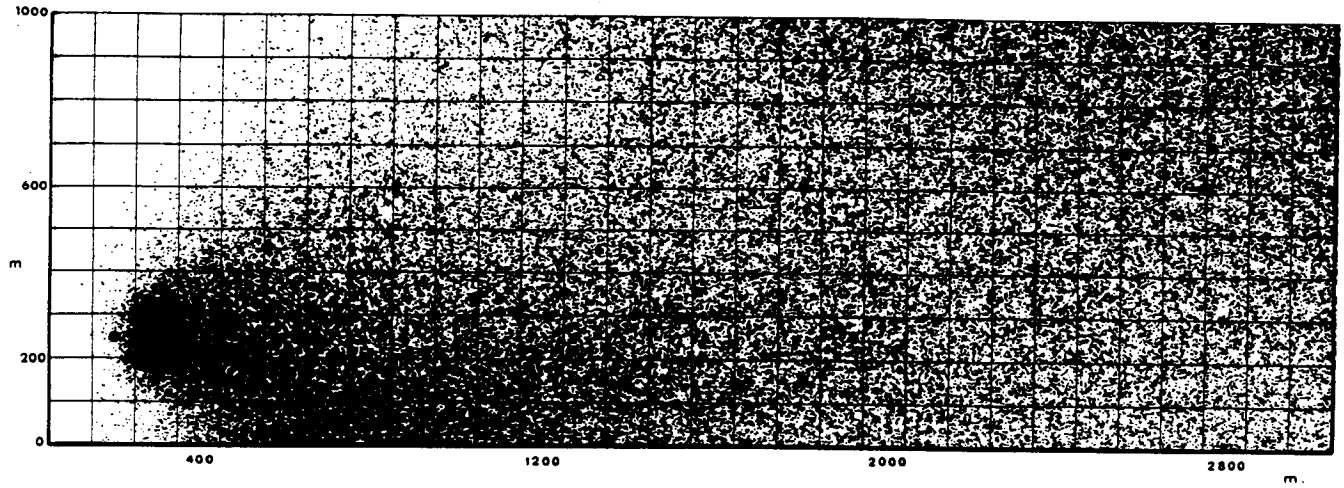


Fig. 1. Example of plume simulation in unstable condition with particle release at 250m.

The main output is a file containing the coordinates (x,y,z) of each particle at each time step. Using an interactive package (written in FORTRAN-77), it is possible to display the "puff" of particles (Fig. 1), to calculate and plot the concentration of pollutant on a suitably selected grid, to draw the isoconcentration lines on the x-y or x-z planes, to determine the standard deviations and centerline of the plume, and so on. Some examples of these possibilities are showed in the following figures.

## 3. SIMULATION OF HOMOGENEOUS TURBULENCE

When turbulence is homogeneous, its average properties are uniform in space. Therefore the turbulent statistics used in performing the simulations, i.e., $\sigma_{u'}$ and $\sigma_{w'}$ (the standard deviation of wind velocity fluctuations) and $T_L$ (the Lagrangian integral time scale), were kept constant with respect to the space coordinates.

It can be shown that MC-LAGPAR generates trajectories whose standard deviations reproduce quite well the particle displacements theoretically deduced by Taylor [20] :

$$\sigma_{Taylor}(n\cdot\Delta t) = 2\sigma_{u'} T_L^2 \left[ \frac{n\cdot\Delta t}{T_L} - \left( 1 - e^{\frac{-n\cdot\Delta T}{T_L}} \right) \right] \qquad (11)$$

Fig. 2 shows the result of this comparison. The agreement is noticeable.

Then, we performed the computation of the concentration field in the (x,z) plane of material continuously emitted by a point source. The parameters of the simulation were the following:

$H_s$ = 400m, $\bar{u}$ = 3m/s, $T_L$ = 144s, $\sigma_{u'} = \sigma_{w'}$ = 0.34m/s, $\Delta t$ = 60s

where $H_s$ is the source height and $\bar{u}$ is the wind speed. The dimensions of the grid cell used to compute the concentrations were defined by $\Delta x = u\cdot\Delta t$ = 180m and $\Delta z$ = 50m. The latter value ($\Delta z$ = 50m) seems to be the best choice in our case, and was evaluated by analyzing several simulations with $\Delta z$ in the range between 5m and 100m: the more the cell increases, the more the concentration tends to reduce its variability. However, $\Delta z$ cannot be too large in order to well represent ground-level concentrations with sufficient spatial resolution.

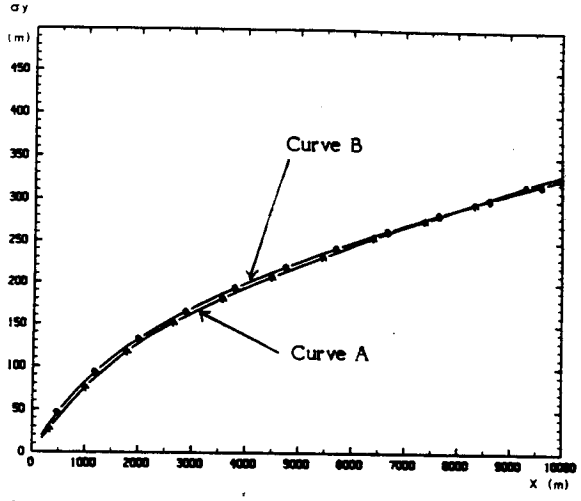


Fig. 2. Standard deviation along cross-wind direction as a function of downwind distance. Curve A: numerical simulation with 3000 particles. Curve B: Eq. 11.

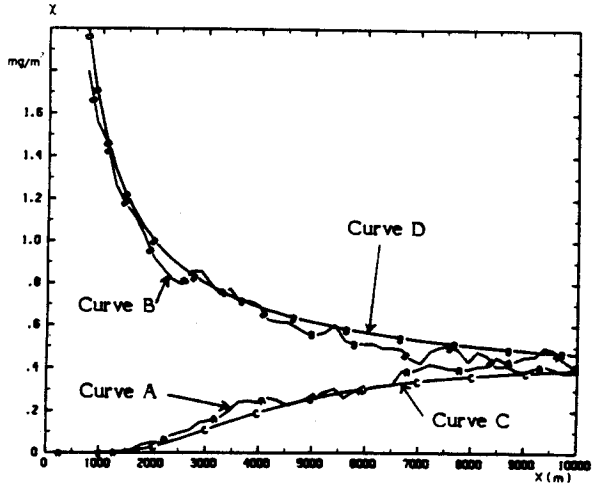


Fig. 3. Concentration as a function of a downwind distance.

Curve A: ground-level with MC-LAGPAR numerical simulation.
Curve B: centerline plume level with MC-LAGPAR numerical simulation.
Curve C: ground-level with analytical solution.
Curve D: centerline plume level with analytical solution.

The results of our simulations have been compared (at ground level and at the centerline plume level) with the results obtained by the two-dimensional analytical solution in homogeneous turbulence (i.e., the Gaussian model), in which $\sigma_z$ was evaluated by Eq. 11. Fig. 3 shows the results of such a comparison, which clearly appears to be satisfactory.

## 4. SIMULATION OF NONHOMOGENEOUS (CONVECTIVE) CONDITIONS

To prescribe the values of the meteorological parameters (stability and height dependent) needed to simulate turbulent diffusion in the planetary boundary layer, we choose the scheme suggested by Hanna [19]. This scheme provides different parametrization of the vertical profiles of

$$\sigma_{u'}\ ,\ \sigma_{v'}\ ,\ \sigma_{w'}\ ,\ T_{L_{u'}}\ ,\ T_{L_{v'}}\ ,\ T_{L_{w'}}$$

for different stability conditions (unstable, neutral, stable), where $T_{L_{u'}}$, $T_{L_{v'}}$, $T_{L_{w'}}$ are the Lagrangian time scales.

In unstable conditions, Hanna suggests :

$$\sigma_{u'} = \sigma_{v'} = u_* \cdot (12 + 0.5\, h_i / |L|)^{1/3}$$

$$\sigma_{w'} \begin{cases} = 0.96 \cdot w_* \cdot \left(\dfrac{3z}{h_i} - \dfrac{L}{h_i}\right)^{1/3} & \text{for } z < 0.03\, h_i \\ = w_* \cdot \min\left[0.96 \cdot w_* \left(\dfrac{3z}{h_i} - \dfrac{L}{h_i}\right)^{1/3} ;\ 0.763 \left(\dfrac{z}{h_i}\right)^{0.175}\right] & \text{for } 0.03\, h_i < z < 0.4\, h_i \\ = 0.722 \cdot w_* \cdot \left(1 - \dfrac{z}{h_i}\right)^{0.207} & \text{for } 0.4\, h_i < z < 0.96\, h_i \\ = 0.37 \cdot w_* & \text{for } 0.96\, h_i < z < h_i \end{cases}$$

$$T_{L_{u'}} = T_{L_{v'}} = 0.15 \frac{h_i}{\sigma_{u'}}$$

$$T_{L_{w'}} \begin{cases} = 0.1 \left(\dfrac{z}{\sigma_{w'}}\right) \dfrac{1}{0.55 + 0.38\,(z - z_o) / |L|} & \text{for } z < 0.1\, h_i \text{ and } (z - z_o) < |L| \\ = 0.59 \dfrac{z}{\sigma_{w'}} & \text{for } z < 0.1\, h_i \text{ and } (z - z_o) > |L| \\ = 0.15 \dfrac{h_i}{\sigma_{w'}} \left(1 - e^{\left(-\frac{5z}{h_i}\right)}\right) & \text{for } z > 0.1\, h_i \end{cases}$$

In our simulations we set :

$h_i$ = 1000 m, $w_*$ = 1.6 m/s, $\bar{u}$ = 2.5 m/s,

$u_*$ = 0.2 m/s $z_o$ = 0.2 m and L = -5 m

Since in nonhomogeneous turbulence the wind profile is not constant with height, the cross-correlation term u'w' must be taken into account (Zannetti [13]). In our simulations, u'w' was set equal to $-u_*^2$ near the surface and allowed to approach zero linearly with the height at the top of the PBL. This trend of u'w' with height was derived from fig. 6.7 of Plate (1982 ) [21].

Fig. 4 shows the differences on the ground-level concentrations due to two vertical wind profiles: 1) constant and 2) power law with height. In the case of the power law profile, its exponent was chosen in order to give an average wind velocity in the PBL equal to the value of the constant wind profile. It appears that using a power law profile, the maximum ground-level concentration comes near the source and its value slightly increases.

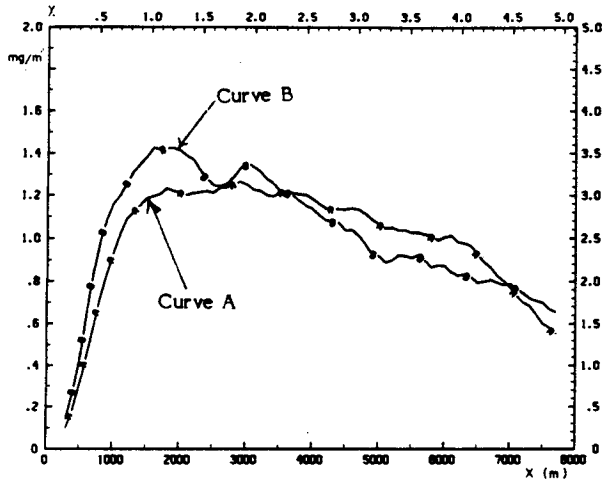


Fig. 4. Ground-level concentration as a function of a downwind distance with:

curve A: constant wind profile ($\bar{u}$ = 2.5 m/s)

curve B: power law wind profile ($u = 1.378 \cdot z^{0.1}$)

the top and right scales report nondimensional distance $(w_*/\bar{u}) \cdot (x/h_i)$ and concentration $(Q/h_i \cdot \bar{u})$.

The effects of the convective plumes on the pollutant dispersion were empirically considered. The measurements of Yamamoto et al. [22] show that the average ascent velocity w of plumes is constant with height in the PBL and it can be calculated that its value is about 0.5-0.6 times $w_*$. A suitable value for the velocity of descent is $0.4 \cdot w_*$ (Briggs 1975 [16]). Therefore, we added to the turbulent vertical velocities a constant vertical velocity due to the convective cells. In other words, to each trajectory a constant vertical velocity (up or down) was attributed in such a way that $\bar{w}$ is zero over all the trajectories and all the heights. This means that the number of particles $N_u$ in updraft, having an higher velocity $w_u$, are less than those ($N_d$ particles) in downdraft. They are calculated by:

$$N_d = N_u \frac{w_u}{-w_d}$$

As also done by Baerentsen and Berkowicz [9], each particle is allowed to jump from an updraft to a downdraft and vice versa with probabilities that depend on the time scales $T_{L_u}$ and $T_{L_d}$ of the two phenomena. That is, setting

$$T_{L_u} = \frac{h_i}{w_u}$$

the probability of a particle to jump from updraft to downdraft is

$$P_{u \rightarrow d} = 1 - e^{-\frac{\Delta t}{T_{L_u}}}$$

To be sure that the same number of particles jumps from up- to downdraft and viceversa we retrieve (for $\Delta t \ll T_{L_u}$ and $t \ll T_{L_d}$)

$$T_{L_d} = \frac{h_i}{-w_d}$$

and the probability of a particle to jump from downdraft to updraft is

$$P_{d \rightarrow u} = 1 - e^{-\frac{\Delta t}{T_{L_d}}}$$

Figs. 5, 6 and 7, show the comparison between the ground-level concentrations obtained from MC-LAGPAR simulations (curve A) and the water-tank experiments of Willis and Deardorff [23],[24],[25] (circles). These last refer to three different source heights (the emissions are nonbuoyant):

$$H_s / h_i = 0.067,\ 0.24,\ \text{and}\ 0.49$$

and Figs. 5, 6 and 7 refer respectively to the same cases.
Fig. 8 shows MC-LAGPAR simulation referred to a source height

$$H_s / h_i = 0.75$$

Concentrations are averaged values over the interval $z / h_i < 0.05$ except for the source height $H_s / h_i = 0.067$, where the average is over $z / h_i < 0.01$. In Figs. 5,6,7 and 8, maximum ground-level concentrations according to the Briggs formula (ref. Eq. 14 in De Baas et al. [8]) are also reported (squares). $-w_d$ and $w_u$ in our simulations have been set equal to 0.4 and 0.6 times $w_*$, respectively.

Looking at Figs. 5, 6, 7 and 8, it appears that the agreement between MC-LAGPAR simulations and experimental data is satisfactory. In particular, the simulations are able to well reproduce the typical behaviour of airborne pollutant dispersion in convectively unstable conditions. In fact, if particles are released near the ground, they first remain at the surface and then rise to the the midlevel of the PBL, whereas if they are emitted from elevated stacks, they first descend and then rise to midlevel [8]. This fact is clearly shown in Figs. 9, 10, 11 and 12, where the contours of the nondimensional concentrations

$$\chi = \left(\frac{Q}{h_i \cdot \bar{u}}\right)$$

of the four numerical simulations are plotted in the x-z plane. The goodness of the agreement is particularly interesting, as the simulations were performed by inserting in the Hanna scheme for unstable conditions a very simple mechanism taking into account the ascent of hot natural plumes.

It must be pointed out that, in our simulations, we did not encounter any unreasonable accumulation of particles in regions of low $\sigma_w$, and, therefore, we found no need to include semi-empirical drift velocity corrections, as performed, for example, by Legg and Raupach [26]. We believe that our realistic treatment of the downdrafts and updrafts, together with the inclusion of the cross-correlation $u'w'$ whose effects are mostly noticeable near the ground, is the main reason why particle accumulation is correctly avoided.

## 5. CONCLUSIONS

A Monte-Carlo model to simulate a turbulent diffusion of pollutants in the atmosphere is presented. The numerical scheme and the input-output assumptions are shown. The results of simulations in homogeneous conditions are in good agreement with those obtained by the analytical solution. Numerical experiments performed in atmospheric convective conditions (nonhomogeneous turbulence) produce concentration fields that satisfactorily agree with Willis and Deardorff's water-tank experiments. Therefore, the MC-LAGPAR computer code has proved to be a flexible and reliable tool to simulate air pollution dispersion in different meteorological situations.

## REFERENCES


[1] Mc Rae, G.J., Goodin W.R., and Seinfeld, J.H. (1981), Development of a second-generation mathematical model for urban air pollution - I. Model formulation, Atmospheric Environment, Vol. 15, pp. 679-696.

[2] Zannetti, P. (1981), An improved puff algorithm for plume dispersion simulation, Journal of Applied Meteorology, Vol. 20, pp. 1203-1211.

[3] Drivas, P.J., Chan, M., and Wayne, L.G. (1977), Validation of an improved photochemical air quality simulation model. AMS Joint Conference on Applications of Air Pollution Meteorology, November 23-December 2, 1977, Salt Lake City, UT.

[4] Hockney, R.W. and Eastwood, J.W. (1981), Computer Simulations Using Particles. McGraw-Hill, New York.

[5] Lamb, R.G. (1978), A numerical simulation of dispersion from an elevated point source in the convective planetary boundary layer, Atmospheric Environment, Vol. 12, pp. 1297-1304.

[6] Lange, R. (1978), ADPIC -- A three dimensional particle-in-cell model for the dispersal of atmospheric pollutants and its comparison to regional tracer studies, Journal of Applied Meteorology, Vol.17, pp. 320-329.

[7] Hanna, S.R. (1981), Lagrangian and Eulerian time-scale relations in the daytime boundary layer, Journal of Applied Meteorology, Vol.20, pp. 242-249.

[8] De Baas, A., Van Dop, H., and Nieuwstadt, F. (1986), An application of the Langevin equation in inhomogeneus conditions to dispersion in a convective boundary layer, Quarterly Journal of the Royal Meteorological Society, Vol. 471, pp. 165-180.

[9] Baerentsen, J.H., and Berkovicz, R. (1984), Monte Carlo simulation of plume dispersion in the convective boundary layer, Atmospheric Environment, Vol. 18, pp. 701-712.

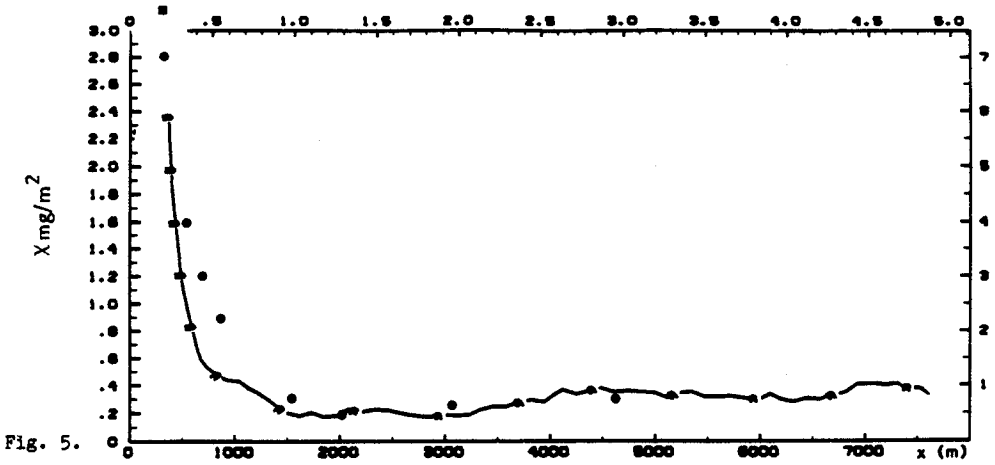


Fig. 5.

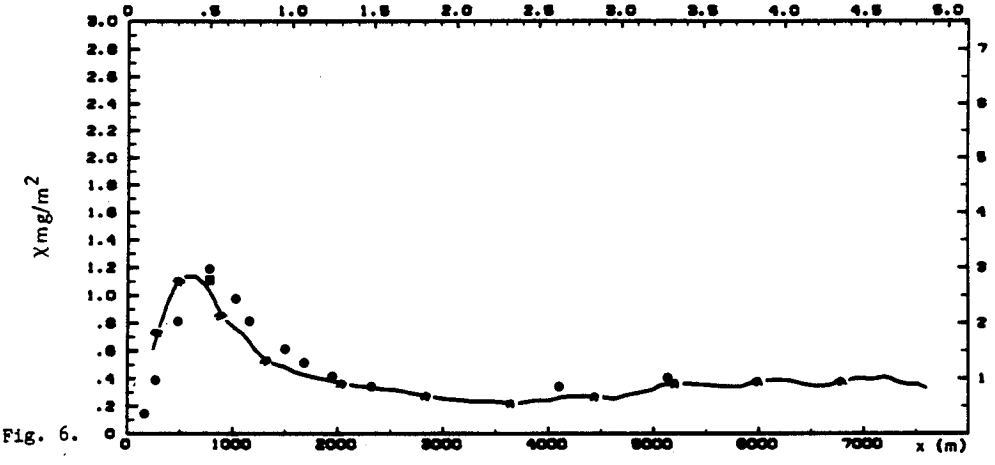


Fig. 6.

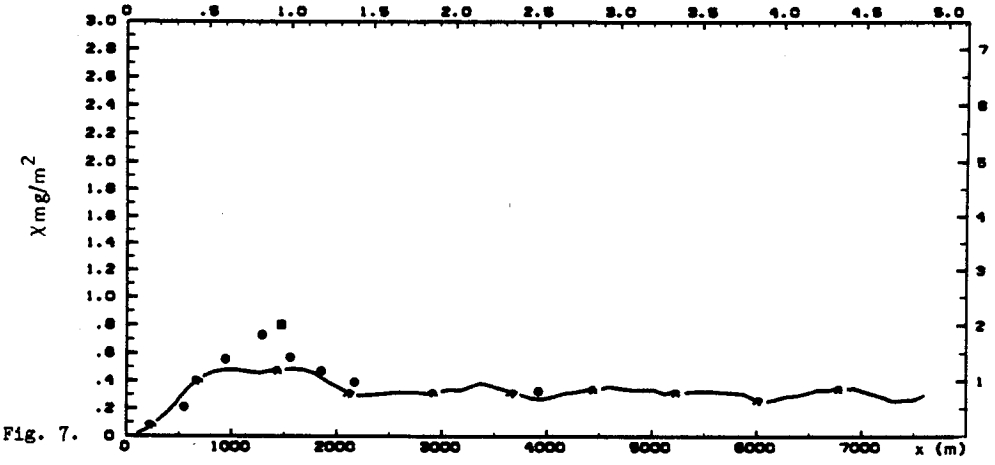


Fig. 7.

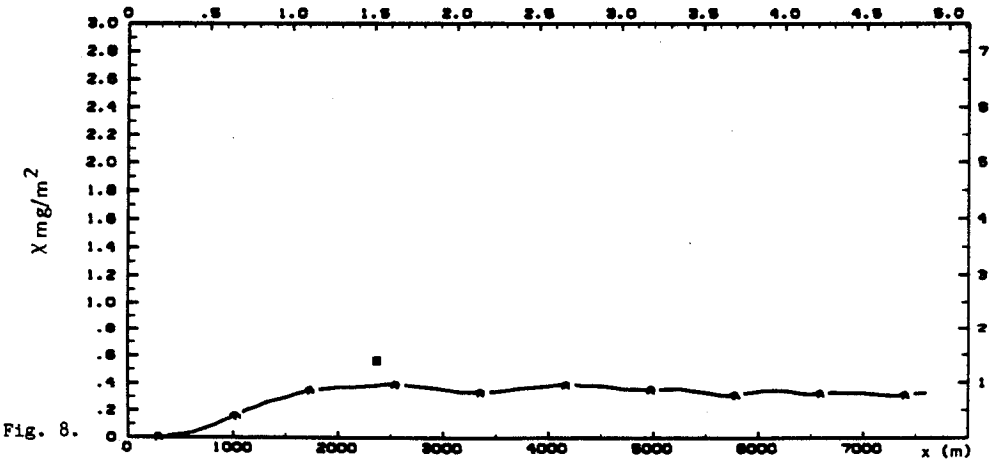


Fig. 8.

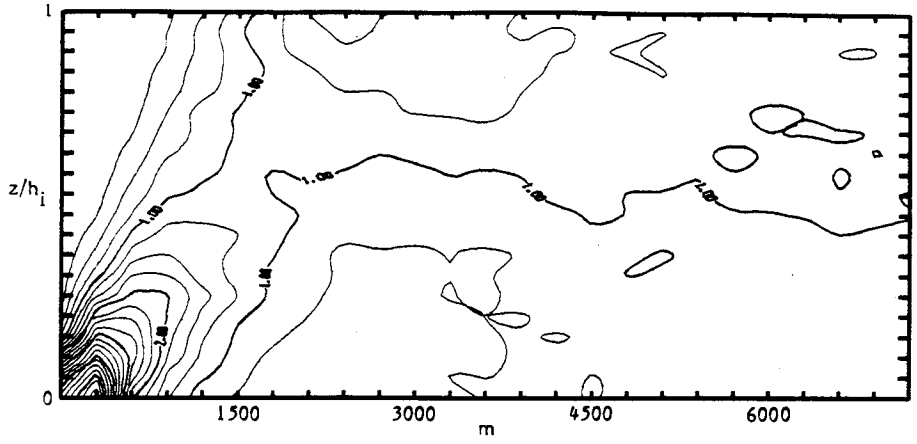


Fig. 9.

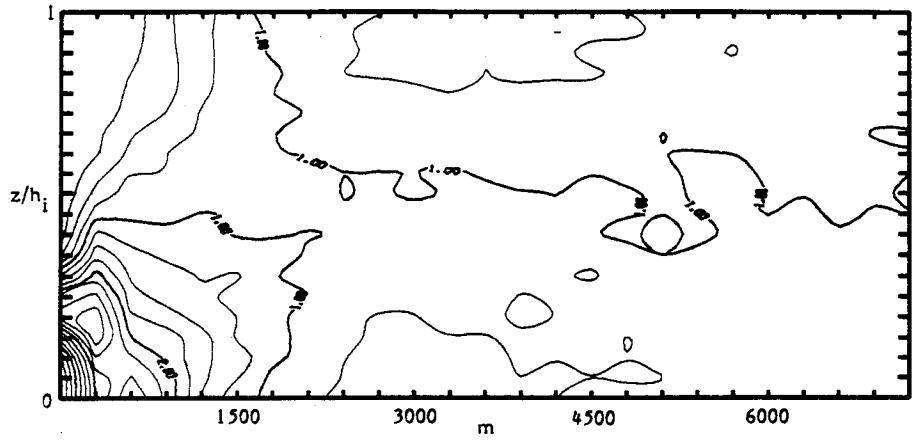


Fig. 10.

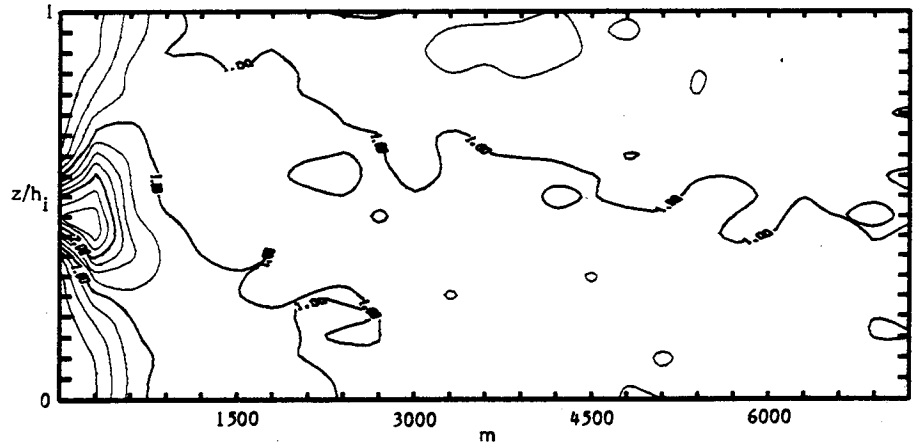


Fig. 11

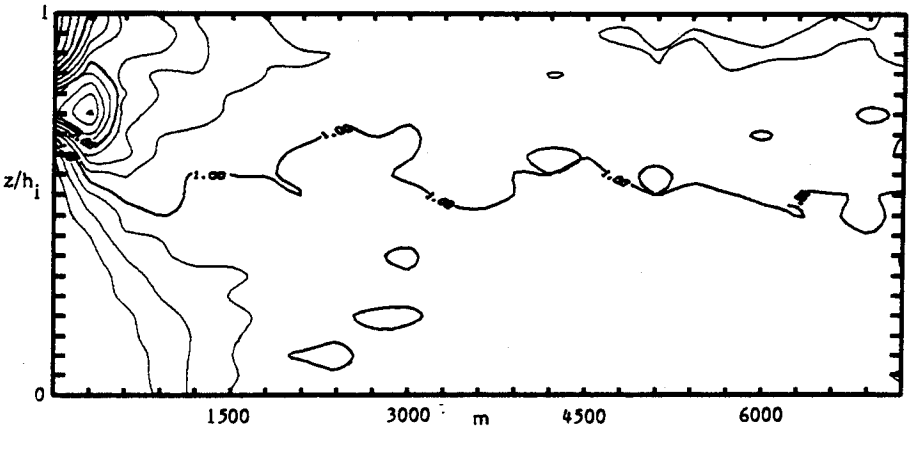


Fig. 12.

[10] McNider, R.T. (1981), Ph.D. Dissertation: Investigation of the impact of topographic circulations on the transport and dispersion of air pollutants. University of Virginia.

[11] Pielke, R.A., McNider, R.T., Segal, M., and Mahrer, Y. (1983), The use of a mesoscale numerical model for evaluations of pollutant tranport and diffusion in coastal region and over irregular terrain, Bulletin of the American Meteorological Society, Vol. 64, pp. 243-249.

[12] Segal, M., Pielke, R.A., Arritt, R.W., Moran, M.D., Yu, C.H., and Henderson, D. (1986) Southern Florida air pollution climatology study and selected episodic impacts, prepared for the Air Quality Division, National Park Service, Department of the interior, Contract NA81RAH00001, Amendment 17, Item 15, 237 pp.

[13] Zannetti, P. (1984), A new Monte Carlo scheme for simulating Lagrangian particle diffusion with wind shear effects, Applied Mathematical Modelling, Vol. 8, pp. 188-192.

[14] Zannetti, P. (1981), Some aspects of Monte Carlo type modeling of atmospheric turbulent diffusion. 7th Conference on Probability and Statistics in Atmospheric Sciences, AMS, Monterey, CA, November.

[15] Zannetti, P. (1986), Monte Carlo simulation of auto- and cross-correlated turbulent velocity fluctuations (MC-LAGPAR II Model), Enviromental Software, Vol.1, pp. 26-30.

[16] Briggs, G.A. (1975), Plume rise predictions, in Lectures on Air Pollution and Enviromental Impact Analyses. D.A. Augen, editor. Boston: American Meteorological Society.

[17] Stern, A.C. (1976), Air pollution, Vol. 1, 3rd edition. Academic press, Orlando, FL.

[18] Anfossi, D. (1985), Analysis of plume rise data from five TVA steam plants, Journal of Climate and Applied Meteorology, Vol. 24, pp. 1225-1236.

[19] Hanna, S.R. (1982), Applications in air pollution modeling. Chapter 7 in Atmospheric Turbulence and Air Pollution Modeling. Nieuwstadt, F.T.M and Van Dop, H., editors, pp. 275-310. Dordrecht: Reidel.

[20] Taylor, G.I. (1921), Diffusion by continuous movements, Proceedings of the London Mathematical Society, Vol. 20, pp. 196-202.

[21] Plate, E.G. (1982), Engineering meteorology. Elsevier

[22] Yamamoto, S., Gamo, M., and Osayuki, Y. (1982), Observational study of the fine structure of the convective atmospheric boundary layer, Journal of the Meteorological Society of Japan, Vol.60, pp. 882-888.

[23] Willis, G.E., and Deardorff, J.W. (1976), A laboratory model of diffusion into the convective planetary boundary layer, Quarterly Journal of the Royal Meteorological Society, Vol. 102, pp. 427-445.

[24] Willis, G.E., and Deardorff, J.W. (1978), A laboratory study of dispersion from an elevated source within a modeled convective planetary boundary layer, Atmospheric Environment, Vol.12, pp. 1305-1311.

[25] Willis, G.E., and Deardorff, J.W. (1981), A laboratory study of dispersion from a source in the middle of the convective mixed layer, Atmospheric Environment, Vol.15, pp. 109-117.

[26] Legg, B.J., and Raupach, M.R. (1982), Markov-chain simulation of particle dispersion in inhomogeneous flows: the mean drift velocity induced by a gradient in Eulerian velocity variance, Boundary Layer Meteorology, Vol. 24, pp. 3-13.